USGS
science for a changing world

Prepared in cooperation with the National Park Service

Assessment of Metal and Trace Element Contamination in Water, Sediment, Plants, Macroinvertebrates, and Fish in Tavasci Marsh, Tuzigoot National Monument, Arizona

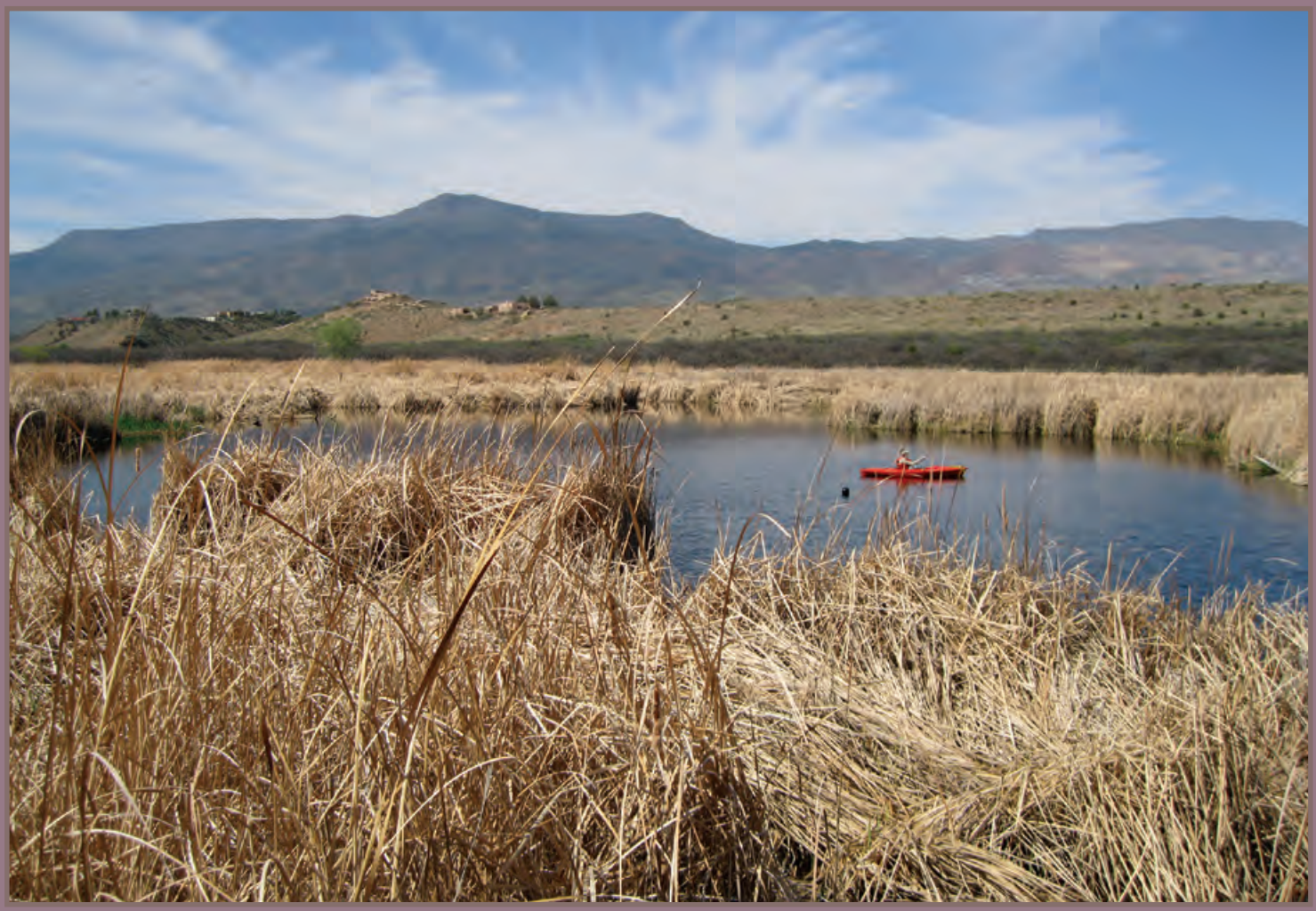

Scientific Investigations Report 2014–5069

U.S. Department of the Interior
U.S. Geological Survey

FRONT COVER
Photograph taken looking westward across a large open water section of Tavasci Marsh with the Tuzigoot Pueblo ruins in the left background and the town of Jerome, Arizona, in the right background. Photo by Matthew Miller, U.S. Geological Survey.

Assessment of Metal and Trace Element Contamination in Water, Sediment, Plants, Macroinvertebrates, and Fish in Tavasci Marsh, Tuzigoot National Monument, Arizona

By Kimberly R. Beisner, Nicholas V. Paretti, Anne M.D. Brasher, Christopher C. Fuller, and Matthew P. Miller

Prepared in cooperation with the National Park Service

Scientific Investigations Report 2014–5069

U.S. Department of the Interior
U.S. Geological Survey

U.S. Department of the Interior
SALLY JEWELL, Secretary

U.S. Geological Survey
Suzette M. Kimball, Acting Director

U.S. Geological Survey, Reston, Virginia: 2014

For product and ordering information: World Wide Web: http://www.usgs.gov/pubprod
Telephone: 1-888-ASK-USGS

For more information on the USGS—the Federal source for science about the Earth,
its natural and living resources, natural hazards, and the environment:
World Wide Web: http://www.usgs.gov
Telephone: 1-888-ASK-USGS

Suggested citation:
Beisner, K.R., Paretti, N.V., Brasher, A.M.D., Fuller, C.C., and Miller, M.P., 2014, Assessment of metal and trace element contamination in water, sediment, plants, macroinvertebrates, and fish in Tavasci Marsh, Tuzigoot National Monument, Arizona: U.S. Geological Survey Scientific Investigations Report 2014–5069, 72 p., http://dx.doi.org/10.3133/sir20145069.

Contents

Figures

Tables

Appendixes

[Available online only at http://pubs.usgs.gov/sir/2014/5069/.]

Conversion Factors

SI to Inch/Pound

Multiply	By	To obtain
	Length	
centimeter (cm)	0.3937	inch (in.)
millimeter (mm)	0.03937	inch (in.)
meter (m)	3.281	foot (ft)
kilometer (km)	0.6214	mile (mi)
meter (m)	1.094	yard (yd)
	Area	
square meter (m^2)	0.0002471	acre
hectare (ha)	2.471	acre
hectare (ha)	0.003861	square mile (mi^2)
square kilometer (km^2)	0.3861	square mile (mi^2)
	Volume	
cubic meter (m^3)	6.290	barrel (petroleum, 1 barrel = 42 gal)
liter (L)	33.82	ounce, fluid (fl. oz)
liter (L)	0.2642	gallon (gal)
cubic meter (m^3)	264.2	gallon (gal)
cubic meter (m^3)	35.31	cubic foot (ft^3)
cubic meter (m^3)	0.0008107	acre-foot (acre-ft)
	Flow rate	
meter per second (m/s)	3.281	foot per second (ft/s)
cubic meter per second (m^3/s)	35.31	cubic foot per second (ft^3/s)
liter per second (L/s)	15.85	gallon per minute (gal/min)
	Mass	
gram (g)	0.03527	ounce, avoirdupois (oz)
kilogram (kg)	2.205	pound avoirdupois (lb)
	Density	
kilogram per cubic meter (kg/m^3)	0.06242	pound per cubic foot (lb/ft^3)
gram per cubic centimeter (g/cm^3)	62.4220	pound per cubic foot (lb/ft^3)
	Radioactivity	
becquerel per liter (Bq/L)	27.027	picocurie per liter (pCi/L)

Temperature in degrees Celsius (°C) may be converted to degrees Fahrenheit (°F) as follows:
°F=(1.8×°C)+32

Temperature in degrees Fahrenheit (°F) may be converted to degrees Celsius (°C) as follows:
°C=(°F-32)/1.8

Specific conductance is given in microsiemens per centimeter at 25 degrees Celsius (µS/cm at 25 °C).

Abbreviations

AES	Arizona Ecological Services
BEST	Biomonitoring of Environmental Status and Trends
BLM	Biotic ligand model
CCC	Criterion continuous concentration
CTU	Cumulative toxicity unit
DOC	Dissolved organic carbon
DOM	Dissolved organic matter
EPA	U.S. Environmental Protection Agency
FI	Fluorescence index
FWS	U.S. Fish and Wildlife Service
ICP-AES	Inductively coupled plasma atomic emission spectrometer
ICP-MS	Inductively coupled plasma mass spectrometer
IQR	Interquartile range
LEL	Lowest effect level
MAR	Mass accumulation rate
NAWQA	National Water Quality Assessment
NCBP	National Contaminant Biomonitoring Program
NIST	National Institute of Standards and Technology
NMS	Nonmetric multidimensional scaling
NPS	National Park Service
PDC	Phelps Dodge Corporation
PEL	Probable effects level
PMC	Percent modern carbon
RPD	Relative percent difference
SEL	Severe effects level
SQG	Sediment quality guidelines
SRS	Standard reference sample
SUVA-254	Specific untraviolet absorption at 254 nm
TEL	Threshold effects level
USGS	U.S. Geological Survey
UVCC	United Verde Copper Company
UVX	United Verde Extension Company

Assessment of Metal and Trace Element Contamination in Water, Sediment, Plants, Macroinvertebrates, and Fish in Tavasci Marsh, Tuzigoot National Monument, Arizona

By Kimberly R. Beisner, Nicholas V. Paretti, Anne M.D. Brasher, Christopher C. Fuller, and Matthew P. Miller

Abstract

Tavasci Marsh is a large freshwater marsh within the Tuzigoot National Monument in central Arizona. It is the largest freshwater marsh in Arizona that is unconnected to the Colorado River and is designated as an Important Bird Area by the Audubon Society. The marsh has been altered significantly by previous land use and the monument's managers are evaluating the restoration of the marsh. In light of historical mining activities located near the marsh from the first half of the 20th century, evaluations of water, sediment, plant, and aquatic biota in the marsh were conducted. The evaluations were focused on nine metals and trace elements commonly associated with mining and other anthropogenic activities (As, Cd, Cr, Cu, Hg, Ni, Pb, Se, and Zn) together with isotopic analyses to understand the presence, sources and timing of water and sediment contaminants to the marsh and the occurrence in aquatic plants, dragonfly larvae, and fish.

Results of water analyses indicate that there were two distinct sources of water contributing to the marsh during the study: one from older high elevation recharge entering the marsh at Shea Spring (as well as a number of unnamed seeps and springs on the northeastern edge of the marsh) and the other from younger low elevation recharge or from Pecks Lake. Water concentrations for arsenic exceeded the U.S. Environmental Protection Agency primary drinking water standard of 10 µg/L at all sampling sites. Surface waters at Tavasci Marsh may contain conditions favorable for methylmercury production.

All surficial and core sediment samples exceeded or were within sample concentration variability of at least one threshold sediment quality guideline for As, Cd, Cr, Cu, Hg, Ni, Pb, and Zn. Several sediment sites were also above or were within sample concentration variability of severe or probable effect sediment quality guidelines for As, Cd, and Cu. Three sediment cores collected in the marsh have greater metal and trace element concentrations at depth for Bi, Cd, Cu, Hg, In, Pb, Sb, Sn, Te, and Zn. Radioisotope dating indicates that the elevated metal and trace element concentrations are associated with sediments deposited before 1963.

Arsenic concentration was greater in cattail roots compared with surrounding sediment at Tavasci Marsh. Concentrations of As, Ni, and Se from yellow bullhead catfish (*Ameiurus natalis*) in Tavasci Marsh exceeded the 75th percentile of several other regional studies. Mercury concentration in dragonfly larvae and fish from Tavasci Marsh were similar to or greater than in Tavasci Marsh sediment. Future work includes a biologic risk assessment utilizing the data collected in this study to provide the monument management with additional information for their restoration plan.

Acknowledgments

National Park Service staff Sharon Kim, Matt Guebard, and Dennis Casper at Tuzigoot National Monument were invaluable in providing background information and field assistance in locating areas of interest. Jessica Anderson and Matthew Garcia with the U.S. Geological Survey diligently worked without complaint for long field days in often muddy locations. The project benefited greatly from the expertise of many USGS scientists.

Introduction

Tuzigoot National Monument was established in 1939, following the discovery of hilltop ruins of a Sinagua pueblo during excavation by the Civilian Conservation Corps, which began in 1933. The boundary of the monument was expanded in 2005 to include Tavasci Marsh, and presently the monument covers 382 acres. Tavasci Marsh has been subject to varied management following Anglo-American settlement in the 1860s (Stoutamire, 2011). Currently, Tuzigoot National Monument resource managers are developing a management and restoration plan for Tavasci Marsh to improve conditions, functions, and ecosystem values provided by this unique freshwater system. Land leveling of the marsh to allow for cattle grazing and increased outflow from Pecks Lake may have resulted in topographic and hydrologic conditions that are extremely favorable for expansion of cattails (*Typha* spp.), which have usurped open water areas and natural transition zones to the adjacent dry mesquite bosque and, to the detriment of other wetland plant communities, now cover almost 70 percent of the marsh area (Ryan and Parsons, 2009). Restoration activities or changes in source water are likely to significantly change water chemistry and affect sediment, plants, macroinvertebrates,

and fish. There is also concern that earth moving and cattail removal activities could potentially remobilize sediment-bound metals and trace elements into the water column.

Tavasci Marsh (fig. 1) is the largest freshwater marsh in Arizona that is unconnected to the Colorado River (Stoutamire, 2011) and is designated as an Important Bird Area by the Audubon Society. Until recently, the marsh was owned by Phelps Dodge Corporation (now Freeport-McMoran Copper and Gold, Inc.) and managed by Arizona Game and Fish Department. In December 2005, the National Park Service obtained 110 acres of land including Tavasci Marsh as part of a larger parcel acquired from Phelps Dodge, and the marsh is now managed as part of Tuzigoot National Monument. Tavasci Marsh and nearby surface waters provide habitat for a number of endangered, threatened, or candidate species of fish, birds, and reptiles, such as the razorback sucker (*Xyrauchen texanus*), spikedace (*Meda fulgida*), Colorado pikeminnow (*Ptychocheilus lucius*), yellow-billed cuckoo (*Coccyzus americanus occidentalis*), bald eagle (*Haliaeetus leucocephalus*), Yuma clapper rail (*Rallus longirostris yumanensis*), and Mexican garter snake (*Thamnophis eques*) (Schmidt and others, 2005).

Tavasci Marsh is potentially influenced by multiple point and nonpoint mining and agricultural sources of contaminants. Most notable are the remnant tailings pile and historical smelter locations evidenced by remnant slag piles from historical mining activities located upstream and adjacent to Tavasci Marsh, Pecks Lake, and the Verde River. Given the location of historical local mine processing sites, it is possible that metals and other trace elements have been transported into Tavasci Marsh. A comprehensive assessment of metal contamination in water, sediment, plants, and biota has never been conducted in Tavasci Marsh, and limited information is available about the source(s), timing, fate, and occurrence of metal contamination in Tavasci Marsh.

Purpose and Scope

The purpose of this report is to provide information to Tuzigoot National Monument resource managers regarding the presence, distribution, and biotic accumulation of mining-related metals and trace elements in Tavasci Marsh to inform the development of their management plan. Our objective was to collect data to assess the current status of the following elements of interest: arsenic (As), cadmium (Cd), chromium (Cr), copper (Cu), mercury (Hg), nickel (Ni), lead (Pb), selenium (Se), and zinc (Zn), which are all potential metal and trace element contaminants from mining operations and have been extensively studied in association with mining and development. We also aimed to develop an understanding of fate and transport of metals and trace elements entering the marsh over time. Mining activities have had significant impacts on surrounding ecosystems that persist beyond the life of the mine (Schmitt, 1998, Church and others, 2007). Early mine operations and processing, before the mid-20th century, were not very efficient or subject to environmental regulations, which resulted in greater loss of metal and trace elements to the environment and more mine waste compared with current practices (Nash and others, 1996, Schmitt, 1998). This report is intended to provide an assessment of metal and other trace element concentrations in Tavasci Marsh, and is not intended to be a biotic risk assessment, which is part of an ongoing study that will utilize the data collected in this report.

Description of Study Area

Tuzigoot National Monument is located in central Arizona in the transition zone between the Basin and Range Province and the Colorado Plateau Province, just south of the Mogollon Rim. Tavasci Marsh lies in the downstream half of an abandoned oxbow of the Verde River east of Clarkdale, Arizona. Directly upstream, in the first half of the oxbow, is the artificially impounded Pecks Lake, which is fed by the Verde River and is one of two primary sources of water into Tavasci Marsh. The other main source is a series of natural springs (including Shea Spring) that seep from the steep hillsides bordering the marsh. Tavasci Marsh flows south and enters the Verde River south of the Tuzigoot Pueblo.

The Pliocene and Miocene Verde Formation comprise the hillside bordering Tavasci Marsh (DeWitt and others, 2008). The Verde Formation consists of clastic limestone and evaporite facies deposited when the Verde Valley was an internally drained closed basin resulting from structural subsidence and/or damming of drainage by late Miocene lava flows (Lindsay, 2000). The two members of the Verde Formation that crop out around Tavasci Marsh are the interbedded member and the limestone member (Lindsay, 2000). The interbedded member makes up the lower part of the hillside bordering Tavasci Marsh and is characterized by alternating limestone and clastic units with localized conglomerate lenses (Lindsay, 2000), which are present at Tuzigoot as a large outcrop on the northern margin of the marsh. The light pink color and iron oxide staining suggest that much of the Verde Formation clastic rock is derived from reworking of the Pennsylvanian-Permian Supai Formation (Lindsay, 2000). The limestone member comprises the upper part of the hillside surrounding Tavasci Marsh and generally consists of white limestone with minimal clastic units indicating a depositional period when water depths may have reached a few meters (Cassell, 1980).

Meteorological data available for Tuzigoot National Monument show an average annual precipitation of 12.67 inches between 1977 and 2012 and an average annual air temperature of 63.2 °F (Western Regional Climate Center, 2013). The precipitation pattern is bimodal with the greatest amount of precipitation falling between July and September followed by the second precipitation season between December and March (fig. 2). Average monthly temperatures are lowest in December and highest in July (fig. 2).

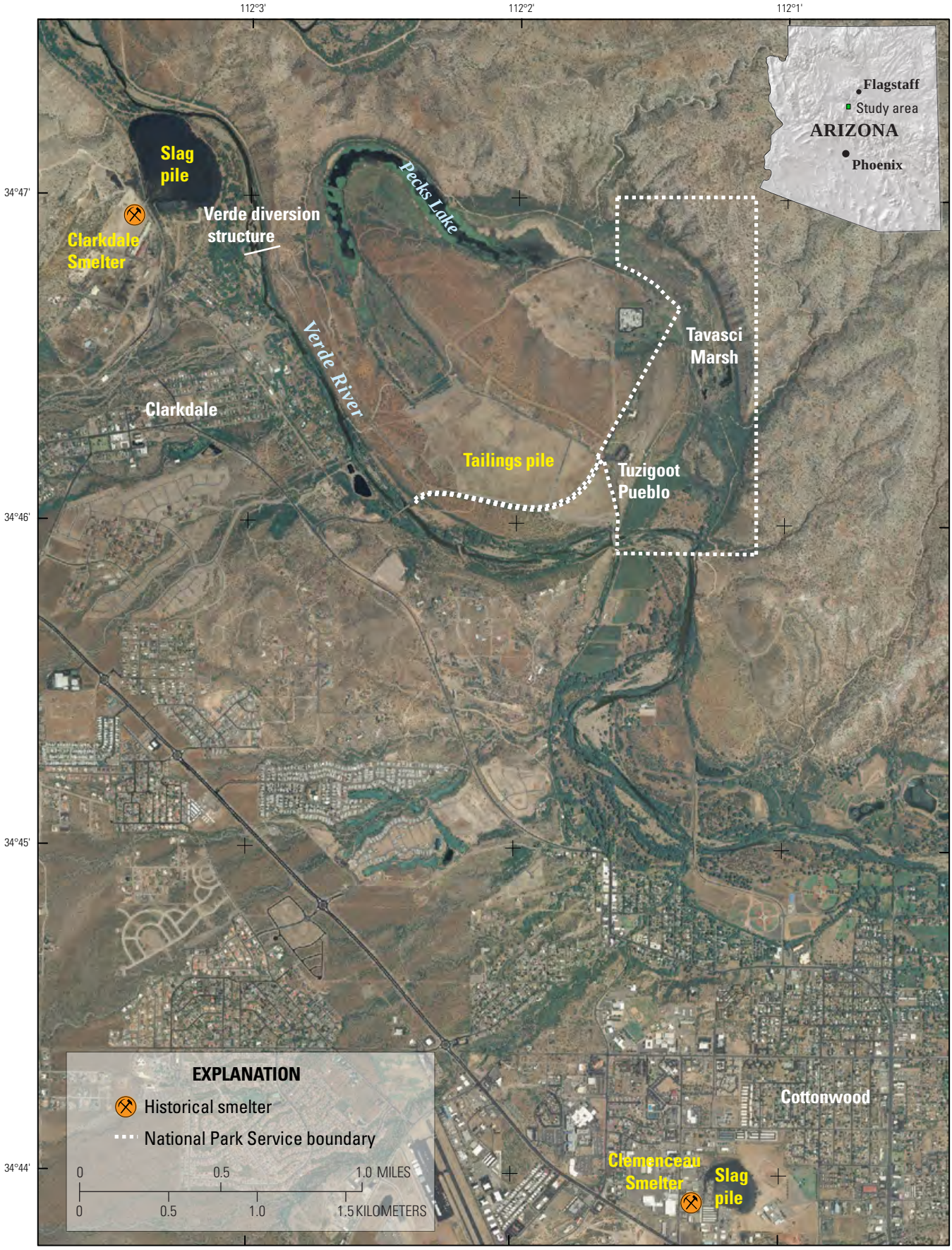

Figure 1. Map of Tavasci Marsh within a regional context.

Historical Overview of Human Development

Human development of Tavasci Marsh and the adjacent parts of the oxbow has drastically altered the marsh from the natural condition. Discussion of human development in this report begins with the late 19th century, as prior utilization of the marsh is subject to anthropologic interpretation. Stoutamire (2011) compiled a comprehensive history of the development and management of Tavasci Marsh and all information below is summarized from his report unless otherwise cited. Timing of management and regional activities are important to the interpretation of results of this study, especially regarding the sediment cores that were analyzed for radioisotopes to obtain ages of sediment exposure to the atmosphere.

The Anglo-American settlement of the upper Verde Valley began in 1865, spurred by the Homestead Act of 1862. Settlement of Tavasci Marsh began in the late 1870s by homesteaders from the eastern United States using minor irrigation systems for subsistence agriculture. Starting in 1890, northern Tavasci Marsh was utilized for raising cattle and ditch systems were developed, diverting water from the Verde River through a tunnel to what is now Pecks Lake and utilizing Shea Spring through installed irrigation ditches.

In 1876, ore deposits near the present-day town of Jerome were explored by Morris Andrew Ruffner, an early resident of Tavasci Marsh, and were subsequently developed for mining by the United Verde Copper Company (UVCC). In 1899, the United Verde Extension Company (UVX) was organized to locate and mine the ore body to the east of the Verde Fault (Anderson and Creasey, 1958). The UVCC and UVX mines are part of the Verde mining district, which is classified as a copper, gold, silver, and zinc stratabound volcanogene massive sulfide deposit of Precambrian age (1.82–1.65 Ga) (Keith and others, 1983). The UVCC mine's host rocks were porphyry and schist and the orebody consisted of a variety of minerals and rocks such as base sulfides with low silica content, siliceous sulfides, oxides or silicates and as a result, selective mining techniques were employed (Alenius, 1968). The greater part of the material in the ore body is quartz porphyry generally replaced by pyrite and chalcopyrite with minor amounts of sphalerite, chalcopyrite, arsenopyrite, and tennantite (Lindgren, 1926). The ore at the UVCC mine was high-grade: some sulfides and contained as much as 40 percent Cu, some siliceous ore contained more than 200 ounces of Ag per ton, and some oxide ore contained more than three ounces of Au per ton (Alenius, 1968). The ore from the UVX mine differs from UVCC mine ore and is dominantly a very high grade chalcocite ore with an average of 15 to 22 percent Cu and only 2 ounces of Ag per ton (Lindgren, 1926). The dominant minerals from the UVX mine are pyrite, chalcocite, cuprite, covellite, and magnetite (Lingren, 1926). The mean chemical composition in the Verde mining area (the average of 12 massive sulfide ore samples from different mines) is 3.3 percent sulfide; 9,540 ppm As; 8,240 ppm Cu; 77 ppm Cd; 9.5 percent Fe; 3,720 ppm Pb; and 18,500 ppm Zn (Nash and others, 1996).

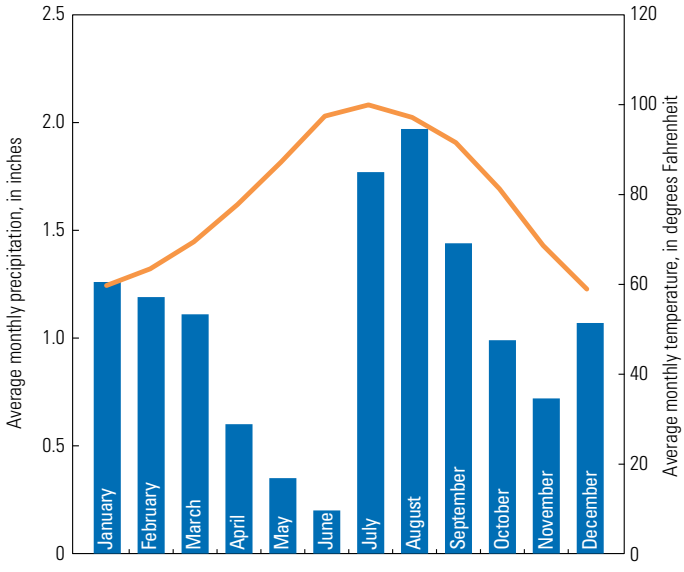

Figure 2. Plot showing monthly average meteorological data from Tuzigoot weather station (028904), from Western Regional Climate Center, 2013; precipitation (blue bars) and temperature (orange line).

Ore was transported from the UVCC and UVX mines to Clarkdale and Clemenceau via railroad then crushed and subsequently smelted. The smelter at Clarkdale began operation in 1915 and included a crushing plant, concentrator, roasting plant, blast furnace and reverbatory furnace, and converters (Lanning, 1930). A study on dust losses in 1918 were reported to be approximately 100 tons per day, including 11,000 pounds of Cu per day from early smelter operations, so the Cottrell plant was constructed at the Clarkdale smelter in 1922 to collect the dust, resulting in 91.5 percent recovery of Cu (Denny, 1930). A concentrator was added in 1927 to improve the smelting process for high-sulphide schist, which ground the ore to a smaller size then underwent flotation milling using lime-burnt (high calcium), cyanide-crude calcium, xanthate-amyl, xanthate-ethyl and pine oil-yarmour reagents. This addition of the concentrator resulted in mill recoveries of approximately 93 percent Cu, 75 percent Ag, and 64 percent Au (Barker, 1930).

The approximate annual smelter capacity at Clarkdale in 1929 was 1,750,000 tons (Lanning, 1930). The smelter operated until 1950 and the UVCC mine closed in 1953 (Anderson and Creasey, 1958). The smelter at Clemenceau was completed in 1918 to handle the ore from the UVX mine, and in 1930 a 200-ton flotation mill was added to handle lower grade copper ore. The Clemenceau smelter closed in 1937 and was followed by the closing of the UVX mine in 1938 (Anderson and Creasey, 1958).

The smelter smoke is reported to have killed farmers' crops throughout the Verde Valley and killed alfalfa crops and native wetland vegetation in Tavasci Marsh. Remnants from the Clarkdale smelter are present as a large slag pile on the western bank of the Verde River across from Pecks Lake

and the remnant slag pile from the Clemenceau smelter is surrounded by development in present day Cottonwood (fig. 1).

In the 1910s, UVCC began purchasing land in the Verde River oxbow encompassing Tavasci Marsh in order to develop a recreational area for mining employees, including a nine-hole golf course and the creation of Pecks Lake. In 1914, a dam and diversion tunnel were created to divert the Verde River into Pecks Lake (Ryan and Parsons, 2009). From 1927 to 1953, Phelps Dodge Corporation (PDC) used the southwestern part of the old oxbow channel as a disposal site for approximately 4 million tons of copper mine tailings. The tailings pile covered approximately 129 acres of the oxbow channel and is approximately 0.5 miles from Tavasci Marsh. In the 1980s, the Town of Clarkdale began using the tailings pile as a discharge location for treated effluent from the wastewater treatment plant and discharged water at a maximum rate of 100,000 gallons per day (Ecology and Environment, Inc., 1994). In the 1990s, the wastewater discharge onto the tailings pile within the oxbow channel was discontinued and in 2007 the pile was capped with a high-density polyethylene liner and three feet of soil and engineered to route water away from the pile during runoff events.

During mining operations, Tavasci Marsh continued to be utilized for farming and cattle grazing and in 1928 became the Clarkdale Dairy. The Clarkdale Dairy operations are reported to have expanded the irrigation system in the marsh and annually removed nearly a foot of sediment and debris from the irrigation ditches to allow for more available land to graze cattle and raise crops. Cattails were seen as a nuisance and burned annually, and many mesquite trees were removed in the early years of development.

In 1935, the purchase of UVCC by the PDC resulted in a new lease for the dairy and the transfer of Tuzigoot hill to the Federal Government for the purposes of establishing Tuzigoot National Monument. In the 1950s, 109 acres of the marsh were leveled to allow for creation of permanent pastures. The Clarkdale Dairy closed in 1958, but the marsh was used to raise beef cattle until 1991.

In 1993, the Arizona Game and Fish Department installed water control structures across the Tavasci and Shea Spring ditches to restore the wetland to its historically smaller size, which was estimated to be approximately 80 acres. By the end of the 1990s the water control structures had fallen into disrepair and the wetland had expanded, largely due to an elaborate system of beaver dams and the resulting spread of cattails.

A condensed timeline of mining and ore processing activities and modifications to Tavasci Marsh is presented below. Additionally, graphs of production over time are presented in figure 3. Ideally, this information could be matched up with sediment core age dating and elemental profiles to understand historical sources of deposition in Tavasci Marsh.

1870s—Settlement of Tavasci Marsh by homesteaders
1882—United Verde Copper Company (UVCC) founded
1890—Northern Tavasci Marsh utilized for raising cattle and ditch systems developed
1899—United Verde Extension Company (UVX) founded
1914—Dam and diversion tunnel built to divert Verde River into Pecks Lake
1915—Clarkdale smelter completed
1918—Clemenceau smelter completed
1922—Cottrell plant constructed at the Clarkdale smelter to reduce dust loss

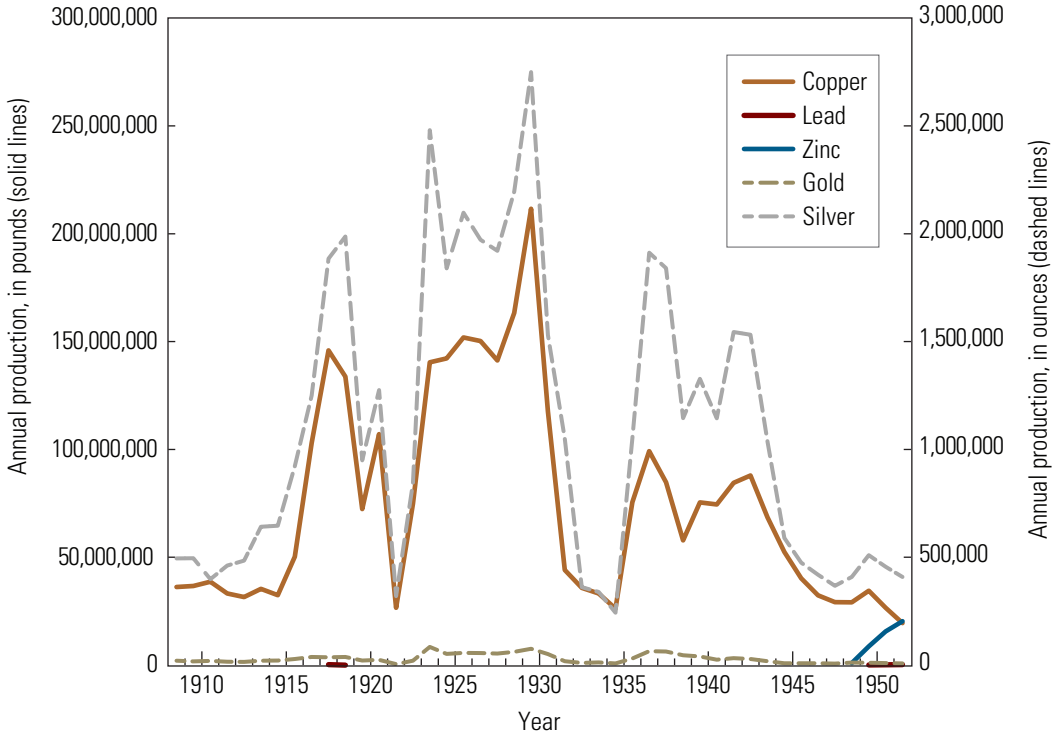

Figure 3. Plot showing annual production of Ag, Au, Cu, Pb and Zn from Verde (Jerome) mining district.

1927—Start of using southwest portion of oxbow for tailings disposal; flotation concentrator added to smelter at Clarkdale
1930—Flotation mill added to Clemenceau smelter
1933–1935—Tuzigoot ruins excavated
1937—Clemenceau smelter closed
1938—UVX mine closed
1939—Tuzigoot ruins designated a National Monument
1950—Clarkdale smelter closed
1950s—109 acres of marsh were leveled for cattle grazing
1953— UVCC mine closed; end of using southwest portion of oxbow for tailings disposal
1958—Clarkdale Dairy closed
1980s—Town of Clarkdale began using the tailings pile as a discharge location for treated effluent from the wastewater treatment plant
1991—End of Tavasci Marsh as cattle pasture
1993—Arizona Game and Fish Department installed water control structures across the Tavasci Marsh and Shea Spring ditches
2005—Tavasci Marsh acquired by the National Park Service
2007—Tailings pile capped and revegetated

Previous Studies

The U.S. Environmental Protection Agency (EPA) requested an Expanded Site Inspection (ESI) under the authority of the Comprehensive Environmental Response, Compensation, and Liability Act of 1980 and the Superfund Amendments and Reauthorization Act of 1980. Ecology and Environment, Inc. carried out the assessment and released an ESI report of the Clarkdale tailings pile, Pecks Lake, and Tavasci Marsh in 1994. Metal concentrations were measured in surface water, groundwater, and sediment throughout the study area. Tailings pile material was sampled directly and contained elevated levels of numerous metals including As, Cd, Cu, Hg, Pb, and Zn (Ecology and Environment, Inc., 1994). Sediment samples were collected starting at the tailings dam at the southwestern end of Pecks Lake and then incrementally along the oxbow through Pecks Lake and Tavasci Marsh. The report notes that numerous metals were released from the tailings pile into Pecks Lake including As, Cd, Cu, Hg, Pb, and Zn (Ecology and Environment, Inc., 1994).

An Aquifer Protection Permit Application prepared for Phelps Dodge Corporation in 1991 describes the native soil beneath the tailings as alluvial deposits of silty to gravelly sand 40 to 50 feet thick. Local groundwater flow in the shallow alluvial aquifer is toward the south. Wells drilled through the tailings pile indicate that locally the top of the water table extends up into the tailings (Ecology and Environment, Inc., 1994). Unfiltered groundwater samples collected from wells in the tailings in 1992 contained total concentrations of Cd, Cr, and Pb above EPA primary maximum contaminant levels (Ecology and Environment, Inc., 1994). Sampling conducted under a previous Site Screening Inspection (SSI) in 1992 documented a release of Cd, Cu, Pb, and Zn to the Verde River from seeps found along the banks of the river (Ecology and Environment, Inc., 1994).

Nash and others (1996) of the U.S. Geological Survey (USGS) conducted a study beginning in 1994 that investigated environmental impacts of mining activities during the period 1860 to 1955 in the Prescott National Forest area of Yavapai County, Arizona, and included analyses of water, soil, and sediment samples. The study found that mining and related mineral-processing activities produced local contamination of moderate to severe magnitude. Soil samples collected around historic smelter locations suggested that substantial amounts of As, Cd, Cu, Pb, and Zn were added to the upper layer of soils (Nash and others, 1996). Concentrations of metals in soils for 1 to 3 miles around smelters tended to be high or very high (determined by Nash and others [1996]) with metal concentrations elevated above background levels up to about 10 to 12 miles from smelter sites (Nash and others, 1996). Older mining technologies were less efficient than modern techniques and consequently more metals and trace elements, particularly As, Cu, Pb, S, Sb, and Zn, were left behind in mine tailings and slag (Nash and others, 1996). Further, many mining, milling, and smelting practices from 1875 to 1925 caused moderate to severe contamination that would not be permitted today due to the lack of health and environmental regulations at the time (Nash and others, 1996).

In 1998, Pecks Lake was placed on the list of Arizona Water Quality Limited Segments (303(d) List) for violations of dissolved oxygen and pH water-quality standards for surface waters. Subsequently, an assessment of total maximum daily load was released in September 2001 (Arizona Department of Environmental Quality, 2001). Recommendations included continuous flow through Pecks Lake with diverted Verde River water and selective harvesting of aquatic macrophytes. Dredging of Pecks Lake was not recommended due to trace element concentrations (As and Pb) that exceeded Arizona soil remediation levels (Arizona Department of Environmental Quality, 2001).

URS Greiner Woodward Clyde (URSGWC), commissioned by the Bureau of Land Management at the request of Phelps Dodge Corporation, conducted a study of Tavasci Marsh in 1999 for geochemical characterization and toxicity testing. Surface water and surface sediment was collected from Tavasci Marsh and surface soil, and rock was collected from the Verde Formation and washes derived from the Verde Formation adjacent to Tavasci Marsh (URSGWC, 1999). Surface water samples were compared with EPA National Ambient Water Quality Criteria and did not exceed the accepted limits (URSGWC, 1999). Toxicity tests showed no statistical difference between the upgradient reference location and marsh locations (URSGWC, 1999), but the reference site was also located in Tavasci Marsh, just north of Shea Spring. Surface sediment samples were compared to freshwater effects range median benchmarks from Ingersoll and others (1996), and only one sample exceeded this threshold for As (URSGWC,

1999). Rock samples were collected from limestone, sandstone, marl/mudstone, and conglomerate facies of the Verde Formation. Sandstone contained the highest mean concentrations of As, conglomerates contained the highest mean concentrations of Ba, marl and mudstones contained the highest mean concentrations of Cr, and limestones (the dominant rock type of the Verde Formation) contained the lowest mean concentrations of As, Ba, Cd, Cr, Cu, Hg, Pb, Se, and Zn (URSGWC, 1999). Surface soils from the wash directly north of Tavasci Marsh contained the highest mean concentrations of Cd, Cu, Pb, and Zn (URSGWC, 1999). Metals concentrations in surface sediment from the marsh were attributed to rocks from the Verde Formation surrounding the marsh (URSGWC, 1999). Metals concentrations in the surface sediment samples from the URSGWC (1999) study had lower metals concentrations compared with surface sediment samples from the Ecology and Environment, Inc., 1994 study.

Following the aforementioned studies, the Clarkdale tailings pile was capped with soil and re-vegetated with native grasses by Phelps Dodge Corporation. Rock-lined channels were installed in 2007 to route stormwater away from the capped area.

Methodology

Determination of Sampling Location, Timing, and Medium

Samples of water, sediment, plant, dragonfly larvae, and fish were collected throughout Tavasci Marsh at sites indicated in figure 4 and table 1. Samples were collected in October and April 2010–2012 to determine if season affected chemistry in the marsh. Water and sediment samples were collected during each of the four sampling trips. Plant samples in Tavasci Marsh consisted of cattails (*Typha* spp.) and watermilfoil (*Myriophyllum* spp.) collected in October and April of 2010–2011. Dragonfly larvae and fish samples were collected the following year in October and April of 2011–2012 to understand how season may affect their body chemistry. Surface sediment samples were collected with cattail samples in October 2010 and with dragonfly larvae samples in April 2012. A reference sample of cattail leaves, roots, watermilfoil, and surface sediment was collected in October 2011 at the Verde reference site on the Verde River, upstream of Tavasci Marsh, for comparison with samples from Tavasci Marsh.

Table 1. Sample location information.

[Latitude and longitude are given in degrees, minutes, and seconds with reference to the NAD83 datum; SW, surface water; GW, groundwater; SS, surface sediment; SC, sediment core; CA, cattail; WM, watermilfoil; DL, dragonfly larvae; FI, fish]

Report short name	USGS site name	USGS site ID	Latitude	Longitude	Sample media
TZG01	Tavasci Marsh TZG01	344626112011900	34° 46′ 25.7″	-112° 01′ 19.4″	SS, CA, DL
TZG02	Tavasci Marsh TZG02	344628112011400	34° 46′ 27.5″	-112° 01′ 13.9″	SC
TZG03	Tavasci Marsh open water	344628112011300	34° 46′ 27.7″	-112° 01′ 12.8″	SW, SS, SC, CA, WM, DL, FI
TZG04	Tavasci Marsh TZG04	344607112011800	34° 46′ 06.9″	-112° 01′ 17.7″	SS, SC, CA, DL, FI
TZG05	Tavasci Marsh TZG05	344621112011900	34° 46′ 20.9″	-112° 01′ 18.7″	SS, CA, DL, FI
TZG06	Tavasci Marsh TZG06	344647112013300	34° 46′ 46.9″	-112° 01′ 33.4″	SS, CA
Shea Spring (TZG07)	A-16-03 15CAC1	344648112012000	34° 46′ 48.0″	-112° 01′ 19.8″	SW, SS, CA, FI
TZG08	Tavasci Marsh TZG08	344640112012300	34° 46′ 40.0″	-112° 01′ 22.9″	SS, SC, CA, DL
TZG09	Tavasci Marsh TZG09	344646112013101	34° 46′ 45.7″	-112° 01′ 31.1″	SC
TZG10	Tavasci Marsh TZG10	344651112012601	34° 46′ 51.2″	-112° 01′ 25.5″	SC
Inflow	Tavasci Marsh inflow	344649112013800	34° 46′ 48.8″	-112° 01′ 37.7″	SW, SS
Outflow	Tavasci Marsh outflow	344600112011700	34° 46′ 00.1″	-112° 01′ 16.7″	SW
Piezometer 1	A-16-03 15CBD1	344651112012801	34° 46′ 51.4″	-112° 01′ 28.2″	GW
Piezometer 3	A-16-03 15CBB1	344654112013401	34° 46′ 53.5″	-112° 01′ 33.5″	GW
Piezometer 6	A-16-03 15CBC1	344650112013601	34° 46′ 50.1″	-112° 01′ 36.0″	GW
Piezometer 7	A-16-03 15CBC2	344649112013301	34° 46′ 48.6″	-112° 01′ 32.9″	GW
Piezometer 8	A-16-03 15CBD2	344647112012901	34° 46′ 47.0″	-112° 01′ 28.7″	GW
Verde reference	Verde River at Reitz Ranch near Clarkdale, Ariz.	344831112031900	34° 48′ 31.4″	-112° 03′ 19.3″	SS, CA, WM

Water sample sites were selected to represent water at the northern end of the marsh, at an open-water site midway through the marsh, and at the outflow of the marsh. Water was flowing at the outflow of Tavasci Marsh during each sampling trip and discharge was measured during each visit except in October 2010. The original sampling plan was to collect a surface water sample of water flowing out of Pecks Lake into Tavasci Marsh (inflow site), but due to damages to the diversion structure on the Verde River, the water level in Pecks Lake was so low that no surface water flowed out of Pecks Lake during the study period. In April 2012, there was a small amount of flowing water present at the inflow site, which was likely seepage from Pecks Lake through the earthen berm, and this water was collected. In light of the lack of water at the inflow site for most of the study, a shallow piezometer at the northern end of the marsh was sampled during each site visit. Four sets of water samples were collected over a two year period at sites Shea Spring (TZG07), piezometer 6, TZG03, and outflow. Four additional piezometers (1, 3, 7, and 8) were sampled in October 2011 to understand the spatial distribution of chemistry in the shallow groundwater at the northern end of the marsh. Water level in piezometers was measured before each sample was collected.

Most of the cattail leaves in the marsh were green during the October 2010 sampling trip then brown in April 2011; both were collected in order to investigate the chemical composition of the brown leaves compared with green leaves. Some of the cattail leaves near Shea Spring (TZG07) were still green in April 2011 and were collected for comparison with nearby brown leaves.

Aquatic macroinvertebrates serve as good biomonitors of contaminants in the aquatic environment because of their ubiquitous presence, ease of collection, relatively sedentary existence, constant exposure to sediments and littoral material, short life span, long immature life-stage, and base trophic position in the food chain (Goodyear and McNeill, 1999). There are also some disadvantages to analyzing aquatic macroinvertebrates, such as the relatively large mass necessary for analytical procedures, which often requires the collection of composite samples that can complicate the interpretation of bioaccumulation information. Additional considerations that may affect trace element concentrations in macroinvertebrates include the adsorption and absorbtion of metals and particulates (Mason and others, 2000; Lavilla and others, 2010), and whether to allow for depuration (emptying of gut

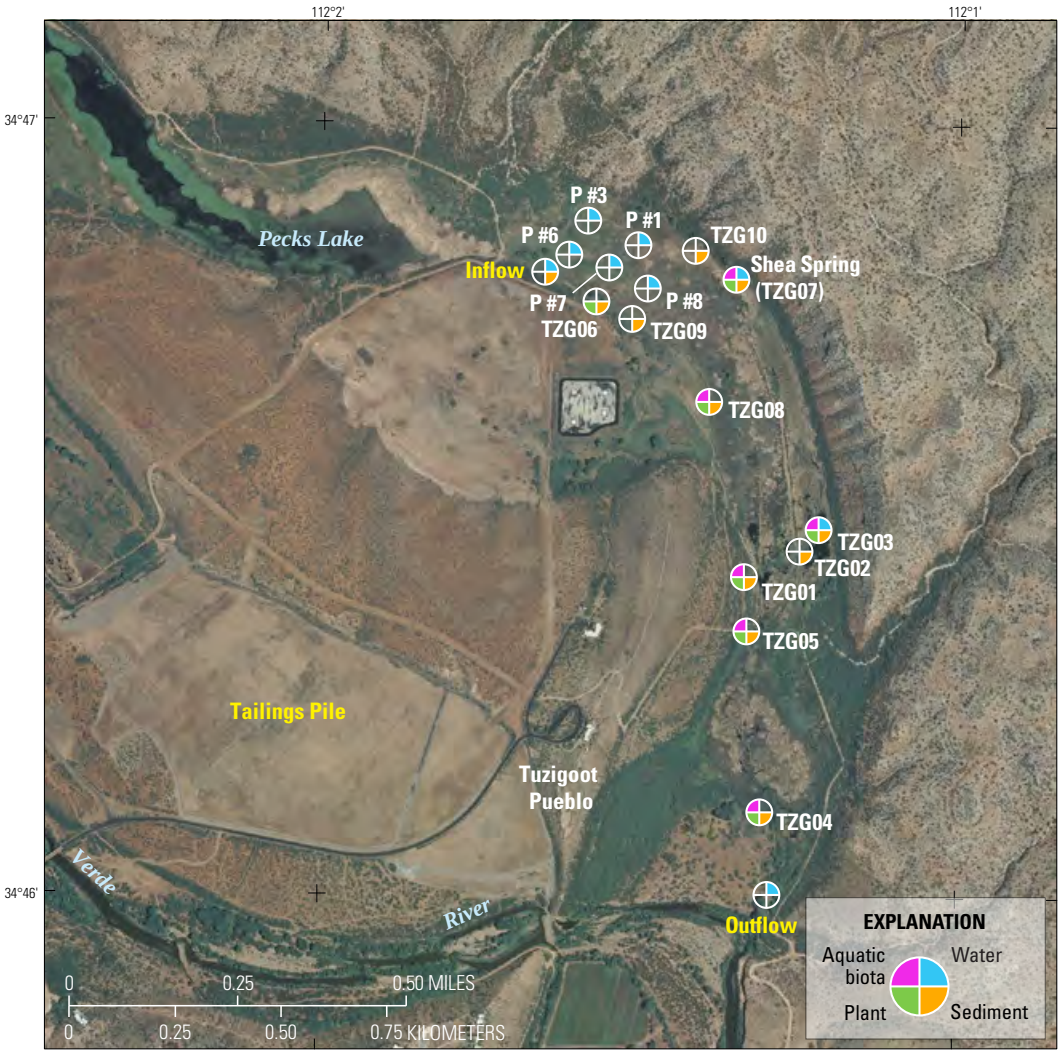

Figure 4. Map of Tavasci Marsh indicating sampling medium and locations. P# sites indicate numbered piezometer sites.

material). Dragonfly larvae were chosen as the representative macroinvertebrate for this study because of their ease of collection, mass, and predatory position in the trophic guild. Clubtail (Gomphidae) and skimmer (Libellulidae) dragonfly larvae were the only macroinvertebrate taxa abundant enough throughout the marsh for major and trace element analysis.

Several fish species were collected throughout the marsh to understand variability in metal bioaccumulation in different trophic guilds. Species collected included an insectivore, western mosquitofish (*Gambusia affinis*); insectivore-predators, yellow bullhead (*Ameiurus natalis*), green sunfish (*Lepomis cyanellus*), and bluegill (*Lepomis macrochirus*); and predator, largemouth bass (*Micropterus salmoides*). Piscivorous fish are often sampled in bioaccumulation/biomagnification studies to understand the transfer of trace metal contamination in the food chain from primary producers to top predators. The habitats sampled at each location in the marsh were different and piscivorous fish were not always present nor were the same species located at each location in the marsh. Western mosquitofish were found at all sampling locations that had fish.

A description of sample sites during the time period of collection for this project is included here to provide context for samples as the marsh may change over time; pictures of sampling sites are shown in figure 5. Numbered sites (TZG##) were named in order of sample collection, and piezometer numbers were based on numbering assignment by the NPS.

Site TZG01 is located at the western margin of the marsh north of an old road crossing and is dominated by a beaver dam and is overgrown with cattails (fig. 5*A*). Site TZG02 is located at the western end of the largest open-water part of the marsh (fig. 5*B*). Site TZG03 is located just to the east of TZG02, also in the largest open water section of the marsh (fig. 5*C*). Site TZG04 is located south of the old road crossing on the western margin of the marsh near a large cottonwood tree (fig. 5*D*). Site TZG05 is located just north of the old road crossing on the western margin of the marsh (fig. 5*E*). Site TZG06 is located at the northwestern end of the marsh in an old irrigation ditch (fig. 5*F*). Shea Spring (TZG07) is the largest and only named spring in the marsh (fig. 5*G*), though there are several unnamed seeps along the northern hillside of the marsh that were not sampled. Groundwater discharges into the bottom of a pool of

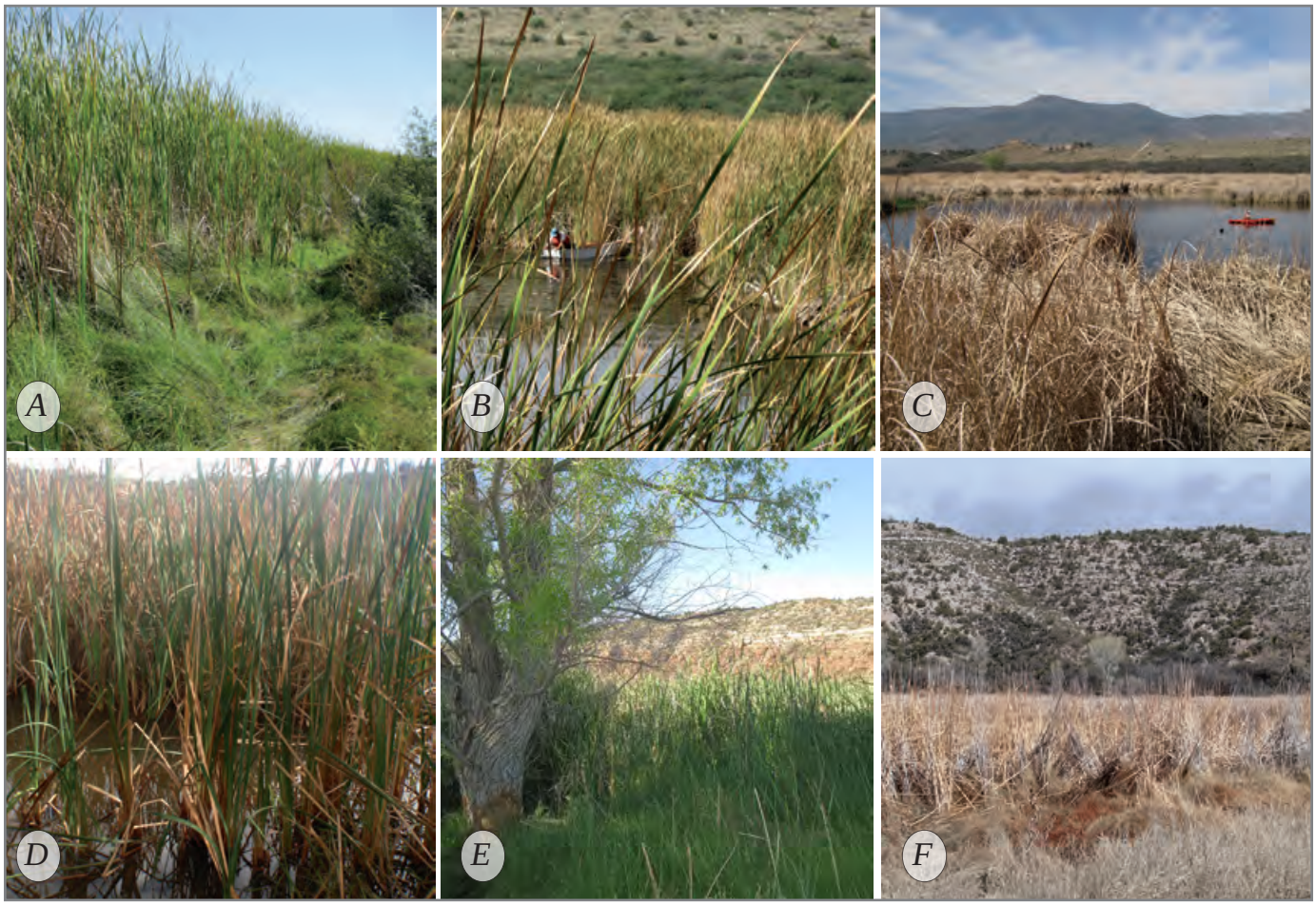

Figure 5. Photos of Tavasci Marsh sampling locations. *A*, TZG01; *B*, TZG02; *C*, TZG03; *D*, TZG04; *E*, TZG05; *F*, TZG06; *G*, Shea Spring (TZG07); *H*, TZG08; *I*, TZG09; *J*, TZG10; *K*, Inflow; *L*, Outflow; *M*, piezometer 1; *N*, piezometer 3; *O*, piezometer 6; *P*, piezometer 7; *Q*, piezometer 8; and *R*, Verde River reference; sampling locations are shown on maps in figures 1 and 5.


G
H
I
J
K
L
M
N
O
P
Q
R

water at several locations at Shea Spring, so that it looks like boiling sands (water pushes the sand up vertically in the water column). The pool is somewhat isolated from the rest of the marsh by a man-made rock wall on the western side of the pool.

Site TZG08 is located in a small open-water section midway between the old road crossing and the northwestern end of the marsh (fig. 5*H*). Site TZG09 is located just south of TZG06 near the same old irrigation ditch (fig. 5*I*). Site TZG10 is located on the northeastern margin of the marsh, on the marsh side of a footpath leading towards Shea Spring (TZG07). There was a fan of eroded sediment at TZG10 originating from the hillside surrounding the marsh (fig. 5*J*). The inflow site is located in the old irrigation ditch leading from Pecks Lake into Tavasci Marsh (fig. 5*K*). The outflow site is located just north of a footbridge for a trail starting from a road in Dead Horse Ranch State Park (fig. 5*L*). The outflow site is a channelized flow of water entrenched between two deeply incised dirt banks.

All of the piezometer sites were installed by the staff of Tuzigoot National Monument during the summer of 2010 and have 2-inch-diameter white PVC pipes with drilled holes on both sides of the pipe below the land surface. Piezometer 1 is located in the marsh just off of the footpath towards Shea Spring (fig. 5*M*). There was standing water and thick cattails around the pipe in October 2011. Piezometer 3 is the northernmost piezometer located in an open field with grasses and no standing water (fig. 5*N*). Piezometer 6 is located southwest of piezometer 3 in the same open field of grasses, but there was a slight amount of standing water during some of the site visits—where we stepped on the ground, the water would pool around our feet (fig. 5*O*). Piezometer 7 is southeast of Piezometer 6, just past a lateral irrigation ditch in an open field of grasses surrounded by cattails (fig. 5*P*). Piezometer 8 is southeast of piezometer 7 and in a similar physical setting as piezometer 7 (fig. 5*Q*).

The Verde reference site is located upstream on the Verde River north of Tavasci Marsh. Samples were collected from the eastern margin of the river in water pooled to the side of the main stream channel where cattails and watermilfoil were growing (fig. 5*R*).

Field Procedures

Water

Water quality parameters including temperature, pH, specific conductance, and dissolved oxygen were measured at each water-sampling site using a Troll-9500 multiparameter meter. The meter was calibrated daily before field measurements using standards supplied by the USGS National Water Quality Laboratory. The temperature probe on the multiparameter meter was checked annually against a National Institute of Standards and Technology (NIST) certified thermometer and found to be within ± 0.1 ˚C. Alkalinity titrations were performed in the field following sample collection using the incremental equivalence method. Blind measurements of sample alkalinity, pH, and specific conductance were made by project staff annually as part of a USGS National Field Quality Assurance program (NFQA) and were within acceptable limits each year of sample collection. Discharge at Tavasci Marsh outflow was measured using a FlowTracker using the midpoint method (Turnipseed and Sauer, 2010).

Samples were collected and processed in accordance with the USGS National Field Manual (U.S. Geological Survey, variously dated). Surface water samples were collected using a cleaned 3-liter Teflon sample bottle that was submerged at the sample site, rinsed once, and then filled to the shoulder. Groundwater samples were collected using clean silicon flexible tubing connected to a peristaltic pump from shallow 2-inch diameter PVC piezometers. Both surface-water and groundwater samples were filtered in a chamber bag using a 0.45-µm capsule filter, which was preconditioned with 2 L of deionized water, and analyzed for major ions, nutrients, and trace elements. Dissolved organic carbon (DOC) samples were filtered through a baked glass fiber filter in a cleaned Teflon apparatus. Sample bottles for cations, metal, and trace element analyses were acidified to pH<2 using ultra-pure nitric acid, and DOC samples were acidified using ultra-pure sulfuric acid immediately following filtering. All samples were kept chilled until they arrived at the laboratory.

Water for mercury and methylmercury analyses was collected as unfiltered samples in precleaned bottles provided by the USGS Wisconsin Mercury Laboratory. Bottles were rinsed three times with sample water before collection for surface water and groundwater. Samples were acidified in a chamber bag following sample collection using ultra-pure hydrochloric acid supplied by the USGS Wisconsin Mercury Laboratory.

A dissolved gas sample was collected at Shea Spring (TZG07) in two 3/8-inch-diameter copper tubes that were sealed with stainless-steel pinch-off clamps (Stute and Schlosser, 2000). There was some upward head pressure from the water discharging at Shea Spring, but not enough to push the water through the sample tube, so a peristaltic pump was placed at the downstream end of the Tygon tubing at the end of the copper tube and used to slowly pull the water through the copper tube before sealing.

Figure 5. Tavasci Marsh sampling location pictures. *A*, TZG01; *B*, TZG02; *C*, TZG03; *D*, TZG04; *E*, TZG05; *F*, TZG06; *G*, Shea Spring (TZG07); *H*, TZG08; *I*, TZG09; *J*, TZG10; *K*, Inflow; *L*, Outflow; *M*, piezometer 1; *N*, piezometer 3; *O*, piezometer 6; *P*, piezometer 7; *Q*, piezometer 8; and *R*, Verde River reference; sampling locations are shown on maps in figures 1 and 5.—Continued

Sediment

All sediment samples were collected in a manner consistent with established procedures that are intended to minimize potential for contamination, including utilizing clean gloves, clean plastic sampling equipment, and clean containers (Shelton and Capel, 1994). During the October 2010 sampling, seven sediment samples associated with each cattail root sample at sites TZG01, -03, -04, -05, -06, -08 and Shea Spring (TZG07) (fig. 4) were collected using clean nitrile gloves and stored in a clean plastic bag. During the April 2012 sampling, three sediment samples were collected from the shallow sediment under the ponded water at sites TZG03, -08, and inflow (fig. 4) in a clean plastic bag. In October 2012, surface sediment was collected from the Verde reference site in association with the cattail root samples. All surface sediment sites had ponded water present above the sediment that was collected. The sediment was wet sieved with native water at the sample site using a cleaned nylon 63-µm mesh (Shelton and Capel, 1994). An additional sediment sample was collected in October 2010 at TZG01, but was not sieved.

Three sediment cores were collected using a slide-hammer-mounted plastic core tube device in October 2010 at sites TZG02, -03, and -04 (fig. 4). Three additional cores were collected in April 2011 at sites TZG08, -09, and -10 (fig. 4) using a modified Hargis corer, a razor-edged piston corer (7.6 cm in diameter) that minimizes soil compaction and allows for cutting through plant material (Hargis and Twilley, 1994). TZG10 was the only core collected from dry surface sediments, and TZG09 was collected from wet surface sediments surrounded by cattails, while all of the others were collected below at least a foot of ponded water. Cores were extruded vertically with a plastic pusher placed at the bottom of the core and pushed upwards, while spacers of known thickness were placed at the top of the core for sectioning. Extruded core intervals were sliced off using a plastic drywall knife. Extrusion rings and cutters were cleaned with 0.2-percent Liqui-nox soap solution, tap water, and then deionized water after each sampling interval. Total core lengths are given in table 2. Cores were sectioned in 2-cm intervals for the entire length of the cores at sites TZG02, -03, -08, and -10. The core at TZG04 was sectioned in 2-cm increments from the top down to 20 cm depth then in 3-cm increments from 20 cm to the bottom of the core. The core at TZG09 was sectioned in 2 cm increments from the top to 14 cm depth and then in 3-cm increments to the bottom of the core.

Table 2. Sediment core sampling dates and lengths, Tuzigoot National Monument, Arizona.

[Site locations are shown in figure 4]

Core site	Sample date	Core length (cm)
TZG02	10/20/2010	24
TZG03	10/20/2010	28
TZG04	10/21/2010	58
TZG08	04/20/2011	23
TZG09	04/19/2011	35
TZG10	04/19/2011	22

Plants

Cattail samples were collected at seven sites (TZG01, -03, -04, -05, -06, -08, and Shea Spring [TZG07]) throughout Tavasci Marsh during October 2010 and resampled at three of the seven sites (TZG01, -06, -07) in April 2011 (fig. 4). At each site, ten cattails with independent rhizome and shoot base were collected by pulling the plant from the sediment. Two leaves from each of the ten plants were cut with stainless steel scissors, rinsed with deionized (DI) water, and composited. Roots were cut from the rhizomes, rinsed with DI water, and composited. The primary aerial shoot or emerging-shoot sprout was cut and composited. Leaf and root samples were cut into small sections then cleaned separately through a series of tap water rinses followed by three DI-water rinses to ensure removal of atmospheric deposition of dust on leaves and sediment from roots. Composite samples were frozen until subsamples could be freeze dried.

In addition to cattail samples, one submerged aquatic macrophyte sample of watermilfoil was collected at TZG03 in October 2010 and resampled in April 2011. The watermilfoil samples consisted of a grab sample of material growing through the water column above the sediment-water interface. The samples were cleaned and processed by the same method as the cattail samples.

Dragonfly Larvae and Fish

Dragonfly larvae were collected using D-frame kick nets and seine nets. An average of 30 individuals was composited per sample site to obtain the needed mass. Because the objective was to measure the environmental concentrations that may realistically be consumed by fish and avian wildlife, samples were not depurated. Following collection, larvae were rinsed with DI water to remove sediment, composited in precleaned Teflon containers provided by the USGS Wisconsin Mercury Laboratory, and then frozen.

Mosquitofish were collected using a seine net at TZG03, -04, -05, and -07. Mosquitofish were composited (average of 20 individuals) into one sample to obtain the needed mass. Largemouth bass, green sunfish, and bluegill were collected using a gill net at TZG03. Yellow bullheads were collected using a LR-24 Smith-Root backpack electrofisher at Shea Spring (TZG07). All fish were measured, rinsed with DI water, placed in clean plastic bags provided by the USGS Wisconsin Mercury Laboratory, and then frozen.

Laboratory Methods

Water

Water samples were analyzed for major ions, trace elements, nutrients, and dissolved organic carbon (DOC) at the USGS National Water Quality Laboratory using methods described in Brenton and Arnett (1993), Fishman (1993), Fishman and Friedman (1989), Garbarino and others (2006), and Patton and Kryskalla (2011). Mercury and methylmercury were analyzed at the USGS Wisconsin Mercury Laboratory using EPA Method 1631, Rev. E for mercury and methods described in DeWild and others (2001) for methylmercury. Stable isotope ratios ($\delta^{18}O$ and $\delta^{2}H$) were measured at the USGS Reston Stable Isotope Laboratory (following methods by Révész and Coplen, 2008a, b) and isotopic ratios are reported relative to Vienna Standard Mean Ocean Water. Radium-226 was analyzed at Eberline Analytical Laboratories in Richmond, Calif. Tritium, $\delta^{13}C$, and ^{14}C were analyzed at the University of Arizona Accelerator Mass Spectrometry Laboratory. Dissolved gas samples were analyzed at the USGS Noble Gas Laboratory using standard methods of gas separation and quadrupole and magnetic sector mass spectrometers (Manning, 2009). Detection limits are presented in appendix A, table 1.

Sediment

All sediment samples were freeze dried prior to analysis. Sediment samples were analyzed at the USGS Central Region Mineral Resources Laboratory for major and trace elements following digestion using hydrochloric, nitric, perchloric, and hydrofluoric acids at low temperature by inductively coupled plasma-atomic emission spectrometry (ICP-AES) and inductively coupled plasma-mass spectrometry (ICP-MS). Calibration on the ICP-AES was performed by standardizing with digested rock reference materials and a series of multielement solution standards. The ICP-MS was calibrated with aqueous standards, and internal standards were used to compensate for matrix affects and internal drifts. Data was deemed acceptable if recovery for all 42 elements was ±15 percent at five times the lower limit of determination (U.S. Geological Survey, 2013a).

Total carbon and carbonate carbon were measured for every sediment sample, and the difference between total carbon and carbonate carbon was used to calculate organic carbon. Total carbon was analyzed using an automated carbon analyzer, where a weighted sample is combusted in an oxygen atmosphere at 1370 °C to oxidize carbon to carbon dioxide. Moisture and dust are removed and the carbon dioxide is measured by a solid-state infrared detector. Carbonate carbon is determined as carbon dioxide by coulometric titration. The sample is treated with hot 2N perchloric acid and the evolved carbon dioxide is passed into a cell containing a solution of monoethanolamine. The carbon dioxide, quantitatively absorbed by the monoethanolamine, is coulometrically titrated using platinum and silver/potassium-iodide electrodes (U.S. Geological Survey, 2013a).

Selenium was determined following digestion using a mixture of nitric, hydrofluoric, and perchloric acids and heating using hydride generation atomic absorption spectrometry (U.S. Geological Survey, 2013a). Mercury was determined following digestion using nitric and hydrochloric acids using a FIMS-100 cold-vapor atomic absorption mercury analyzer (U.S. Geological Survey, 2013a). A separate subsample of some sediment core samples were also analyzed for Hg and methylmercury at the USGS Wisconsin Mercury Laboratory using the methods described in Olund and others (2005) and DeWild and others (2005). Detection limits are presented in appendix B, table 1.

Radioisotope Analysis

A split of each freeze-dried sediment core section was analyzed by the USGS National Research Program in Menlo Park, Calif., for age dating of the sediment core using ambient levels of naturally occurring and bomb-fallout radioisotopes (^{210}Pb, ^{226}Ra, and ^{137}Cs). Freeze-dried sediment was ground to a powder, and then packed into counting vials to obtain constant geometry among samples. Water content of sediments was determined by weight loss during freeze drying. Sediment bulk density (grams dry sediment per cubic centimeter) was estimated from the geometric volume of the coring device assuming complete recovery of sediment during subsectioning of the core. Some water and sediment material may have been lost from the top few intervals of TZG02, -03, and -04 because of very high porosity.

Radioisotope activities were measured simultaneously by gamma spectrometry based on previously published methods (Van Metre and others, 2004; Fuller and others, 1999). The supported ^{210}Pb activity, defined by its long-lived progenitor, ^{226}Ra, was determined for each core interval from the 352-KeV and 609-KeV gamma-emission lines of ^{214}Pb and ^{214}Bi (daughters of ^{226}Ra), respectively. Self-absorption of the gamma emission lines by the sample matrix was corrected using an attenuation factor for each counting container calculated with an empirical relationship between self absorption and bulk density developed for this geometry based on the method of Cutshall and others (1983).

Age dating was accomplished by identifying the earliest layer of unsupported ^{210}Pb and then analyzing each progressively shallower layer to determine age and the rate of accretion using established models of sediment accumulation (Van Metre and others, 2004). Sediment deposited after 1952 is identified by the peak in ^{137}Cs, which is derived from atmospheric fallout from above-ground nuclear weapons testing in the 1950s and first half of the 1960s. The first occurrence is commonly assigned a date of 1952, with maximum deposition occurring in 1963 and 1964. Atmospheric fallout decreased after that period with no measurable fallout detected after 1976 (Callender and Robbins, 1993).

The dry sediment mass (in g/cm^2) of each core interval was calculated from the dry mass recovered, the interval geometric volume and interval thickness. The interval dry mass (g/cm^2) was summed over the length of the core from the surface downward to obtain the cumulative sediment mass with depth. For cores TZG02 and TZG03, the constant rate of supply (CRS) sedimentation model was used to determine sediment mass accumulation rates, MAR, which is given in dry g/cm^2/yr (Van Metre and others, 2004, and references within). The unsupported ^{210}Pb versus cumulative mass is used instead of depth to account for compaction. Activity of unsupported ^{210}Pb decreases exponentially over time according to its decay rate (half-life 22.3 years) in a system with constant sediment accumulation. Unsupported ^{210}Pb results from emanation of ^{222}Rn gas from continental land masses, decay in the atmosphere to ^{210}Pb, and subsequent deposition onto the marsh surface and the watershed, where it is adsorbed to sediment particles.

Particle Size and Color Analysis

Sediment core sections were analyzed for particle size distribution using a dry sieve method. Sieve sizes were chosen to cover full phi breaks in the sand size range down to the sand/silt and clay break, which were most applicable to the majority of the samples. The deepest four core sections from core TZG08 contained larger particles that were less than 16 mm but greater than 0.5 mm and those particles were sorted through sieves in the gravel size range. Table 3 presents the particle size breaks used to characterize the sediment cores.

Grain size distribution was measured using the remains of the freeze-dried core sections that were not needed for chemical analysis. If sufficient material was available, then 50 g of sediment was utilized per core section; the minimum amount of sediment used for grain-size analysis was 12 g. The sieves were stacked in order of decreasing particle size and placed in a sieve shaker for 5 minutes. Following the agitation, the material left on each sieve and in the bottom pan was weighed; the incremental weights were summed to obtain the percent of material finer than each sieve break (appendix B, table 4).

Sediment color was determined for all core sections using the Munsell Soil Color Book (Munsell Color, 2009). Color was determined on dry sediment with indoor lighting.

Table 3. Particle size analysis distribution breakdown.

[Particle name refers to anything larger than the given sieve size and less than the next largest sieve size. Particles larger than 0.5 mm were only found in the lowest 4 core sections from TZG08]

Phi units	Particle name (Wentworth class)	Sieve size (mm)	Standard mesh (US)
-4	Coarse gravel	16	5/8”
-3	Medium gravel	8	5/16”
-1	Very fine gravel	2	10
1	Coarse sand	0.5	35
2	Medium sand	0.250	60
3	Fine sand	0.125	120
4	Very fine sand	0.0625	230

Periphyton-Diatom Analysis

A split from eight freeze dried core sections from TZG04 were sent to EcoAnalysts, Inc., for periphyton taxonomic identification and enumeration. Periphyton is sensitive to changes in water chemistry and serves as a useful indicator of water quality. Changes in community structure can be used to assess past ecological conditions and provide information regarding limnologic changes through time.

Plant

Plant samples were freeze dried then homogenized in a blender with stainless steel blades that was cleaned between each sample. All freeze-dried samples were ashed and analyzed by the USGS Central Region Mineral Resources Laboratory by the same procedures and for the same elements as the sediment samples.

Some samples were split prior to ashing and analyzed for selenium, mercury, and methylmercury. Selenium was analyzed using the same laboratory procedure as the sediment samples. Mercury and methylmercury were analyzed by the USGS Wisconsin Mercury Laboratory using a sulphuric- and nitric-acid digestion for total mercury and a nitric-acid digestion for methylmercury (DeWild and others, 2001). Detection limits are the same as the sediment samples presented in appendix B, table 1 and apply to values before ash correction.

Dragonfly Larvae and Fish

Larvae were not depurated and were sent in whole for analysis, in order to understand the total metals available to species eating the larvae. All fish were sent in for analysis whole with the exception of one largemouth bass that was sent as a fillet.

Dragonfly larvae and fish samples were freeze-dried and homogenized by the USGS Wisconsin Mercury Laboratory using ultra clean procedures. Percent moisture was determined as the difference in weight before and after freeze drying. Following processing, the samples were analyzed for total mercury and a subset was also analyzed for methylmercury using a sulphuric and nitric acid digestion for total mercury and a nitric acid digestion for methyl mercury (DeWild and others, 2001).

After mercury analysis, samples were sent to the USGS Central Region Mineral Resources Laboratory for major and trace element analysis. Freeze-dried samples were digested using 4 mL of double-distilled HNO_3 and 2 mL of ultrapure H_2O_2 in a microwave digestion system. The samples were allowed to sit in the digestion vessels until they cooled to

room temperature. The resulting clear sample solutions were quantitatively transferred to 50-mL polypropylene centrifuge tubes and diluted to 15 mL, using the scribed volume marks on the tubes, with deionized water (Wolf and others, 2009). The final sample solutions contained approximately 20 percent by volume nitric acid and were directly analyzed by ICP-MS using the 42 element method described in Briggs and Meier (2002). Detection limits for fish and larval samples are presented in appendix D, table 1.

Organic Material

A split of the water filtered for DOC analyses was submitted to the University of Colorado Dissolved Organic Matter Laboratory for spectroscopic characterization of the dissolved organic matter (DOM) in the sample.

The fulvic acid fraction of organic material was extracted from the splits of 37 freeze-dried core sections (evenly distributed throughout the depth of each core) at the University of Colorado Dissolved Organic Matter Laboratory using two wet chemical methods (Wolfe and others, 2002). The first method, which was used to extract organic material from the cores collected at sites TZG02, -03, and -04, is a less time-consuming method in which the core sections were agitated for 24 hours in 1.0 N tetrasodium pyrophosphate, $Na_4P_2O_7$ (ratio of 1 mg sediment core to 1 ml $Na_4P_2O_7$), and the solution was then filtered through a 0.7 µm GF/F-grade glass-fiber filter. Following spectroscopic analyses of the extracts from these cores, it was determined that values were lower than expected and a more time-consuming and chemically aggressive technique (modified from Schnitzer, 1982) for extraction of the fulvic acid organic material was needed. In this method, which was used to extract organic material from the cores collected at TZG08, -09, and 10, core sections were agitated for 24 hours in 0.5 N NaOH (solid to liquid extraction ratio of 1:10 by volume) under N_2. Following extraction the samples were acidified to pH 1.0 with 6.0 M HCl and centrifuged. The filtrates (for samples extracted using the first method) and supernatants (for samples extracted using the second method) were diluted with deionized water such that the dissolved organic carbon (DOC) concentration of the solutions was between 1 and 3 mg/L. Samples were stored in the dark at 4 °C for less than 1 week prior to analysis by absorbance and fluorescence.

To investigate differences in DOM characteristics among plant types, DOM was leached from dried plant material. Subsets of the plant material were cleaned as described above and then dried at 100 °C for 12 hours. Additionally, to investigate the potential for detection of a DOM signature in the sediment core data that may be indicative of historical burning of the marsh, a subset of the dried green cattail leaves collected in October 2010 were burned prior to leaching. Approximately 25 g of dried green leaves, 25 g (preburning mass) of burned green leaves, and 10–15 g of root material from cattails collected at sites TZG03, -04, -06, and -07 in October 2010 were leached in 750 mL of deionized water in the dark for 164 days (approximate water residence time in the marsh calculated using volume of water in marsh and discharge at the outflow site). We collected 15 g of dried cattail shoot material and 25 g of dried watermilfoil at TZG03 in October 2010, as well as approximately 25 g of dried brown cattail leaves from TZG01, -06, and -07 in April 2011, and all these samples were also leached by the same methodology. Leachates were filtered through 0.7 µm GF/F-grade glass fiber filters and analyzed by absorbance and fluorescence.

Organic matter was measured in surface water samples, groundwater samples, sediment extracts, and plant leachates by collecting spectra of absorbance and three-dimensional fluorescence at the University of Colorado Dissolved Organic Matter Laboratory. Absorbance scans were collected from 190 to 1,100 nm at 1-nm increments using a 1-cm pathlength quartz cuvette on an Agilent 8453 UV-Visible spectrophotometer. To avoid inner-filter effects, all samples were diluted such that the absorbance at 254 nm was less than 0.1 prior to fluorescence analysis (Ohno, 2002; Miller and others, 2010) on a Fluoromax-4 fluorometer. The effectiveness of the instrument-specific fluorescence emission correction file in removing instrument bias was verified by comparison of quinine sulfate emissions scans collected and instrument-corrected monthly with NIST reference spectra for quinine sulfate. Lamp scans, cuvette checks, and water Raman scans were collected daily to ensure stable instrument function. Three dimensional fluorescence sample and blank scans were collected over an excitation range of 240–450 nm, at a 10 nm interval, and an emission range of 300–600 nm, at a 2-nm interval in a 1 cm path length quartz cuvette. Scans were collected in ratio (S/R) mode and bandwidth was 5 nm for both excitation and emission. Fluorescence spectra were corrected using Mathworks Matlab software following the methods of Cory and others (2010). Blanks, samples, and Raman spectra of water were instrument-corrected with the instrument-specific excitation and emission correction files, samples were inner-filter corrected (McKnight and others, 2001), samples and blanks were normalized to the area under the water Raman curve, and samples were blank subtracted.

Specific ultraviolet absorbance at 254 nm (SUVA-254) was calculated as the ratio of the decadic absorption coefficient at 254 nm to the DOC concentration (Weishaar and others, 2003) for surface water and groundwater samples. SUVA-254 values generally range from zero to six in natural waters, with higher values being indicative of more aromatic carbon and lower values being indicative of less aromatic carbon. Fluorescence index (FI) values were calculated as the ratio of the fluorescence intensity at an emission of 470 nm to the intensity at 520 nm at an excitation wavelength of 370 nm (McKnight and others, 2001; Cory and others, 2010) for surface-water samples, groundwater samples, sediment core extracts, and plant leachates. FI values in natural waters generally range from 1.2 to 1.8, with higher values being indicative of more microbially derived DOM and lower values being indicative of more terrestrially-derived or higher plant-derived DOM.

Quality Assurance

Water samples are supported by blank and replicate analyses. Solid samples (sediment, plant, dragonfly larvae, and fish) are supported primarily by replicate sample analyses and standard reference materials. Relative percent difference (RPD) was used to evaluate variability in replicate pairs using

$$RPD = \frac{C_e - C_r}{\left(\frac{C_e + C_r}{2}\right)} \times 100 \quad (1)$$

where C_e is concentration of the environmental sample; and

C_r is concentration of the replicate sample.

If more than three replicate pairs were available for a sample medium, a median RPD was calculated for each element analyzed. Sediment core replicates were analyzed by a more robust statistical analysis to quantify variability, as there were 11 replicate pairs available for most elements and 46 replicate pairs for total and carbonate carbon.

Water

Field blank samples were collected during the October 2010 and October 2011 field visits for analysis of major ion, trace element, mercury, nutrient, radioisotope, and dissolved organic material using certified inorganic and organic blank water supplied by the USGS National Water Quality Laboratory and mercury-free blank water from the USGS Wisconsin Mercury Laboratory. Detections of DOC in blank samples during October 2010 and April 2011 were less than the laboratory reporting level but greater than the long term laboratory detection level and both blank detections were less than the DOC concentration in the blank sample from October 2011 which was reported as <0.23 mg/L. The low level detections of DOC in the blanks are much lower than the most of the DOC concentrations in the samples collected, with the exception of Shea Spring (TZG07). DOC concentrations at Shea Spring (TZG07) were all above the laboratory reporting limit and ranged between 0.30 and 0.48 mg/L. Bias in the blank sample concentrations is not quantifiable given the limited amount of data available, but because the blanks were all below the laboratory reporting limit and the environmental samples were all above the laboratory reporting limit, there appears to be a distinct difference between the Shea Spring (TZG07) and blank samples.

In the blank sample collected during October 2010, there was a low level detection of total Hg (0.04 ng/L), which is also the laboratory reporting limit. The next blank sample collected in October 2011 was below the detection limit for total Hg. The October 2010 detection was 6 percent of the lowest environmental sample (0.64 ng/L) from Shea Spring (TZG07) during the same sampling trip, which does not indicate significant sample contamination. There was a low level detection of Ca (0.079 mg/L) from the blank sample collected during October 2011. The Ca detection was 0.2 percent of the lowest Ca value among the environmental samples (36.1 mg/L), therefore Ca concentrations in the environmental samples are not likely to be biased due to contamination. Low concentrations of ^{226}Ra were detected in both blank samples (0.056 and 0.022 pCi/L), but the inorganic blank water used was not certified for radioisotopes. Blank sample results are presented in appendix A, table 7.

Sequential replicate samples were collected during the April 2011 and April 2012 field visits for measurement of major ions, trace elements, mercury, nutrients, stable isotopes, radioisotopes, DOC, absorbance at 254 nm, and florescence index. Surface water replicate samples from April 2011 were collected as a second grab sample from site TZG03 immediately following the environmental sample. Groundwater replicate sample from April 2012 was collected from piezometer 6. Replicate sample results are presented in appendix A, table 8.

Relative percent difference was used to evaluate variability in replicate pairs by analyte and the majority of the pairs were within ±20 percent. RPD values outside of that range occurred for Cl, nitrate+nitrite, Al, Cr, Ni, Sb, Se, U, V, ^{226}Ra, and absorbance at 254 nm. The aforementioned analytes were all within ±40 percent, with the exception of nitrate+nitrite (127 percent) and Cr (-149 percent). However, the concentration differences within the two pairs with larger RPDs were small; nitrate+nitrite was 0.07 mg/L different and Cr was 0.47 µg/L different between the two pairs.

Cation and anion charge balances were calculated for all water samples collected with major ion data. Charge balances for all samples were less than ±5 percent between cations and anions, with the exception of one sample at piezometer 1 (6.9 percent difference), with a majority of the samples within ±2.5 percent. Good charge balance indicates that there were no major cations or anions missing from the analysis and that the analytical values are reasonable. Charge balance is presented in appendix A, table 3.

Sediment

One surface sediment replicate from site TZG05 was analyzed for major and trace elements as a separate grab sample from the same sample container as the environmental sample. A total of ten sediment-core replicate samples with a least one replicate from each of the core locations (TZG02, -03, -04, -08, -09, and -10) were analyzed for major and trace elements in a separate lab batch after analysis of the environmental sample. Replicate pair results are presented in appendix B, tables 8 and 9. Sediment core replicates are separate subsamples of the original sample, not a split, and therefore provide a measure of the variability within a sample as well as the lab analysis variability. Replicate variability among all cores and samples was determined by calculating the standard deviation for each replicate pair and taking the average of the standard deviations. Relative standard deviation was also calculated for each replicate pair but was not more

consistent than standard deviation over the range of sample values. All Ag concentrations measured in sediment samples were less than the reporting limit of 1 ppm, so Ag variability could not be quantified.

Uncertainty at the 90-percent confidence level was calculated for each element based on the average standard deviation of replicate pairs and is presented in table 4 using

$$\text{Uncertainty} = \pm Z_{\left(1-\frac{\alpha}{2}\right)}(SD_{reps}) \quad (2)$$

where α is the level of significance (0.90);
Z is the Z-score for given level of significance (1.645); and
SD_{reps} is the average of the standard deviations of the replicate pairs.

Fifteen sediment-core samples were submitted to the USGS Wisconsin Mercury Laboratory and the USGS Central Region Mineral Resources Laboratory for analysis of total mercury and results are in appendix B, table 10. Samples were individual subsamples of the core interval and reported values may also represent variability within a core section. Sample pairs analyzed by each laboratory were compared, following the same method as the sediment replicates described above, to understand how the similarity of values from each laboratory. The range of Hg concentrations in all samples was 19.5 to 296 parts per billion (ppb) and the variability of Hg concentration between the labs was 11.4 ppb with a 90-percent confidence interval uncertainty of ±18.8 ppb.

Standard reference samples (SRS) are homogenized materials that have been analyzed at multiple laboratories to obtain a common value and distribution statistics. The analysis of SRS along with environmental samples provides an understanding of how accurate the reported laboratory values are. Two standard reference samples were obtained through the USGS Geochemical Reference Materials program; they were selected for having chemical concentrations similar to those found in the Tavasci Marsh sediment samples: Cody Shale (SCo-1) and Green River Shale (SGR-1b). These two standard reference samples were analyzed along with three different batches of Tavasci Marsh samples and results are presented with published reference sample values in appendix B, table 11.

Elements Ba, Co, Li, and Pb had all laboratory results within one standard deviation of the reported concentrations for both SCo-1 and SGR-1b (SCo-1, Smith, 1995; SGR-1b, Wilson, 2001). For all samples of SCo-1, Mo, Ni, Sr, and V were within one standard deviation of the reported concentration. For all samples of SGR-1b, As, Ce, Cu, Sb, Sc, U, and Zn were within one standard deviation of the reported concentration. The rest of the elements with reported concentrations either have no reported standard deviation or not all replicates were within one standard deviation of the reported value.

Percent recovery was calculated as the laboratory average for the three standard reference sample analyses divided by the published reported concentration of the standard reference

Table 4. Results of sediment-sample replicate variability analysis.

[Variability and uncertainty values are the same unit as sample concentration; %, percent; ppm, parts per million or milligrams per kilogram]

Element	Concentration range from Tavasci Marsh environmental sediment samples	Units	Variability	Uncertainty (90% confidence)
Total carbon (C)	2.84–25.1	%	0.55	± 0.90
Carbonate carbon (C)	<0.003–4.37	%	0.31	± 0.50
Organic carbon (C)	1.04–25	%	0.64	± 1.06
Aluminum (Al)	2–5.35	%	0.16	± 0.26
Calcium (Ca)	2.34–15.5	%	0.89	± 1.46
Iron (Fe)	1.08–2.87	%	0.07	± 0.12
Potassium (K)	0.6–1.83	%	0.07	± 0.12
Magnesium (Mg)	0.95–6.85	%	0.24	± 0.39
Sodium (Na)	0.13–0.71	%	0.01	± 0.02
Sulfur (S)	0.02–1.25	%	0.01	± 0.02
Titanium (Ti)	0.13–0.44	%	0.01	± 0.02
Arsenic (As)	8–82	ppm	3.4	± 5.59
Barium (Ba)	355–681	ppm	20.8	± 34.2
Beryllium (Be)	0.6–2	ppm	0.17	± 0.28
Bismuth (Bi)	0.22–1.96	ppm	0.05	± 0.08
Cadmium (Cd)	0.4–5.1	ppm	0.15	± 0.25
Cerium (Ce)	19–66.4	ppm	3.8	± 6.25
Cobalt (Co)	5–13.5	ppm	0.57	± 0.94
Chromium (Cr)	18–91	ppm	7.3	± 12.0
Cesium (Cs)	<5–29	ppm	1.4	± 2.30
Copper (Cu)	19.7–389	ppm	13.9	± 22.9
Gallium (Ga)	4.4–14.4	ppm	0.52	± 0.86
Indium (In)	0.05–0.38	ppm	0.02	± 0.03
Lanthanum (La)	8.7–34.4	ppm	1.9	± 3.13
Lithium (Li)	11–37	ppm	1.0	± 1.64
Manganese (Mn)	128–1550	ppm	22.4	± 36.8
Molybdenum (Mo)	0.26–4.25	ppm	0.08	± 0.13
Niobium (Nb)	4.9–29.2	ppm	1.1	± 1.81
Nickel (Ni)	13.9–38.6	ppm	1.9	± 3.13
Phosphorus (P)	340–2310	ppm	37.3	± 61.4
Lead (Pb)	17.9–93.6	ppm	4.1	± 6.74
Rubidium (Rb)	31.8–92.9	ppm	2.5	± 4.11
Antimony (Sb)	0.46–2.57	ppm	0.08	± 0.13
Scandium (Sc)	3.1–11.2	ppm	0.46	± 0.76
Tin (Sn)	1.4–8.4	ppm	0.24	± 0.39
Strontium (Sr)	152–433	ppm	10.2	± 16.8
Tellurium (Te)	<0.1–1.6	ppm	0.07	± 0.12
Thorium (Th)	3–12.7	ppm	0.41	± 0.67
Thallium (Tl)	0.2–0.5	ppm	0.01	± 0.02
Uranium (U)	1.7–7.2	ppm	0.23	± 0.38
Vanadium (V)	39–103	ppm	3.8	± 6.25
Tungsten (W)	0.3–2.3	ppm	0.09	± 0.15
Yttrium (Y)	5.2–20.6	ppm	0.78	± 1.28
Zinc (Zn)	50–308	ppm	7.8	± 12.8
Selenium (Se)	0.6–4.4	ppm	0.19	± 0.31

sample. The majority of the elements analyzed with reported values for the standard reference samples were within 80–120 percent recovery, which is considered an acceptable range for this study. Only one element, Y, had a percent recovery less than 80 percent in both SCo-1 and SGR-1b (71 and 73 percent, respectively). The percent recovery of Cr was also just outside of the acceptable range for both standard reference materials (79 percent for SCo-1 and 122 percent for SGR-1b). Two elements, As and S, had percent recoveries greater than 120 percent in SCo-1 (127 and 131 percent, respectively). Cd and Nb had recoveries over 120 percent in SGR-1b, 122 and 139 percent, respectively. One element, Ga, had 69 percent recovery in SGR-1b. The sample concentrations from this study of the elements described above may be slightly greater or less than the reported values. Further SRS analysis and determination of matrix similarities of these SRS compared with Tavasci Marsh sediments would be needed to quantify measurement errors.

For radioisotope analysis, detector efficiency for each isotope was determined from NIST traceable standards. Reference materials NIST and the International Atomic Energy Agency were used to check detector calibration. The reported uncertainty in the measured activity was calculated from the random counting error of samples and background spectra at the one-standard-deviation level was typically within ±10 percent.

Plant

Plant samples were quality assured by analyzing replicate cattail samples as a separate grab sample from the same sample bag as the environmental cattail samples. One leaf replicate at site TZG03 was collected in October 2010 and one root replicate was collected from site TZG01 in April 2011. At the Verde Reference site a replicate of both the leaf and root sample were collected.

Replicate samples provide an indication of the variability of each element due to analytical method and differences within grab samples from a composite sample. Relative percent difference (RPD) between a replicate pair was calculated for each element analyzed. For all samples, Ag was less than the laboratory reporting limit and P was greater than the instrumental range. Only one sample's replicate pair had values greater than the instrumental range for Cs, Se, Tl, Hg, and methylmercury, and these concentrations are therefore not included in the median calculation of RPD. The RPD values for the aforementioned analytes were all less than ±14 percent for the single replicate pairs. The majority of the other elements had a median RPD within ±20 percent, with the exception of Ti, As, In, Li, Nb, Pb, Sc, Sn, and W. Titanium had the greatest median RPD at -49 percent. The greatest RPD values for each element were mostly from root samples, with the exception of As, Ba, Cd, Li, Pb, Sc, and Sn, and may indicate that there is greater elemental variability in root concentrations than in leaves. Replicate sample results are presented in appendix C, table 3.

Dragonfly Larvae and Fish

Dragonfly larvae and fish samples were quality assured by collecting and analyzing replicate samples of the same species at the same location and time as the original sample. A total of four replicate dragonfly larvae and six replicate fish samples were collected and results are presented in appendix D, tables 4 and 7. Replicate samples provide an indication of the variability of each element due to analytical method and within different sample collections at the same site.

Two replicate samples of dragonfly larvae were collected at TZG03 and TZG08. The majority of elements had values less than the reporting level (and were below reporting for both replicates) except for Bi, Nb, Sn, Th, Tl, and W, and the reported value was equal to the reporting level for half of these elements (Bi, Nb, and Tl). More than half of the remaining replicate pairs were within ±20 percent RPD and the values are presented in appendix D, table D4. The replicate results indicate that there is high variability in the dragonfly larvae for many of the analyzed elements and additional samples would be needed to quantify the variations.

Four dragonfly larvae replicate samples were analyzed for Hg and two for methylmercury. The RPD of replicate samples from TZG03 and -08 were less than 10 percent and the replicate sample from TZG05 had the greatest RPDs: -21 percent for Hg and -28 percent for methylmercury (see appendix D, table 4 for full results).

Three replicate samples of fish were collected from TZG03 and Shea Spring (TZG07). Relative percent difference between the two replicates was calculated for each element. Twelve elements (Be, Bi, Ho, In, Li, Nb, Sb, Tb, Te, Th, Tm, and W) were below the instrumental reporting limit for all replicate pairs. The majority of elements with values less than the reporting level were less for both replicate pairs (except for Ag, Dy, Eu, Ge, Sn, Ta, Tb, and Yb), and the reported value was equal to the reporting level for more than half of these elements (Dy, Eu, Ge, Tb, and Yb). More than half of the replicate pairs with values above the reporting limit were less than ±20 percent RPD and the values are presented in appendix D, table 7. The replicate results indicate that there is high variability in the fish samples for many of the analyzed elements and additional samples would be needed to quantify this variability.

Six fish replicate samples were analyzed for Hg and four for methylmercury. Most replicate pairs were less than ±20 percent RPD except for the Largemouth bass at TZG03 (RPD of 33 percent for Hg and 30 percent for methylmercury) and the Yellow bullhead from October 2011 at Shea Spring, TZG07 (RPD of 29 percent for Hg and 31 percent for methylmercury) (appendix D, table 7).

Additionally, three tissue SRS were analyzed with the dragonfly larvae and fish samples: DORM-3 (fish protein), TORT-1 (lobster hepatopancreas), and DOLT-4 (dogfish liver tissue). It should be noted that all of the environmental samples for this study were analyzed during the same laboratory batch run along with the three SRS. Concentrations in SRS relative to published reference sample values, DORM-3 (National Research

Council Canada, 2008a), TORT-1 (National Research Council Canada, 1983), and DOLT-4 (National Research Council Canada, 2008b), are presented in appendix D, table 8.

Elements in the tissue standard reference samples having laboratory results within uncertainty of the reported concentrations were As, Cd, and Ni for DORM-3; Cr, Cu, Mo, and Zn for TORT-1; and Ag, As, Ni, and Se for DOLT-4 (appendix D, table 8). Percent recovery was calculated as the laboratory concentration for the SRS analyses divided by the published reported concentration of the SRS. The majority of the elements analyzed and compared to reported values for the standard reference samples were within 80–120 percent recovery, which is considered acceptable for this study. Iron recovery in DOLT-4 was 121 percent and 142percent in TORT-1. Copper recoveries were slightly greater than 120 percent for DORM-3 and DOLT-4 (127 and 124 percent, respectively). Tin recoveries were greater than 120 percent for samples DORM-3 and TORT-1 (152 and 144 percent, respectively). All other elements with percent recoveries greater than 120 percent (Ca, K, Mg, Na, Co, Mn, Ni, P, Pb, and V) were from TORT-1; K had the highest percent recovery at 154 percent (appendix D, table 8). The sample concentrations of the elements described above may be slightly greater or less than the reported values. Further SRS analysis and determination of matrix similarities of these SRS compared with Tavasci Marsh whole fish would be needed to quantify measurement errors.

Statistical Analysis and Equations

Arithmetic averages were used throughout the report, and a variety of statistical techniques were employed in data interpretation. The statistical software JMP (version 10) was used to construct boxplots for data sets of five values or more. The horizontal line within the box represents the distribution median. The ends of the box represent the 25th and 75th quantiles, and the difference between the 25th and 75th quantiles is called the interquartile range (IQR). The lines that extend from each end are whiskers, from the ends of the box to the outermost data point that falls within the distances computed as follows: 1st quartile - 1.5*(IQR) 3rd quartile + 1.5*(IQR) (SAS, 2007). If the data points do not reach the computed ranges, then the whiskers are determined by the upper and lower data point values (not including outliers).

Correlation statistics were determined in JMP. The Kendall's tau correlation test, a nonparametric test that measures the monotonic dependence of predicted variables, is a common method for trend-testing in hydrology (see, for example, Helsel and Hirsch, 2002). The main advantages of using Kendall's tau are that the distribution of this statistic has slightly better statistical properties than a Spearman's rho, and there is a direct interpretation in terms of probabilities of observing concordant and discordant pairs (Helsel, 2005). The test statistic makes no assumptions about the normality of the data distribution. Further, the Kendall's tau (τ_b) correlation test was used because the procedure makes more efficient use of tie situations.

Chemical data are often below a threshold where the analytical capabilities are unable to detect a compound or the laboratory uncertainty is too high. These data are referred to as censored data and typically reported as less than a threshold that represents a minimum concentration that the laboratory deems statistically valid for that constituent. Censored data must be treated differently than measured values and a common approach is to substitute the censoring threshold with half the censoring threshold or zero. These substitution procedures will bias the statistics and produce false conclusions (Helsel, 2005).

ProUCL for Environmental Applications for Data Sets with and without Non Detect Observations (version 5.0.00; U.S. Environmental Protection Agency, 2013c) was used to analyze censored data. A Kaplan-Meier estimator was used for computing the general statistics and boxplots for trace element concentrations that were below one or more laboratory reporting limits. By this method, quantiles can be calculated to incorporate the concentrations that are below the reporting limit, rather than allowing the substitutions for less-than values used in other analysis techniques to carry undue weight in the distribution descriptive statistics. Typically this estimator is used in survival functions for lifetime data, but it is well suited to compute descriptive statistics for censored chemical data. There is no assumption of a distribution and no substitution is used in the analysis (for example, the reporting limit or half the reporting limit; Helsel, 2005).

Nonmetric multidimensional scaling (NMS) ordination in PRIMER v. 6 software was used to examine patterns in periphyton community structure (Clarke and Gorley, 2006). NMS is a non-parametric multivariate ordination technique that uses ranks of the sample similarities to build a graphical representation of sample patterns in a specified number of dimensions. Unlike other ordination methods, NMS preserves relative distance in multivariate space by retaining the rank order of among-sample similarities (for example, units are arbitrary) (Clarke, 1993). Interpretation of a NMS plot in two-dimensional space, therefore, is relatively straightforward; samples close in proximity are more similar than those located farther apart. The starting point for any multivariate ordination is the similarity or distance matrix selected to represent the sample similarity. This is computed from the correlation or resemblance between every pair of sample data (square array, with row by column) to build a relational matrix (triangular matrix). For example, the assemblage (number of different taxa and their abundance) at one location is compared to the assemblage collected at another location. This sample comparison process is continued for each site assemblage.

A fourth-root transformation (similar to a logarithm transformation) was used to normalize the data distribution before calculating the Bray-Curtis similarity matrix. A Bray-Curtis similarity matrix is a resemblance matrix well suited for examining these data because of the flexibility to include nondetects into the matrix. A Bray-Curtis similarity matrix is most commonly used with species abundance data sets because of the frequent absence (zero count) of species

between samples. NMS analysis was performed on the Bray-Curtis similarity matrix and plotted in two-dimensional space to reduce misinterpretation of multivariate patterns. A measure of stress is provided from the NMS analysis as a diagnostic to determine how well the data are represented by the NMS ordination. Lower stress values are desired and stress values below 0.20 generally indicate that the NMS ordination is providing an accurate representation of the data in multivariate space.

A seriation-trajectory was overlaid on the NMS ordination to show the change in assemblage through the sediment core. The RELATE function in the PRIMER-E software is a nonparametric seriation procedure that was used to test for the statistical significance of the temporal changes in biotic assemblages at each site. A Spearman's rho correlation coefficient was used assess the strength and significance of trend.

Principal components analysis (PCA) was used to visualize trace metal concentrations for the nine elements of interest in all solid sample media collected in the marsh. Multiple samples for a given site were first averaged and then data were normalized (subtracting the mean and dividing by the variance) for computing a Euclidean distance matrix, which is implicit matrix underlying a PCA analysis (Clarke and Warwick, 2001). PCA generates linear combinations of variables that are represented with principal component vectors. The first principal component (PC1) accounts for the greatest proportion of variance (minimizes the sum of squares) in the data and each successive orthogonal component accounts for next greatest proportion of the variance. Contributions from the variables are expressed as loadings where the highest loadings (greatest) are interpreted as the most significant. Directionality of the loadings (±) is also interpretable, indicating increasing or decreasing variable values.

An empirical relationship based on stable isotopic ratios of ^{18}O and ^{2}H in precipitation of the Verde River watershed was developed by Blasch and others, 2006. The equations have been modified to solve for elevation based on isotopic signature.

$$z = -200\delta^{2}H - 8919 \quad (3)$$

$$z = -1428.6\delta^{18}O - 8589 \quad (4)$$

where z is the elevation of precipitation in feet;
$\delta^{2}H$ is the hydrogen isotopic ratio of the water; and
$\delta^{18}O$ is the oxygen isotopic ratio of the water.

The following equation was used to calculate the relative contribution from the two distinct water sources (Shea Spring [TZG07] and shallow groundwater at the north end of Tavasci Marsh) to the TZG03 and outflow sites using stable isotopic ratios of hydrogen ($\delta^{2}H$) and oxygen ($\delta^{18}O$). This approach assumes that the only sources of water contributing to the TZG03 and the outflow sites are from Shea Spring (TZG07) and shallow groundwater measured at piezometer 6. While this is likely an oversimplification of the system, it provides some initial insight into the relative amounts of water from each source.

$$\delta_{sample} = \chi\delta_{Shea\ Spring} + (1-\chi)\delta_{Piez\ 6} \quad (5)$$

where δ the hydrogen ($\delta^{2}H$) or oxygen ($\delta^{18}O$) isotopic ratio of the water; and
χ proportion of the sample originating from Shea Spring (TZG07) water (equation modified from Clark and Fritz, 1997).

Concentrations of DOC predicted to occur under conditions of conservative transport were calculated using the average of the calculated proportions of water estimated to be contributing to the TZG03 and outflow sites from Shea Spring (TZG07) and piezometer 6 on each date (average estimates were based on $\delta^{2}H$ and $\delta^{18}O$ values; see equation 5). Specifically, on each of the four sampling dates the DOC concentrations expected to occur in the absence of production or removal of DOC at the TZG03 and outflow sites were calculated as:

$$DOC_i = \chi_i DOC_{Shea\ Spring} + (1-\chi_i)DOC_{Piez\ 6} \quad (6)$$

where DOC_i is the conservative estimate of DOC concentration at site *i* (TZG03 or outflow); and
χ_i is the proportion of the sample originating from Shea Spring (TZG07) at site *i* calculated as the average of the estimates based on $\delta^{2}H$ and $\delta^{18}O$ values from equation 5.

Isotopic values of ^{14}C and $\delta^{13}C$ were used to calculate a relative age for water from the time of recharge as precipitation to discharge in Tavasci Marsh. Uncorrected age of the water assumes that the ^{14}C value is only dependent on radioactive decay using the following equation with a Libby half-life of 5,568 years.

$$t = -8033 \times \ln\left(\frac{A_w}{A_o}\right) \quad (7)$$

where t is the age of the water sample in years;
A_w is the ^{14}C value of the water sample in percent modern carbon (pmc); and
A_o is the ^{14}C value of the original recharge water (100 pmc).

Corrected age of the water was calculated using ^{14}C, $\delta^{13}C$, pH, and alkalinity, and accounts for water interacting with soil CO_2 gas and carbonate rock. Several equations exist

for calculating a corrected age and two are used in this report for comparison. The first is the Ingerson and Pearson model, which uses an isotopic balance approach (modified from Ingerson and Pearson, 1964):

$$t = -8033 \times \ln\left(\frac{A_w}{\frac{(A_g - A_c)(\delta^{13}C_w - \delta^{13}C_c)}{\delta^{13}C_g - \delta^{13}C_c} + A_c}\right) \quad (8)$$

where
- t is the age of the water sample in years;
- A_w is the ^{14}C value of the water sample in percent modern carbon (pmc);
- A_g is the ^{14}C value of the soil CO_2 (in pmc);
- A_c is the ^{14}C value of the carbonate rock (in pmc);
- $\delta^{13}C_w$ is the carbon isotopic ratio of the water (in per mil);
- $\delta^{13}C_c$ is the carbon isotopic ratio of the carbonate rock (in per mil); and
- $\delta^{13}C_g$ is the carbon isotopic ratio of the soil CO_2 (in per mil).

The second equation used to estimate the age of the water sampled is the Tamers model, which uses a chemical balance approach for waters close to pH neutral (modified from Tamers, 1967):

$$t = -8033 \times \ln\left(\frac{A_w}{\frac{(a + 0.5b)\,A_g + 0.5bA_c}{a + b}}\right) \quad (9)$$

where
- t is the age of the water sample in years;
- A_w is the ^{14}C value of the water sample in percent modern carbon (pmc);
- A_g is the ^{14}C value of the soil CO_2 (in pmc);
- A_c is the ^{14}C value of the carbonate rock (in pmc);
- a is the concentration of CO_2 (in mol/L); and
- b is the concentration of HCO_3 (in mol/L).

Biotic data (plants, dragonfly larvae, and fish) are presented in this report as dry weight values, because that is how the laboratory reported the values. Some results from other studies used for comparison are reported as wet weight, but were converted for comparison with this study using

$$DW = \frac{WW}{\left[1 - \left(\frac{\text{percent sample moisture}}{100}\right)\right]} \quad (10)$$

where
- WW is wet weight; and
- DW is dry weight.

Data Used for Comparison

Water

Water concentrations from Tavasci Marsh were compared with EPA water-quality standards for drinking water and aquatic life (table 5, U.S. Environmental Protection Agency, 2013a).

Table 6 presents the aquatic-life standards based on site-specific water-quality values to which the standards need to be adjusted. Standards for Cd, Cr, Pb, Ni, Ag, and Zn were calculated based on hardness values (U.S. Environmental Protection Agency, 2013b, appendix B). Copper standards were calculated using the biotic ligand model, which utilizes water temperature, pH, DOC, humic acid, Ca, Mg, Na, K, SO_4, Cl, alkalinity, and sulfite (U.S. Environmental Protection Agency, 2007). Humic acid fraction of DOC was not measured during the study, so the default value of 10 percent was utilized. Sulfite was not measured during the study, therefore a small value of 0.01 mg/L was assumed for all samples.

Table 5. Water-quality standards for drinking water and aquatic life.

[Values are in µg/L unless otherwise noted; NA, not available; MCL, maximum contaminant level; CMC, criteria maximum concentration (acute); CCC, criterion continuous concentration (chronic)]

Element	Primary drinking-water standard	Aquatic-life water standard (freshwater)	
	MCL	CMC	CCC
Antimony (Sb)	6	NA	NA
Arsenic (As)	10	340	150
Barium (Ba)	2,000	NA	NA
Beryllium (Be)	4	NA	NA
Cadmium (Cd)	5	a	a
Chromium (Cr)	100	a,b	a,b
Copper (Cu)	1,300	c	c
Iron (Fe)	NA	NA	1,000
Lead (Pb)	15	a	a
Mercury (Hg) (ng/L)	2,000	NA	NA
Methyl mercury (ng/L)	NA	1,400	770
Nickel (Ni)	NA	a	a
Selenium (Se)	50	d	5
Silver (Ag)	NA	a	NA
Uranium (U)	30	NA	NA
Zinc (Zn)	NA	a	a
^{226}Radium (Ra) (pCi/L)	5	NA	NA

[a]Calculated based on hardness (see table 6).

[b]Concentration for chromium (III).

[c]Calculated using the biotic ligand model (see table 6).

[d]Selenium speciation needed and was not analyzed for during this study. Additionally, traditional methods for predicting effects based on direct exposure to dissolved concentrations are not appropriate for Se (Chapman and others, 2009).

Sediment

Metal and trace element concentrations measured in marsh sediments were compared to several published sediment quality guidelines (SQG) as a preliminary indication of potential risk to biologic communities. Sediment samples were also compared with published elemental concentrations from local and regional studies for context.

The EPA presents SQGs intended as screening tools to indicate level of concern, but due to the complex nature of biological-effect correlations the SQG's are nonenforceable (U.S. Environmental Protection Agency, 1997). The SQGs were derived from both environmental sites and laboratory experiments to assess the incidence of adverse biological effects in aquatic organisms using trace-element concentrations in sediment according to dry weight. The EPA cautions against the use of the SQGs to indicate direct cause-and-effect relations because sediments may contain a combination of elements that collectively contribute to the adverse biological effects, causing the SQGs to be potentially over- or underprotective for environmental sites (U.S. Environmental Protection Agency, 1997). Two SQGs used in this report are the threshold effects level (TEL) and the probable-effects level (PEL). The TEL represents the concentration below which toxic biological effects rarely occur. Toxic effects usually or frequently occur at concentrations above the PEL.

Table 6. Site-specific water-quality criteria values for aquatic life from Tavasci Marsh.

[Aquatic life water standards for freshwater are given in µg/L; NA, not applicable; CMC, criteria maximum concentration (acute); CCC, criterion continuous concentration (chronic)]

Sample site	Sample date	Cadmium (Cd)[a]		Chromium (Cr)[a,b]		Copper (Cu)[c]		Lead (Pb)[a]		Nickel (Ni)[a]		Silver (Ag)[a]		Zinc (Zn)[a]	
		CMC	CCC	CMC	CCC	CMC	CCC	CMC	CCC	CMC	CCC	CMC	CCC	CMC	CCC
Shea Spring (TZG07)	10/19/2010	4.9	0.46	1,203	156	2.5	1.5	172	6.7	1,013	113	15	NA	254	256
Shea Spring (TZG07)	04/21/2011	5.3	0.49	1,293	168	2.3	1.4	188	7.3	1,092	121	18	NA	274	276
Shea Spring (TZG07)	10/17/2011	5.2	0.48	1,262	164	2.4	1.5	182	7.1	1,064	118	17	NA	267	269
Shea Spring (TZG07)	04/16/2012	4.9	0.47	1,211	157	2.2	1.3	173	6.7	1,020	113	16	NA	256	258
TZG03	10/20/2010	4.9	0.46	1,199	156	10	6.5	171	6.7	1,010	112	15	NA	253	255
TZG03	04/20/2011	5.8	0.52	1,393	181	13	8.1	207	8.1	1,179	131	21	NA	296	298
TZG03	10/18/2011	5.9	0.53	1,416	184	8.6	5.4	211	8.2	1,199	133	22	NA	301	303
TZG03	04/17/2012	6.0	0.54	1,432	186	9.7	6.0	214	8.4	1,213	135	22	NA	304	306
Inflow	04/18/2012	8.9	0.71	1,995	260	37	23	325	13	1,709	190	45	NA	429	432
Outflow	10/20/2010	7.9	0.65	1,802	234	40	25	287	11	1,538	171	36	NA	386	389
Outflow	04/20/2011	7.4	0.62	1,711	223	39	24	269	10	1,458	162	32	NA	366	369
Outflow	10/18/2011	7.1	0.61	1,653	215	32	20	257	10	1,407	156	30	NA	353	355
Outflow	04/17/2012	7.0	0.60	1,627	212	20	13	252	9.8	1,384	154	29	NA	347	350
Piezometer 6	10/22/2010	11	0.81	2,336	304	124	77	395	15	2,011	223	62	NA	504	509
Piezometer 6	04/21/2011	10	0.80	2,288	298	34	21	385	15	1,968	219	60	NA	494	498
Piezometer 6	10/19/2011	9.3	0.73	2,066	269	27	17	340	13	1,771	197	48	NA	444	448
Piezometer 6	04/18/2012	11	0.83	2,390	311	39	24	406	16	2,060	229	65	NA	517	521
Piezometer 1	10/20/2011	15	1.0	3,100	403	28	17	556	22	2,694	299	113	NA	676	681
Piezometer 3	10/20/2011	8.7	0.70	1,956	254	41	26	317	12	1,675	186	43	NA	420	423
Piezometer 7	10/20/2011	9.7	0.76	2,146	279	20	12	356	14	1,843	205	52	NA	462	466
Piezometer 8	10/21/2011	8.5	0.69	1,924	250	9.9	6.2	311	12	1,646	183	41	NA	413	416

[a]Calculated based on hardness (equations in U.S. Environmental Protection Agency, 2013b, appendix B).

[b]Concentration for chromium (III).

[c]Calculated using the biotic ligand model.

Table 7. Sediment quality guidelines (SQGs) for selected trace elements from various sources.

[All values are in parts per million (ppm) except for Hg, in parts per billion (ppb); LEL, lowest effect level; SEL, severe effect level; TEL, threshold effects level; PEL, probable effects level; TEC, threshold effect concentration; PEC, probable effect concentration]

Trace element	Persaud and others (1993)		EPA (1997)		MacDonald and others (2000)	
	LEL	SEL	TEL	PEL	TEC	PEC
Arsenic (As)	6	33	7.24	41.6	9.79	33
Cadmium (Cd)	0.6	10	0.676	4.21	0.99	4.98
Chromium (Cr)	26	110	52.3	160	43.4	111
Copper (Cu)	16	110	18.7	108	31.6	149
Lead (Pb)	31	250	30.2	112	35.8	128
Mercury (Hg) (ppb)	200	2,000	130	696	180	1,060
Nickel (Ni)	16	75	15.9	42.8	22.7	48.6
Zinc (Zn)	120	820	124	271	121	459

Table 8. Metal and trace-element concentrations in sediment samples from local, regional, and national studies, compared to sediment in Tuzigoot National Monument.

[All values are in parts per million (ppm), except for mercury, in parts per billion (ppb); nc, not computed]

Element	Arsenic (As)	Cadmium (Cd)	Chromium (Cr)	Copper (Cu)	Mercury (Hg) (ppb)	Lead (Pb)	Nickel (Ni)	Selenium (Se)	Zinc (Zn)
U.S. baseline bed sediment (average)[1]	8.1	0.5	66	24	80	24	28	0.8	100
Western U.S. baseline bed sediment (average)[2]	7.4	0.47	60	32	40	18	25	0.50	100
Prescott National Forest surface soil (average)[3]	13	1.3	nc	78	10	34	nc	nc	100
Prescott National Forest surface soil (maximum)[3]	120	7.6	nc	370	110	140	nc	nc	320
Prescott National Forest deep soil (average)[3]	9.0	0.4	nc	55	10	17	nc	nc	83
Prescott National Forest anomaly threshold[3]	10	1.0	nc	70	nc	30	nc	nc	90
At Pecks Lake tailings dam[4]	623	<1	nc	953	1,300	512	nc	nc	625
300 ft away from Pecks Lake tailings dam[4]	224	12.3	nc	932	910	273	nc	nc	1,800
Tavasci Marsh surface sediment[4] (average)	35	3.05	nc	146	200	66.6	nc	nc	162
Tavasci Marsh surface soil (average)[5]	11.7	1.8	10.1	40.1	nc	24.1	nc	nc	45.5
Verde Formation Limestone (average)[5]	nc	nc	9.8	3.1	nc	9.7	nc	nc	9.7
Verde Formation Sandstone (average)[5]	15.6	0.6	29.7	12.8	nc	31.2	nc	nc	31.2
Verde Formation Marl/ mudstone (average)[5]	4.1	<0.24	31.6	12.6	nc	31.9	nc	nc	31.9
Verde Formation Conglomerate (average)[5]	nc	nc	26	7	nc	20.9	nc	nc	20.9

[1]Reported in Horowitz and Stephens, 2008.

[2]Reported in Paul and others (2012); calculated from bed-sediment trace-element concentrations for sites in Alaska, Arizona, California, Colorado, Idaho, Missouri, Montana, Nebraska, Nevada, New Mexico, Oregon, Utah, Washington, and Wyoming.

[3]Reported in Nash and others (1996); concentrations from 60 soil samples located near historic mining sites in the Prescott National Forest; surface soil samples were collected from the top 2 inches, and deep soil samples were collected from between 5 and 8 inches.

[4]Reported in Ecology and Environment, Inc. (1994), where the tailings dam is at the boundary with Pecks Lake.

[5]Reported in URS Greiner Woodward Clyde (1999); which for calculation of average values, substituted the detection limit for values reported as less than the detection limit.

Persaud and others (1993) also developed SQGs for several trace elements and defined a lowest-effect level (LEL) and a severe-effect level (SEL). The LEL represents sediment concentrations that have no effect on the majority of sediment-dwelling organisms. The SEL represents sediment concentrations that are considered heavily polluted and likely to affect the health of sediment-dwelling organisms.

MacDonald and others (2000) developed consensus-based SQGs for several trace elements that were computed as the geometric mean of several previously published SQG: the threshold-effect concentration (TEC) and the probable-effect concentration (PEC). The TEC is similar to the TEL and represents the concentration below which adverse effects are not expected to occur. Likewise the PEC represents the concentration above which adverse effects are expected to occur more often than not. SQGs are presented in table 10 and are included in selected figures for reference.

The range of uncertainty of individual sample concentrations (based on replicate analysis; table 4) should be considered when sample concentrations are near a SQG for a given element to understand the likelihood of a SQG exceedance. If the sample concentration is less than the SQG minus the uncertainty, then the sample does not exceed the SQG with 90-percent confidence. If the sample concentration is greater than the SQG plus the uncertainty, then the sample exceeds the SQG with 90-percent confidence. For sample concentrations within the range of uncertainty around the SQG, the sample exceedance of the SQG is uncertain at the 90-percent confidence level.

Sediment data from other local, regional, and national studies are included in table 8 to provide context for the sample concentrations found in Tavasci Marsh.

Plants

Plant data from other studies are included in table 9 to provide context for the sample concentrations found in Tavasci Marsh. Taylor and Crowder (1983) studied the uptake and accumulation of Cu, Ni, Zn, Fe, Mn, Mg, and Ca in several different tissues of *T. latifolia* in wetlands affected by mining smelters. Ye and others (1997) investigated cattails used for treating wastewater from a Pb and Zn mine compared with an uncontaminated site. Grisey and others (2012) looked at the performance of cattails for removal of metals in wetlands receiving landfill leachate. They observed some seasonal variation in the roots and shoots for certain metals. Sasmaz and others (2008) sampled cattail sediment, roots, leaves, and water for several trace elements in wetlands supplied by treated waste water. Sasmaz and others (2008) observed greater uptake in the roots when compared to the surrounding sediment concentrations for Cd, Cu, Pb, Ni, and Zn.

Dragonfly Larvae and Fish

Macroinvertebrate data from other studies are included in table 10 to provide context for the sample concentrations found in Tavasci Marsh. As part of the NAWQA, the USGS has conducted several studies in northern Idaho, mostly within the Coeur d'Alene Basin, which has been heavily impacted by mining (for example, Farag and others, 1998; Maret and others, 2003). A study by Farag and others (1998) did not depurate the dragonfly larvae, which makes their data more directly comparable with ours. Maret and others (2003) report data for Cd, Pb, and Zn in caddis flies from reference sites not heavily impacted by mining compared

Table 9. Concentrations of select metals and trace elements in cattail parts, as reported in previous studies.

[All values are in parts per million (ppm) dry weight; nc, not computed; sed, sediment sample near base of plant.]

Element	Cadmium (Cd)			Chromium (Cr)			Copper (Cu)			Lead (Pb)			Nickel (Ni)			Zinc (Zn)		
	Sed	Root	Leaf	Sed	Root	Leaf	Sed	Root	Leaf	Sed	Root	Leaf	Sed	Root	Leaf	Sed	Root	Leaf
Uncontaminated roadside site[1]	1.4	2.1	0.6	nc	nc	nc	nc	nc	nc	26	25	19	nc	nc	nc	86	46	22
Contaminated settling pond from Pb-Zn mine[1]	20	1.5	0.6	nc	nc	nc	nc	nc	nc	5,686	1,108	40	nc	nc	nc	3,009	946	122
Wetlands near smelter sites[2]	nc	nc	nc	nc	nc	nc	3,738	38	nc	nc	nc	nc	9,372	52	nc	343	120	nc
Lagoon inflow receiving landfill leachate (fall)[3]	3.3	2.51	nc	92.1	2.23	nc	322.3	5.1	nc	39.17	13.9	nc	56.42	6.03	nc	657.2	45.5	nc
Lagoon inflow receiving landfill leachate (spring)[3]	3.3	2.51	nc	92.1	2.25	nc	322.3	11.29	nc	39.17	19.1	nc	56.42	4.95	nc	657.2	36.1	nc
Wetlands supplied by treated wastewater[4]	0.23	0.44	0.21	60	44	21	45	50	30	10	13	8	50	55	40	70	340	215

[1]Average values reported in Ye and others (1997); plant tissue samples were ashed as in this report.
[2]Reported in Taylor and Crowder (1983).
[3]Average values reported in Grisey and others (2012); sediment samples not reported by season.
[4]Average values reported in Sasmaz and others (2008); plant tissue samples were ashed as in this report.

with mining-impacted sites. A study by Lavilla and others (2010) investigated bioaccumulation of trace elements in dragonfly larvae due to anthropogenic sources of pollution in Spain. They report data for three species of dragonfly larvae that were depurated before analysis, and two of the reported species are burrowers like the Gomphidae and Libellulidae collected from Tavasci Marsh. A study on caddis fly larvae in mining-impacted streams in California (Cain and others, 2000) includes sediment and whole-body data for mining-impacted sites and reference site and was also used for comparison with this study.

The link between trace metal bioaccumulation and the long-term effects on fish is not well understood. Laboratory studies have demonstrated dose/response effects in controlled settings and these studies are mostly used for determining toxicity thresholds from dietary or external exposures. Transferring the information from a controlled laboratory setting to the environment is challenging because of the heterogeneous physical characteristics and complex chemical interactions in a marsh environment. For this investigation, existing fish contaminant databases were accessed and data compiled to develop a better understanding of concentrations observed in Tavasci Marsh. Developing a distribution of possible concentrations observed in similar fish collected in the West provided a reference for which Tavasci Marsh concentrations could be compared. Data was retrieved from the National Contaminant Biomonitoring Program (NCBP), the NAWQA Program, the USGS Biomonitoring of Environmental Status and Trends (BEST) Program's Large River Monitoring Network, and the U.S. Fish and Wildlife Service (FWS) Arizona Ecological Services (AES). Data compilation focused on the fish from the families Centrarchidae (sunfishes), Ictaluridae (catfish), and Cyprinidae/Pocillidae (small minnows/livebearers).

The NCBP, NAWQA, and BEST data collections were conducted as part of larger regional assessments for their respective agencies and programs. These studies captured a gradient of fish metal bioaccumulation across the larger landscape likely measuring larger nonpoint land-use effects. The AES dataset was more targeted on site-specific impacts, such as point-source mining or industrial activities, than the other, more regional studies, which capture a wider range of accumulated concentrations. As a result the three regional datasets were combined to compare to the AES and Tavasci Marsh datasets. The data sources and retrievals are described in detail below and data used from other studies is presented in appendix D, table 9.

The NCBP dataset (http://www.cerc.usgs.gov/data/ncbp/ncbp.html) contains data on polychlorined biphenyls, pesticides, and trace elements that may threaten fish and wildlife (Schmitt and Brumbaugh, 1990). The NCBP database houses results of analyses on whole-body fish composite samples (5 fish per sample) collected from 1960 to 1986. Data was retrieved from seven western states (Arizona, California, Idaho, Nevada, New Mexico, Oregon, and Washington). Fish tissue samples were analyzed for As, Cd, Cu, Pb, Hg, Se, and Zn. A total of 67 fish were used in the comparison distribution; 51 from the sunfish family and 16 from the catfish family.

Table 10. Macroinvertebrate studies of select metals and trace elements.

[All values are in parts per million (ppm), except for mercury, which is in parts per billion (ppb) dry weight; nc, not computed]

Element	Arsenic (As)		Cadmium (Cd)		Copper (Cu)		Mercury (Hg) (ppb)		Lead (Pb)		Zinc (Zn)	
	Sed	Macro	Sed	Macro	Sed	Macro	Sed	Macro	Sed	Macro	Sed	Macro
River with upstream mining impacts, Idaho[1]	107.5	3	14.5	6	77	32	1,780	110	2,390	74	2,543	973
Reference sites, Montana and Idaho[2]	nc	nc	1	0.58	nc	nc	nc	nc	52	2.94	69	181
Test site from mining-impacted streams, Idaho[2]	nc	nc	24	6.68	nc	nc	nc	nc	1,851	142	2,022	707
Reference site, Spain[3]	nc	2.21	nc	0.341	nc	25.6	nc	nc	nc	1.93	nc	67
Polluted site, Spain [3]	nc	5.62	nc	0.334	nc	20.9	nc	nc	nc	2.54	nc	59.7
Reference site, California[4]	nc	nc	0.4	0.06	61	14.5	60	80	14	0.59	110	113
Mining-impacted site in California[4]	nc	nc	2.7	2.16	240	37.5	400	40	36	1.26	410	169

[1]Average elemental concentrations reported in Farag and others (1998); macro data are for carnivore benthic macroinvertebrate class.

[2]Average elemental concentrations reported in Maret and others (2003); macro data are for whole-body caddis flies and sediment data are from a weak-acid extraction.

[3]Average elemental concentrations for point 3 (not polluted) and point 10 (polluted); dragonfly larvae (*Onychogomphus uncatus*) were depurated before analysis; data from Lavilla and others (2010).

[4]Average elemental concentrations in whole body caddisfly larvae at station 6 (reference) and station 1 (mining impacted) are from Cain and others (2000); samples were not depurated before analysis.

Table 11. U.S. Fish and Wildlife Service studies utilized for fish comparison.

Study citation	Land use	Location and fish used
Marr, 2008	Mining	Lynx Lake, 2 sunfish and 12 catfish; Granite Basin Lake, 21 sunfish
Marr and Schotborgh, 2003	Wood treatment, wastewater discharge, mining	Watson Lake, 26 sunfish, 10 small minnow/livebearer; Lynx Lake, 5 sunfish; Granite Creek, 4 sunfish and 4 small minnow/livebearer
Andrews and King, 1997	Mining	Gila River, 2 sunfish, 3 small minnow/livebearer; Mineral Creek, 1 sunfish, 1 small minnow/livebearer
King and others, 1997	Agriculture, urban, mining	Lower Gila River (5 locations), 10 sunfish, 11 catfish
King and Andrews, 1996	Agriculture, urban, mining	Lower Colorado River (2 locations), 2 catfish
Andrews and others, 1995	Mining	Little Colorado River (3 locations) 3 small minnow/livebearer
King and others, 1992	Mining, agriculture, wastewater discharge, gunpowder manufacture	San Pedro River, 1 sunfish, 6 small minnow/livebearer; Babocomari River, 1 sunfish; Aravaipa Creek, 1 small minnow/livebearer
Baker and King, 1994	Mining, agriculture	Upper Gila River (8 locations), 2 sunfish, 10 catfish

The NAWQA is a long-term monitoring program that provides an understanding of water-quality conditions and trends across the United States and includes an aquatic-ecology resource component in addition to surface- and groundwater quality. NAWQA started in the early 1990s and continues to monitor the Nation's water quality. Whole-body-tissue contaminant data collected by the USGS is housed in the National Water Information System (NWIS) at http://waterdata.usgs.gov/nwis (U.S. Geological Survey, 2013b). Data were retrieved from NWIS for Arizona and California. Most samples were analyzed for suite of 24 trace elements. Fourteen fish were used in the analysis: 2 catfish and 12 small minnow/livebearers.

The BEST program's Large River Monitoring Network examined fish health in multiple river basins by using a suite of organismal and suborganismal endpoints, which monitor and assess the effects of environmental contaminants in fish (Hinck and others, 2006). In 2003, the Colorado River Basin (CDRB) was sampled for whole fish and analyzed for organic and inorganic contaminants. A suite of 19 trace elements were analyzed in fish tissue and the data can be obtained at http://www.cerc.usgs.gov/data/best/search/Colorado.htm. A total of 22 fish were used; 12 were sunfish and 10 catfish.

The FWS has an environmental-contaminants program within the AES that identifies environmental contaminant problems affecting National Wildlife Refuge lands, migratory birds, and threatened and endangered species. They focus on locations and regions that have significant impacts from anthropogenic stressors related to activities such as mining, agriculture, industrial processes, and wastewater. As part of this investigation, data from 8 different studies conducted in Arizona from 1992 to 2008 were retrieved independently and compiled to develop a distribution of fish bioaccumulation data that could be compared to the regional studies and the Tavasci Marsh datasets. Reports can be found at http://www.fws.gov/southwest/es/arizona/, and table 11 includes a brief explanation reports. A total of 139 fish were used for the distribution and of those, 75 were sunfish, 38 catfish, and 26 minnow/livebearer.

Assessment of Chemistry in Water, Sediment, Plant, Dragonfly Larvae, and Fish

Water

Water Quality Parameters

Water temperature, pH, specific conductance, and dissolved oxygen were measured in every water sample. The pH was generally neutral; all field measurements were between 6.8 and 7.8. Specific conductance average and standard deviation was lowest at Shea Spring (TZG07) (548±4.2 µS/cm) and higher towards the outflow (657±32 µS/cm at TZG03 and 778±65 µS/cm at outflow). Specific conductance was highest in the shallow groundwater at the north end of the marsh at piezometer 1 (1,440 µS/cm) (fig. 6).

A multiparameter meter was deployed to continuously measure and record dissolved oxygen, pH, specific conductance, and temperature at the TZG03 site for 23 hours beginning in early afternoon on April 18, 2011. The unit stopped recording values at 2 a.m. but began again at 8 a.m. (MST). Temperature showed a strong diurnal fluctuation of 3 °C with the lowest temperatures occurring around 9 a.m. The other parameters did not fluctuate like temperature but did exhibit some small oscillations (fig. 7).

Three temperature sensors were placed at TZG03 along a stainless steel cable at 1.5, 3, and 4.5 feet above the sediment/water interface. These sensors recorded continuously between November 2010 and April 2012. The coolest temperatures were recorded in the winter and warmest temperatures recorded in the summer (fig. 8). Temperature was similar in October and April during each site visit. Daily fluctuations

in water temperature were observed at all three depths. The water column at the TZG03 site was thermally stratified with a difference of up to 0.8 °C every 1.5 feet (fig. 8-inset). Thermal stratification was apparent for a few weeks after the temperature probes were reset during each October and April sampling trip, however the temperature at all depths then became very similar, which may have been due to the wind moving the cattails around the open water site TZG03, which could have pushed the temperature sensor cable to a different area and moved the temperature sensors closer together.

Dissolved Oxygen

Average and standard deviation of dissolved oxygen in the four measurements collected was 7.06 ± 0.44 mg/L (89±5.4 percent saturation) at Shea Spring (TZG07), while the shallow-groundwater site at the north end of the marsh (piezometer 6) was lower, around 2.05±0.74 mg/L (22±8.8 percent saturation). At TZG03, dissolved oxygen concentrations in surface water over the course of this study were low, averaging 2.75±0.78 mg/L (30±9.2 percent saturation), which is below the Arizona standard for fresh water fisheries of 6.0 mg/L.

During the overnight multiparameter meter deployment at TZG03, dissolved oxygen decreased from 4.15 to 2.5 mg/L between 10 p.m. and 8 a.m. (fig. 7). In other wetland systems, photosynthesis during daylight hours can lead to an increase in dissolved oxygen above 100 percent saturation followed by depletion of dissolved oxygen to near zero values at night (Naftz and others, 2011). Aquatic macrophytes are present in most open water sections of Tavasci Marsh but do not appear to produce a lot of dissolved oxygen through respiration during the day. The consistency of dissolved-oxygen concentrations over time at TZG03 implies that plant respiration and gas exchange from the atmosphere are not greater than the oxygen consumption occurring in the marsh. The large amount of decaying cattail material may be contributing to the depletion of dissolved oxygen in Tavasci Marsh, similar to conditions found in Pecks Lake (Arizona Department of Environmental Quality, 2001). The causes of the low dissolved oxygen measurements in the marsh were not tested in this project.

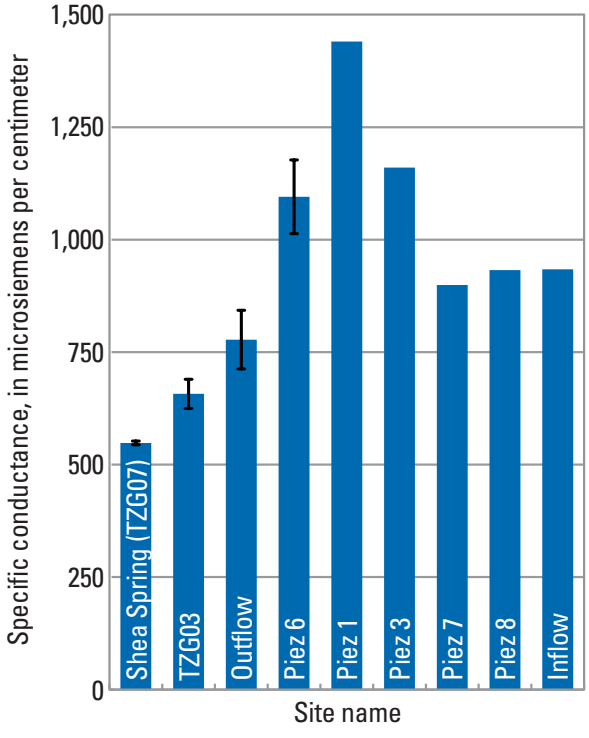

Figure 6. Histogram of average specific conductance values from Tavasci Marsh. Error bars represent one standard deviation. Only one sample was collected from inflow and from piezometers 1, 3, 7, and 8.

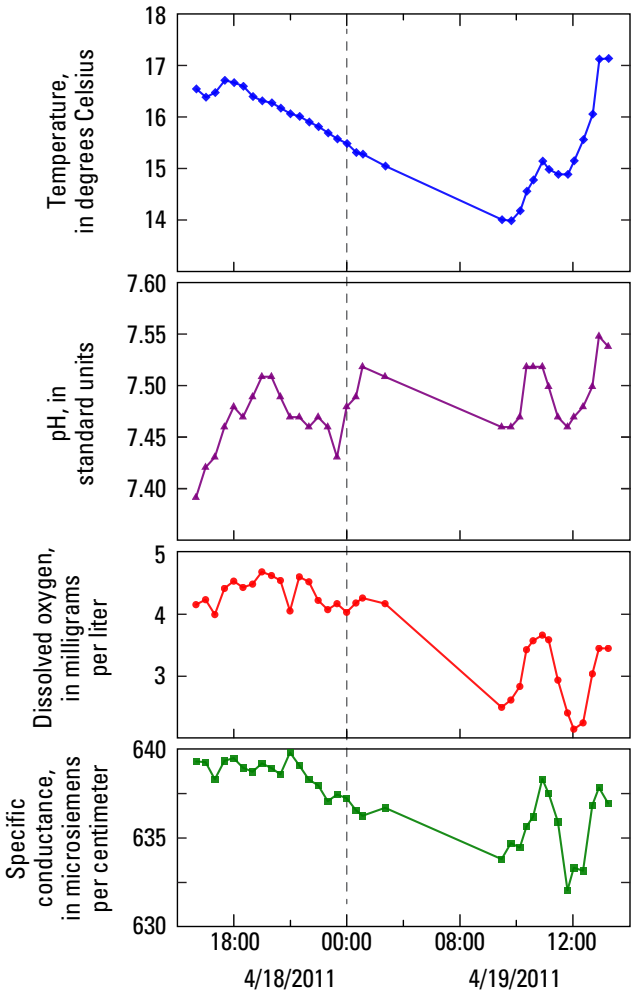

Figure 7. Plots of water-quality parameters measured at TZG03 over a 23-hour period in April 2011.

Water Chemistry

The concentration of As in all water samples exceeded the EPA maximum contaminant level in drinking water of 10 µg/L (U.S. Environmental Protection Agency, 2013a), and the concentration of As in the October 2010 piezometer 6 sample exceeded the EPA criterion of continuous concentration (CCC) for aquatic life of 150 µg/L (U.S. Environmental Protection Agency, 2013b) (table 5). Neither standard directly applies to the use of water at the sites, but are given for reference. Total dissolved As concentrations at Shea Spring (TZG07) were consistent for all water samples and averaged 21.7±0.8 µg/L. Piezometer 6 was more variable and had the highest average dissolved concentration of As, 90±47 µg/L. The difference in As concentrations between piezometer 6 and the surface-water sites (Shea Spring, TZG03, and outflow) may be due, in part, to electron shuttling by terrestrially-derived DOM at piezometer 6, resulting in the mobilization of Fe and As (Mladenov and others, 2010). Arsenic is known to be naturally elevated in waters of the Verde Valley (Owen-Joyce and Bell, 1983; Foust and others, 2004, Johnson and others, 2011), and the Verde Formation is thought to be the source of the elevated As, the sandstone member contains higher concentrations than the rest of the unit (URS Greiner Woodward Clyde, 1999).

One sample (2,830 µg/L Fe at piezometer 1) exceeded the EPA chronic aquatic life standard of 1,000 µg/L for Fe. No other elements measured exceeded the EPA water-quality standards for either drinking water or aquatic life. Piezometer 1 was the only site with a H_2S odor and water was ponded at the surface around the well pipe. There was a small amount of dissolved oxygen (1.8 mg/L, 20 percent saturation) present in the pumped water sample, and dissolved barium and iron were elevated (1,320 and 2,830 µg/L, respectively). In this study, "dissolved" refers to water that passed through a 0.45 µm filter, however, studies have shown that small colloidal material can pass through this filter and that constituents may not be present only as dissolved ions (Cidu and Frau, 2007). Dissolved iron at Shea Spring (TZG07) was less than the detection limit of 3.2 µg/L for all but one sample (7.1 µg/L), which was much lower than all other samples collected in Tavasci Marsh; average and standard deviation for surface water (inflow, TZG03, and outflow) was 53.8±17.9 µg/L and shallow groundwater (excluding piezometer 1) was 310±142 µg/L. Shea Spring (TZG07) discharges from bedrock through fine sand, while all of the other sites have darker fine-grained material with more organic material, which may be related to the higher dissolved iron compared to Shea Spring (TZG07).

Mercury samples were unfiltered and analyzed for both total and methylmercury. Methylmercury is the more mobile and bioavailable form of Hg and is used in the EPA aquatic life standard. Hg concentrations in unfiltered water samples were low compared to drinking-water and aquatic-life standards throughout Tavasci Marsh (table 5); average total Hg in surface water was 0.69±0.48 ng/L and methylmercury in surface water was 0.20 ± 0.12 ng/L. Concentrations in groundwater averaged 4.72 ± 3.04 ng/L total Hg and 0.12 ± 0.04 ng/L methylmercury. (Piezometer 1 was excluded from this average because it was the only site with a H_2S odor and also had the greatest Hg concentrations: 60.3 total mercury and 0.62 ng/L methylmercury). The average percentage of methylmercury in total Hg was greater in surface water (29±10 percent) than groundwater (4±3 percent; all sites included in average) in Tavasci Marsh. Surface waters may contain bacteria or other factors favorable for converting Hg to methylmercury—an important consideration if the concentration of total Hg in water were to increase because of sediment disturbance or continued input from atmospheric sources.

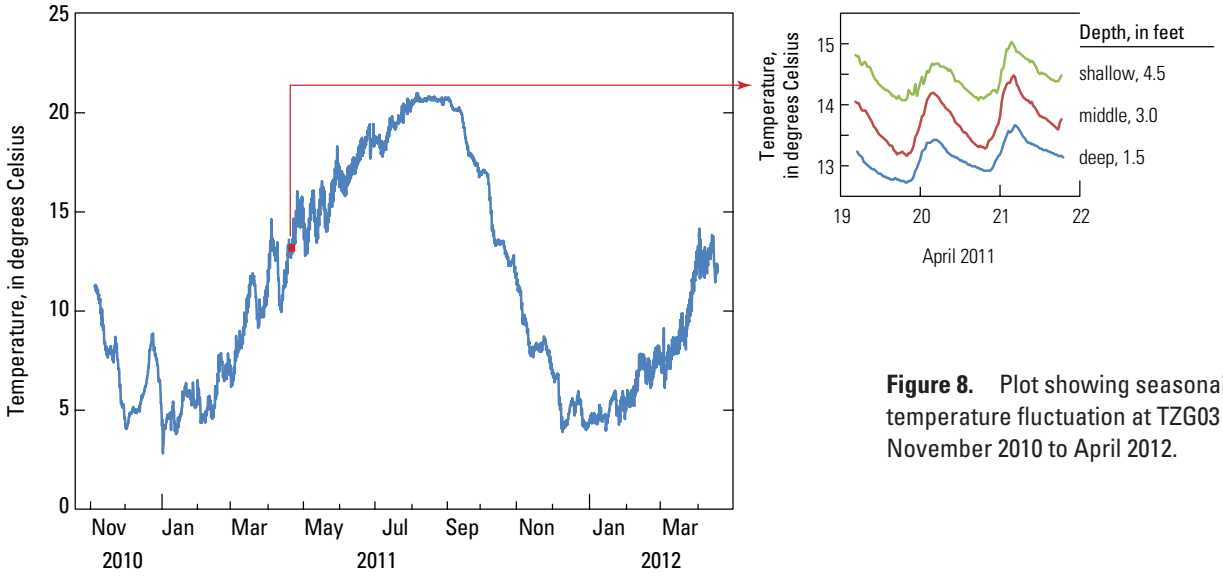

Figure 8. Plot showing seasonal water temperature fluctuation at TZG03 from November 2010 to April 2012.

Water Cumulative Toxic Units

The cumulative effect of all metals and trace elements present in the water can be estimated by using a toxic-unit approach where the water concentration is divided by the water-quality standard for each element of interest and then summed to produce a cumulative toxic unit (CTU) where values greater than 1 indicate potential toxicity to aquatic biota (Wildhaber and Schmitt, 1996; Allert and others, 2013). This approach assumes toxicity effects from each element are additive, which is a simplification but provides a basic estimate of cumulative toxicity potential. All water samples from Tavasci Marsh were below the detection limit for Cd, several other species (Cu, methylmercury, Pb, and Zn) had some samples with concentrations below the reporting limit, and some reporting limits were close to the water quality standards. Therefore, censored values below the reporting limit were not included in the cumulative toxicity estimate following the approach in Wildhaber and Schmitt, 1996. The piezometer 6 water sample from October 2010 is the only sample with a CTU greater than 1 (1.15), and the majority of the toxic unit sum is due to a high As concentration, which exceeded the water-quality standard. Arsenic was also the dominant contributor to the cumulative toxic unit values at all sites except for three samples from TZG03, for which dissolved Cu concentrations were the dominant contributor to cumulative toxic unit values but did not exceed the water-quality standard (fig. 9). None of the surface-water samples, where aquatic life was living during this study, had greater than 0.3 CTU, which indicates that metal and trace element concentrations in the water column do not pose a significant threat to aquatic life at this time.

Major Ion Geochemistry

Major-ion chemistry indicates that water from Tavasci Marsh is calcium-magnesium-bicarbonate type water. Limestone units in the Interbedded and Limestone members of the Verde Formation are present on the hillsides surrounding the marsh as well as below the marsh (inferred from well log information). Limestone weathering may be the dominant source of major ions to the waters of the marsh.

Water at Shea Spring (TZG07) had a smaller proportion of Mg compared to groundwater from piezometer 6 and compared to other constituents discussed above. Sites TZG03 and outflow had intermediate values, indicating a mixture of the two source waters (fig. 10). Major-ion chemistry of the groundwater from the other piezometers sampled during October 2011 was also intermediate, with piezometer 1 having a signature more similar to Shea Spring (TZG07) (fig. 10). Piezometer 1 is located near Shea Spring (TZG07) (fig. 4) and has standing water at the surface, so the origin of water at piezometer 1 may be from groundwater seeps of similar source to Shea Spring (TZG07).

The major-ion signature of the Verde River at Clarkdale (U.S. Geological Survey, 2013b), which is the source of water to Pecks Lake, was more similar to Shea Spring (TZG07) for cations but more similar to piezometer 6 for anions (fig. 10). Verde River water that is diverted to Pecks Lake may undergo ion exchange with sediments as it moves towards Tavasci Marsh.

Another potential source of water in the area is the leachate from the tailings pile material, which is located at the beginning of the abandoned oxbow of the Verde River adjacent to the marsh (fig. 1). The groundwater under the tailings pile was not sampled during this project, but water chemistry data are available from the early 1990s (Plumb, 1999). Major-ion chemistry of the groundwater beneath the tailings pile is magnesium-sulfate type water, which is very different from the water samples collected from Tavasci Marsh and the Verde River at Clarkdale (fig. 10), suggesting that the groundwater beneath the tailings pile is not contributing a significant amount of water to Tavasci Marsh.

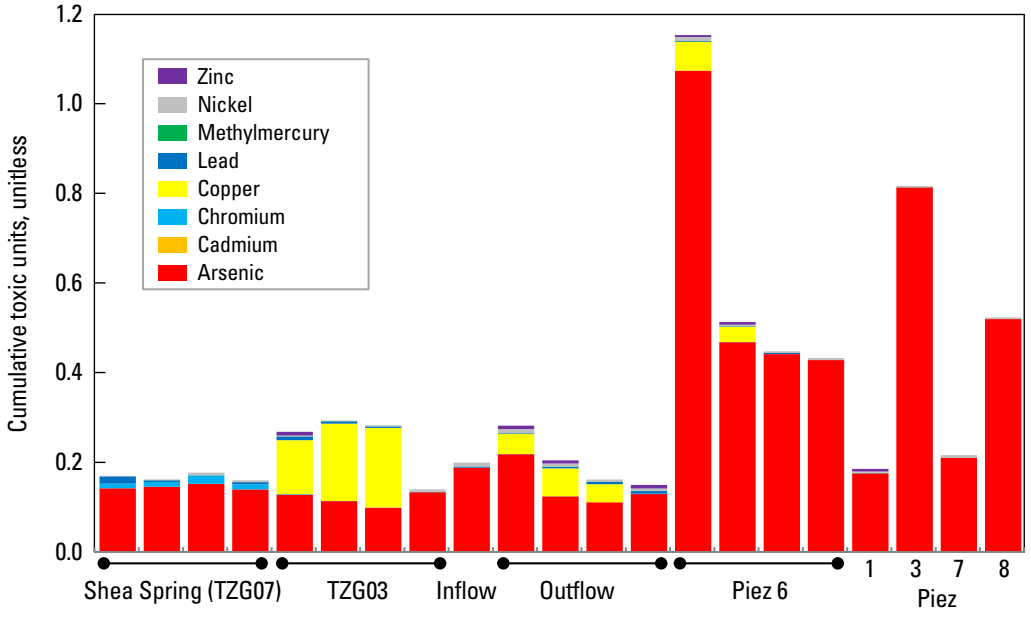

Figure 9. Bar chart showing cumulative toxic unit contribution by element for water samples collected at Tavasci Marsh. Piez, piezometer.

Stable Isotopes, Radioisotope Age Dating, and Dissolved Gases

Stable isotope ratios of ^{18}O and ^{2}H vary in water due to several factors including source of moisture for precipitation, precipitation elevation, and evaporation. A local meteoric water line (LMWL) was developed for Flagstaff (Blasch and others, 2006) and utilized for studies of the Verde River watershed (which includes Tavasci Marsh). Their study found that precipitation isotope ratios in the Verde River watershed decrease (have a more depleted signature) with increasing elevation and they developed equations to calculate isotope signature based on elevation (Blasch and others, 2006). Isotopic ratios that plot to the right of the LMWL indicate the water has undergone evaporation (Clark and Fritz, 1997).

The isotopic signature of the shallow groundwater at piezometer 6 is more enriched than the surface water sites sampled for stable isotopes (fig. 11). In April 2011, the isotopic signature of piezometer 6 plots to the right of the LMWL (fig. 12). The inflow sample from Pecks Lake seepage in April 2012 had the most enriched stable isotopic values of all samples (-4.62 for ^{18}O and -49.2 per mil for ^{2}H) and showed a more evaporated signature than piezometer 6 (fig. 11*D*). Enriched isotopic values are representative of low elevation or warmer precipitation and indicate that the shallow groundwater in the vicinity of piezometer 6 has a localized recharge source. Based on the precipitation-isotope-versus-elevation equations from Blasch and others (2006, equations 3 and 4), the expected isotopic signature for precipitation at 3,330 feet (the elevation of Tavasci Marsh) is -8.34 and -61.24 per mil for ^{18}O and ^{2}H, respectively, and is similar to the average of samples from piezometer 6 of -7.68 and -60.97 per mil for ^{18}O and ^{2}H, respectively.

Between 2009 and 2012, the average isotopic signature of the Verde River at Clarkdale (09504000), which is located upstream of the Pecks Lake diversion, was -11 and -78.5 per mil for ^{18}O and ^{2}H, respectively (U.S. Geological Survey, 2013b), which indicates input of higher elevation winter recharge (7,125- and 6,781-ft elevation for ^{18}O and ^{2}H equations, respectively) and is more similar to water from Shea Spring (TZG07) compared to the enriched samples from inflow or piezometer 6. The Verde River is the water source to Pecks Lake, but the different isotopic signatures of the river and inflow water samples suggest that either there is significant evaporation from the lake or there is another localized source of water to the lake. The shallow groundwater at piezometer 6 and Shea Spring (TZG07) water appear to be sources of water to the Tavasci Marsh system.

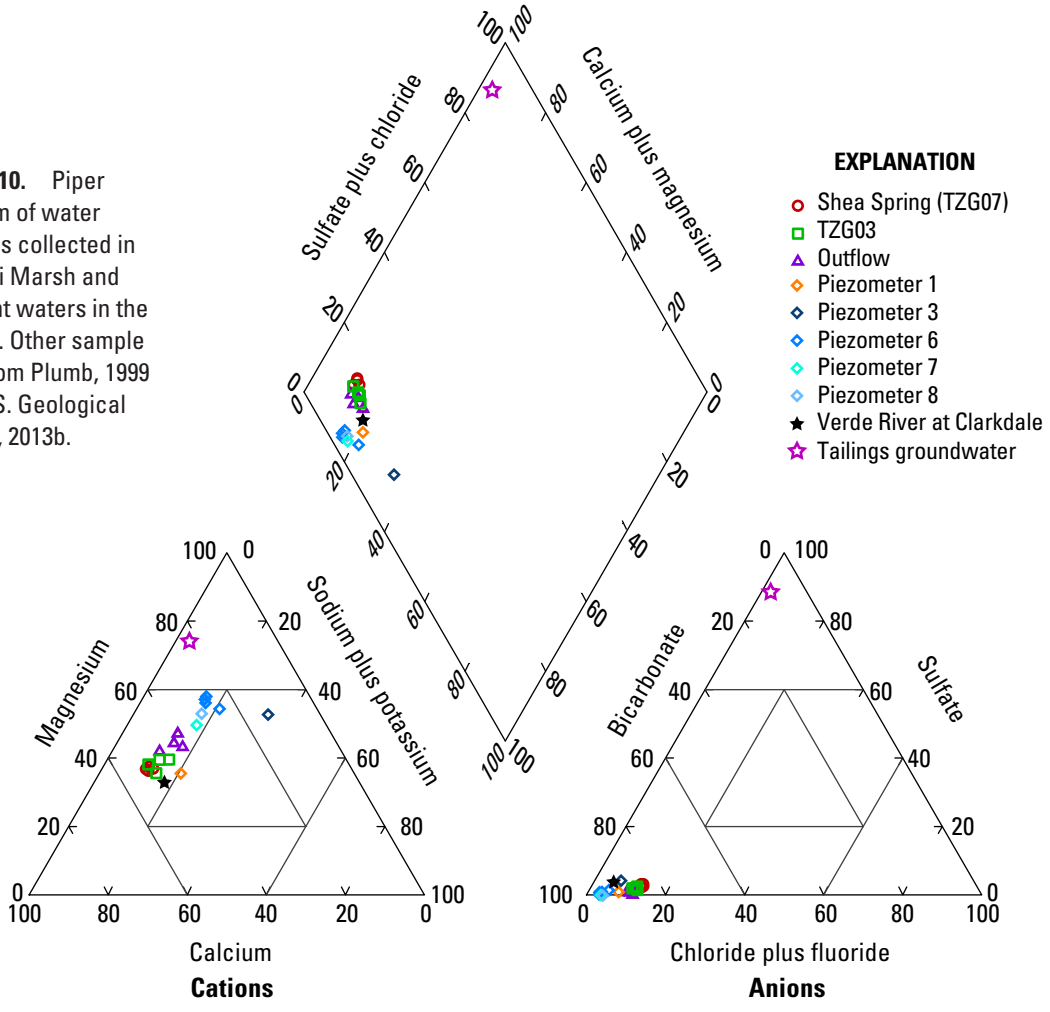

Figure 10. Piper diagram of water samples collected in Tavasci Marsh and relevant waters in the vicinity. Other sample data from Plumb, 1999 and U.S. Geological Survey, 2013b.

Table 12. Proportion of water originating from Shea Spring (TZG07) based on calculations using equation 5.

[Site locations are shown in figure 4. A value of 1 (for both δ^2H and δ^{18}O) indicates that the sample was comprised of water from only Shea Spring (TZG07); value of 0 indicates no water from Shea Spring (TZG07) was present in sample]

Sample date	TZG03		Outflow	
	δ^2H	δ^{18}O	δ^2H	δ^{18}O
October 2010	0.57	0.55	0.45	0.25
April 2011	0.78	0.76	0.54	0.51
October 2011	0.78	0.83	0.49	0.51
April 2012	0.82	0.80	0.65	0.67

Proportions calculated with the stable isotope data indicate a majority of the open water present at TZG03 originates from Shea Spring (TZG07) while water at the outflow is approximately half from Shea Spring (TZG07) and half from the shallow groundwater at Piezometer 6 (table 12). Calculated proportions were similar using δ^2H and δ^{18}O with the exception of October 2010 at the outflow site, which showed an evaporated signature compared to the other samples (fig. 11*A*) and accordingly a lower proportion of Shea Spring (TZG07) water was calculated using δ^{18}O (table 12).

Shea Spring (TZG07) and piezometer 6 were then sampled for ^{14}C, δ^{13}C, and tritium to understand the groundwater age and contribution of modern precipitation (<60 years old) to these sites. Shea Spring (TZG07) water had 30.1±0.3 pmc and a δ^{13}C of -8.7 per mil, which corresponds to an uncorrected age of 9,645 years old using equation 7. The uncorrected radiocarbon age does not take into account the water interacting with various carbonate rock species in the subsurface, which tend to have older radiocarbon ages and therefore can make the water appear older than it is. Corrected ages were calculated using equation 8 (modified from Ingerson and Pearson, 1964) and equation 9 (modified from Tamers, 1967) assuming ^{14}C values of 0 pmc for carbonate rock and 100 pmc for soil CO_2, and assuming δ^{13}C values of 0 per mil for carbonate rock and -22 per mil for soil CO_2 (Hart and others, 2010). Corrected ages of 2,211 and 5,069 years old were calculated using equations 8 and 9, respectively for the Shea Spring (TZG07) water sample collected in June 2011. The corrected ages are less than the uncorrected age, indicating that interaction with carbonate rock in the subsurface may have affected the ^{14}Cvalue of the water. These age values are estimates, and a more detailed study understanding changes in water chemistry along the flowpath from recharge to discharge at Shea Spring would be needed to obtain a more accurate age of the water.

Tritium, ^{3}H, is a radioactive isotope of hydrogen with a half-life of 12.32 years, and large amounts of it were released into the atmosphere by above-ground nuclear testing in the 1950s and 1960s. Presence of tritium in groundwater can indicate that a component of water was in contact with the atmosphere in the last 60 years. Tritium was not detected at Shea Spring (TZG07), indicating that there is little or no modern precipitation in the water. In contrast, we measured

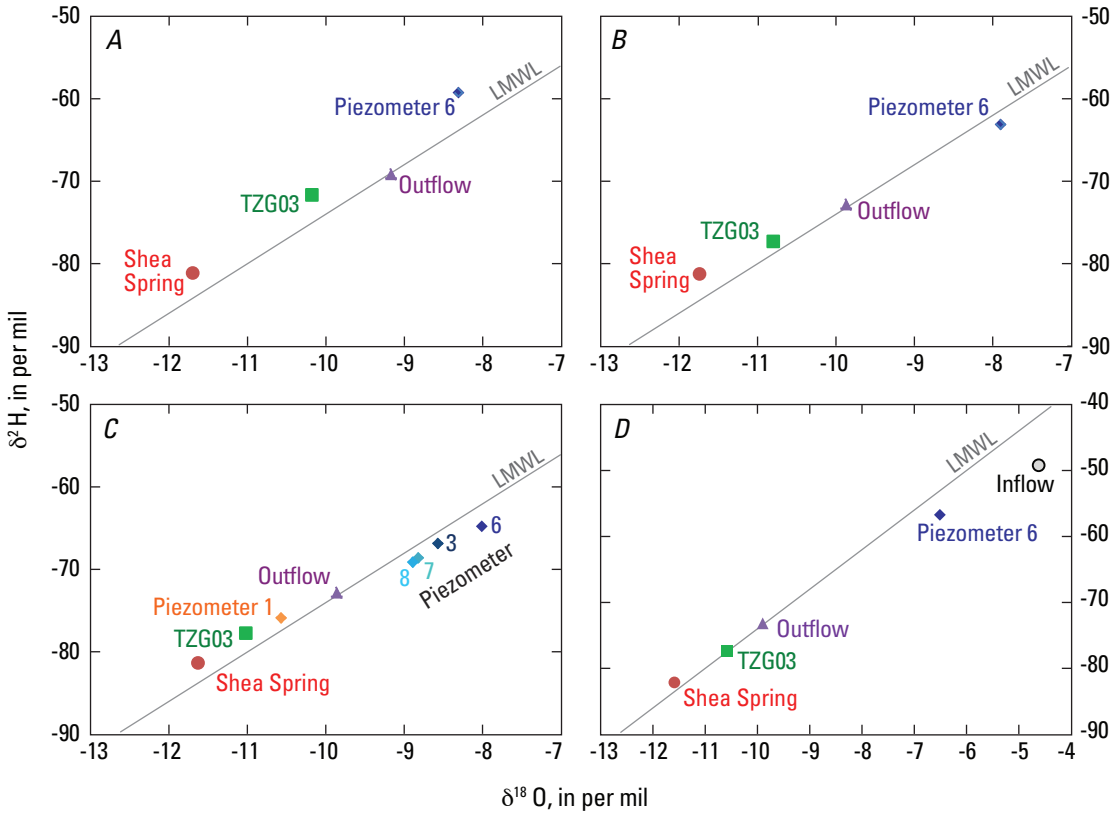

Figure 11. Scatter plot of isotopic signatures of water samples collected at Tavasci Marsh. Values are relative to VSMOW. *A*, October 2010; *B*, April 2011; *C*, October 2011; and *D*, April 2012. LMWL, local meteoric water line, from Blasch and others (2006).

Table 13. Measured dissolved organic carbon (DOC) concentrations.

[DOC concentrations predicted assuming conservative transport; and the ratio of measured to predicted DOC concentrations at TZG03 and outflow water-sampling sites. Conservative transport estimates of DOC are based on equation 6]

Sample date	TZG03			Outflow		
	Measured (mg/L)	Predicted (mg/L)	Measured: predicted	Measured (mg/L)	Predicted (mg/L)	Measured: predicted
October 2010	5.32	10.03	0.53	6.23	14.63	.43
April 2011	3.06	1.80	1.70	4.93	3.41	1.45
October 2011	2.93	1.36	2.16	5.36	2.83	1.90
April 2012	3.19	2.04	1.56	5.21	3.28	1.59

2.7 tritium units (TU) at piezometer 6, which indicates that there is some component of modern precipitation in the water. Water at piezometer 6 had a ^{14}C value of 96.6±0.4 pmc and a $\delta^{13}C$ of -8 per mil. The high ^{14}C pmc and presence of tritium indicate the water at piezometer 6 is modern and therefore age calculation is not resolvable using equations 7, 8 and 9.

Shea Spring (TZG07) water was also analyzed for noble gas concentrations to estimate the elevation and temperature where the water discharging at the spring originally entered the subsurface as precipitation. Using methods in Stute and Schlosser (2000), we calculate that the recharge elevation and temperature range for Shea Spring (TZG07) is between 6,060 and 7,220 feet and between 9.9 °C and 8.6 °C. The recharge elevation range calculated by this method is a bit lower than the elevation predicted using stable isotopes in equations 3 and 4 of (8,075 and 7,374 ft elevation for ^{18}O and ^{2}H, respectively), but this result—high-elevation recharge from both methods—implies that precipitation recharge is occurring in the mountainous regions to the east and north of Tavasci Marsh. The temperature of the Shea Spring, 20.3 °C, is warmer than the average annual air temperature measured at Tuzigoot National Monument of 17.3 °C (fig. 2), and implies that the water is being warmed as it moves through the subsurface following recharge as precipitation.

Dissolved Organic Material

Gains or losses of organic material during water transport through Tavasci Marsh were examined using DOC concentrations. Averages and standard deviations of DOC concentrations ranged from 0.4±0.08 mg/L at Shea Spring (TZG07) to 7.7±6.2 mg/L for all piezometer data combined (fig. 12*A*). Average DOC concentrations at the TZG03 and outflow sites were 3.6±1.1 mg/L and 5.4±0.6 mg/L, respectively. Assuming that all water is sourced from Shea Spring and shallow groundwater (observed at piezometer 6) and that there is no reactive loss of DOC, concentrations measured at TZG03 and at the outflow site suggest that there was approximately a 50 percent loss in DOC during

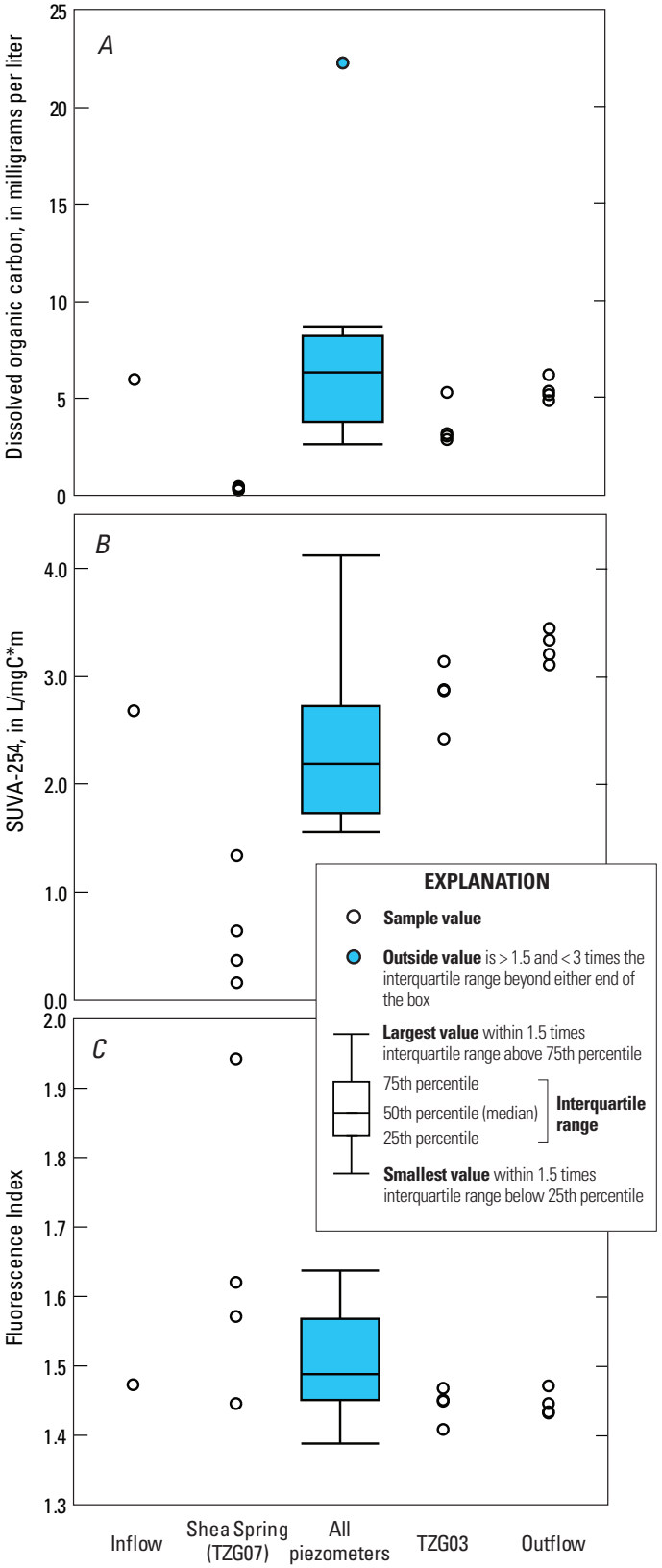

Figure 12. Box plots of dissolved organic carbon (DOC) concentration and related measurements at water-sampling sites in Tuzigoot National Monument, Arizona. *A*, Concentration of DOC, in milligrams per liter. *B*, Specific Ultraviolet Absorbance at 254 nm (SUVA-254); and *C*, fluorescence index. Data from all piezometers were combined.

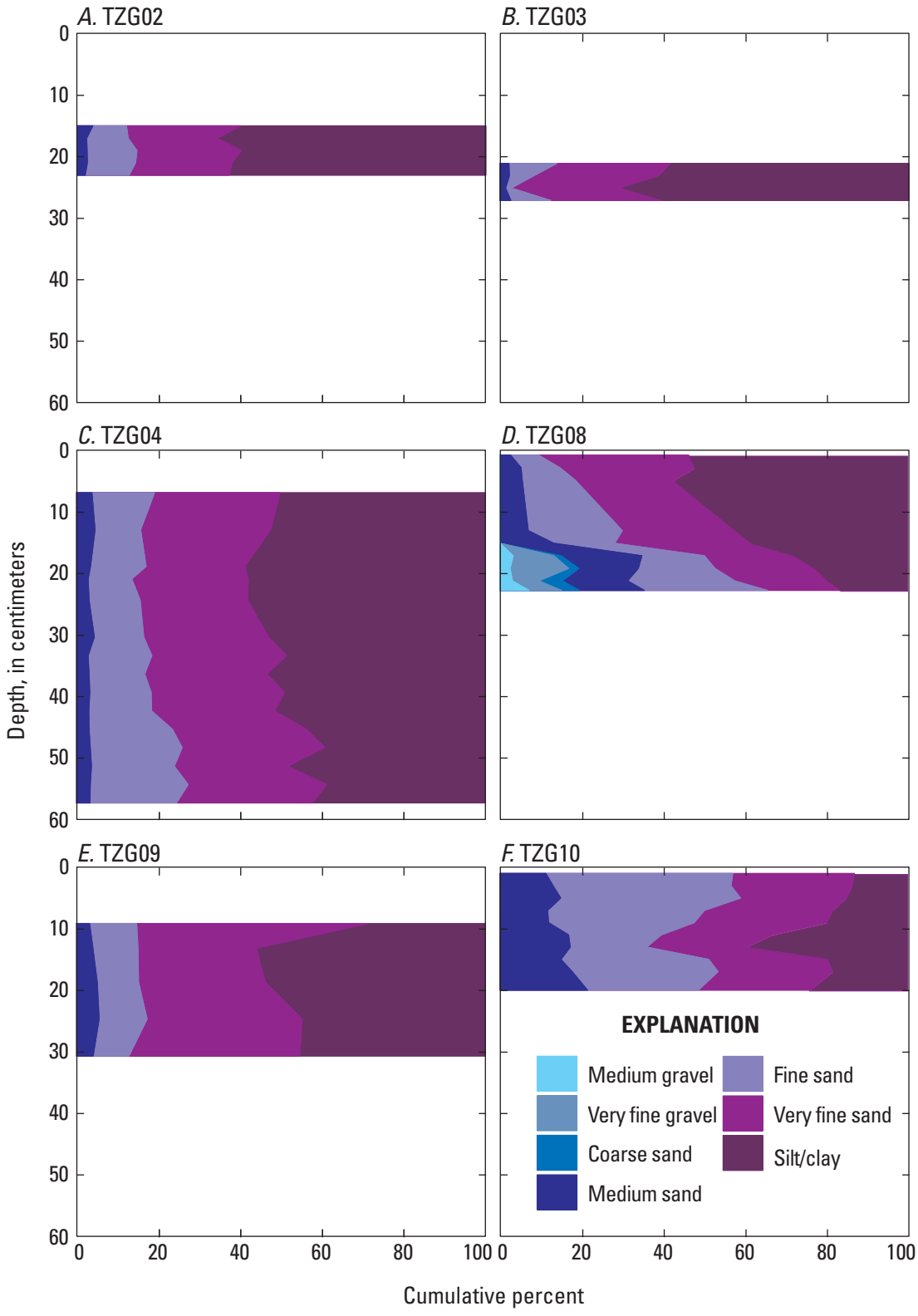

Figure 13. Plots of particle size distribution for all cores collected from Tavasci Marsh. *A*, TZG02; *B*, TZG03; *C*, TZG04; *D*, TZG08; *E*, TZG09; and *F*, TZG10.

transport in October 2010 (table 13). However, this result may be biased by the influence of evaporation as indicated by the isotopic signature at the outflow site in October 2010. In contrast, in April and October 2011, there was a increase in DOC concentration during transport from the sources to all other sample sites ranging from 45 percent at the outflow to 116 percent at TZG03.

We measured specific ultraviolet absorption at 254 nm (SUVA-254) in order to investigate properties of dissolved organic matter in the water of Tavasci Marsh. Fe concentrations greater than 0.5 mg/L can influence absorbance and fluorescence measurements (Weishaar and others, 2003), and two of the water samples—Piezometer 1 sampled in October 2011 and Piezometer 6 sampled in April 2012—had Fe concentrations above this threshold and therefore spectroscopic results for DOM characterization of these two samples are not included in the following analysis. Average SUVA-254 values ranged from 0.6±0.5 L/mgC*m at Shea Spring (TZG07) to 3.3 ± 0.1 L/mgC*m at the outflow (fig. 13*B*); indicating a low degree of aromaticity at Shea Spring (TZG07) and an intermediate degree of aromaticity at the outflow. Average SUVA-254 values at the other three sites were similar to the outflow value: 2.7 L/mgC*m at the inflow, 2.7±0.8 L/mgC*m for all piezometers combined, and 2.8 ± 0.3 L/mgC * m at TZG03. Fluorescence indexes (FIs) generally followed the opposite pattern of the SUVA-254 data. Average FIs ranged from 1.44±0.03 at TZG03 to 1.65±0.21 at the Shea Spring (TZG07) site (fig. 13*C*); indicating a mix of terrestrially-derived or higher-plant-derived and microbially-derived DOM at TZG03 and a possible higher microbial source of DOM at Shea Spring (TZG07). Average FIs at the other three sites were intermediary between TZG03 and Shea Spring (TZG07), but more similar to TZG03 with an FI of 1.47 at the inflow site, 1.51±0.09 for all piezometers combined, and 1.45±0.02 at the outflow site.

Taken together, the DOC concentration, SUVA-254, and FI data suggest that Shea Spring (TZG07) contributes microbially-derived, low-DOC water with low aromaticity to the marsh; whereas the shallow groundwater contributes a mix of terrestrially- and microbially-derived DOC of intermediate concentration and aromaticity to the marsh. Additionally, the SUVA-254 and FI data suggest that the calculated DOC gain of up to 116 percent and 90 percent (table 13) during transport from the assumed source areas to the TZG03 and outflow sites, respectively, is from a terrestrially derived source or degradation of higher plant material that contributes aromatic DOM to the marsh. If our assumption is correct that Shea Spring (TZG07) and the shallow groundwater around piezometer 6 are the only (or major) sources of water to the marsh, then it is likely that degradation of the abundant cattails in the marsh are contributing to patterns in marsh DOM biogeochemistry, and more generally, water quality in the marsh. In addition, cattail-derived organic material may be contributing to higher As and Fe concentrations through electron shuttling processes (Mladenov and others, 2010).

Sediment

Tavasci Marsh

Sediments collected at Tavasci Marsh were primarily clay or fine sand with larger sandy material present in isolated locations as transported erosional material from the Verde Formation around the margin of the marsh. Decaying plant material and roots were also associated with collected sediments. Sediments were generally oxic and only one water sampling location (piezometer 1) was characterized by a sulfur smell (no sediment sample was collected at this site).

Surface Sediment

Surface sediment samples were collected from cattail root samples in October 2010. Additional surface sediment samples were collected at inflow, TZG03, -01 and -08 at the site of dragonfly larvae samples in April 2012.

In the following discussion of sample results, SQG exceedances refer to sample concentrations (plus uncertainty) that exceeded the 90-percent confidence interval of the SQG (tables 4 and 7). For sample concentrations within the range of uncertainty around the SQG determined for this study, exceedance of the SQG is not certain at the 90-percent confidence level. All surface-sediment sample sites exceeded an SQG for several elements. Most of the exceedances were of the LEL, TEL, or TEC, but five sites (inflow, TZG01, TZG03, TZG05, and Shea Spring [TZG07]) also had at least one element that exceeded a SEL, PEL, or PEC. Elemental exceedances by site are given in table 14.

Sediment Cores

Six sediment cores were collected in Tavasci Marsh (fig. 4) to assess depositional history and establish elemental profiles. Sediment-core samples were not sieved prior to metal and radioisotope analyses in order to preserve depositional character. Previous studies of metal concentrations in sediment of Tavasci Marsh only focused on surface sediment and no subsurface sediment data has previously been published.

Particle Size and Color Distribution

Particle size and color was determined for core sections with sufficient material available following all other analysis. All cores (TZG02, -03, -04, -08, -09, and -10) had some remaining material, but only the lower sections of TZG02 and -03 were analyzed because of high water content in upper sections. The majority of the 48 core sections analyzed for particle size distribution were composed of particles <0.25 mm (fine sand) with an average and standard deviation of 91.4±9.2 percent <0.25 mm; followed by less than very fine sand (0.125 mm) with 73.0±17.2 percent finer than 0.125 mm. All sediment cores analyzed for particle size distribution contained particles in the silt/ clay size range (less than 0.063 mm) with 43.5±16.5 percent finer than 0.063 mm (fig. 13).

Table 14. Exceedance of sediment-quality guidelines (SQG) in surface-sediment samples from Tavasci Marsh.

[Exceedance refers to concentrations greater than the SQG plus uncertainty at the 90-percent confidence level; within uncertainty refers to concentrations within the range of uncertainty at the 90-percent confidence level around the SQG; LEL, lowest effect level; SEL, severe effect level; TEL, threshold effects level; PEL, probable effects level; TEC, threshold effect concentration; PEC, probable effect concentration; --, no exceedance; location of sites shown in figure 4; elements in bold red exceed or are within uncertainty of the respective column for SEL, PEL, or PEC, and exceedance of the respective LEL, TEL, or TEC is implied, composite refers to a single surface sediment sample from TZG01 that was not wet sieved before sample analysis]

Site	LEL and SEL		TEL and PEL		TEC and PEC	
	Exceeds	Within uncertainty	Exceeds	Within uncertainty	Exceeds	Within uncertainty
Inflow	Cd, Cr, Ni, Pb, **As**	Zn, **Cu**	Cd, Ni, Pb, **As**	Cr, Zn, **Cu**	Cd, Cu, **As**	Cr, Ni, Pb, Zn
TZG01 (composite)	Cd, Cr, Ni, Pb, Zn, **As, Cu**	--	Cd, Cr, Ni, Pb, Zn, **Cu, Zn**	**As**	Cd, Cr, Ni, Pb, Zn, **As, Cu**	--
TZG01 (wet sieved)	As, Cd, Cr, Ni, Pb, Zn, **Cu**	--	As, Cd, Cr, Ni, Pb, Zn, **Cu**	--	As, Cd, Cr, Ni, Pb, Zn	**Cu**
TZG03 (October 2010)	As, Cd, Cu, Ni, Zn	Cr, Pb, **Cu**	As, Cd, Cu, Ni, Pb, Zn	**Cu**	Cd, Cu, Zn	As, Cr, Ni, Pb
TZG03 (April 2012)	As, Cd, Cu, Ni, Pb, Zn	Cr, **Cu**	As, Cd, Cu, Ni, Pb, Zn	**Cu**	As, Cd, Cu, Pb, Zn	Cr, Ni
TZG04	Cd, Cr, Cu, Ni	As, Pb, Zn	Cd, Cr, Cu, Ni	As, Pb, Zn	Cd, Cr, Cu, Ni	As, Zn
TZG05	As, Cd, Ni, Pb, Zn	Cr, **Cu**	As, Cd, Ni, Pb, Zn	**Cu**	Cd, Cu, Ni, Zn	As, Cr, Pb
TZG06	Cd, Cr, Cu, Ni	As, Pb, Zn	Cd, Cu, Ni	As, Pb, Zn	Cd, Cu	As, Cr, Ni, Pb, Zn
Shea Spring (TZG07)	As, Cd, Cr, Ni	Pb, Zn, **Cu**	As, Cd, Ni	Cr, Pb, Zn, **Cu**	Cd, Cr, Cu	As, Ni, Pb, Zn
TZG08 (October 2010)	As, Cd, Cr, Cu, Ni	Pb, Zn	As, Cd, Cu, Ni	Cr, Pb, Zn	As, Cd, Cu	Cr, Ni, Pb, Zn
TZG08 (April 2012)	As, Cd, Cr, Cu, Ni, Pb	Zn	As, Cd, Cu, Ni, Pb	Cr, Zn	As, Cd, Cu	Cr, Ni, Pb, Zn

The only core that contained particles larger than 0.5 mm was TZG08. The deepest 4 intervals of TZG08 contained gravel-sized sediments (between 2 and 16 mm; table 3, fig. 13*D*). The gravel particles were mainly subangular white (10YR 8.5/1) limestone but there were also some subrounded to rounded particles that ranged from weak red (10R 5/3) to green and purple sandstone.

Sediment color in all sediment core sections ranged from brown (7.5YR 5/3) to light gray (10YR 7/2). Color name and definition are listed in appendix B, table 4.

Radioisotope Age Dating

Sediment mass accumulation rate (MAR) versus depth was determined from the ^{210}Pb profile using the CRS method (Appleby and Oldfield, 1992), which assumes a constant rate of input of unsupported ^{210}Pb activity per gram of sediment and determines a sediment accumulation rate for each core interval by mass balance (in units of grams per centimeter squared per year, g/cm^2/yr). The method allows for variations in rate of sediment accumulation with depth. The age of each sediment interval is determined at its mid-depth and subtracted from the core collection date to assign calendar year for each interval.

The anthropogenic radionuclide ^{137}Cs can provide a means to test the ^{210}Pb chronology because of its well-known atmospheric input history. In sediments, ^{137}Cs is derived from atmospheric fallout from above-ground nuclear weapons and the first occurrence is commonly assigned a date of 1952, with maximum deposition occurring during the years 1963 and 1964, and no measurable fallout after 1976 (Callender and Robbins, 1993). The profile of ^{137}Cs in an undisturbed sediment profile should reflect this history of atmospheric fallout and provides time horizons (first occurrence and highest activity) to derive sediment accumulation rates.

The activity of ^{210}Pb in the sediment core from TZG02 decreases with depth to the supported activity at 16 cm, which is defined by ^{226}Ra activity (fig. 14*B*). The ^{210}Pb activity decreases exponentially with respect to cumulative sediment dry mass until reaching the supported activity defined by ^{226}Ra (fig. 14*C*). An exponential decrease is expected for decay of the unsupported ^{210}Pb activity over time by its characteristic decay rate (half-life 22.3 years) in a system with constant sediment accumulation rate. At site TZG02, sediments had a very high water content (>94 percent) in the upper 10 cm (fig. 14*A*) and likely a high component of organic material. This zone comprises a small fraction (<3 pecent) of the total sediment mass sampled, and the transition to more consolidated

sediments between 10 and 15 cm marks a switch to much lower water content and clay-like consistency that extends to the bottom of the core. The lower ^{226}Ra activity of the unconsolidated upper 10-cm zone is consistent with more organic material. The ^{226}Ra activity increases by as much as a factor of three in the more consolidated sediments below, consistent with higher inorganic or clay content that underlies the less consolidated material of the upper 10 cm (fig. 14).

The resulting age model, depicted in figure 14*D* using the CRS method, is linear with depth in the upper 10 cm (to 2001), consistent with a near-constant MAR. Deposition date decreases at greater rate below 10 cm suggesting a large increase in MAR with increasing depth below. The large uncertainty in the deposition dates older than 1990 are the result of a very small difference between the total ^{210}Pb and the supported activity. The uncertainty in age is estimated by propagating the measured activity to the calculated MARs and the resulting deposition dates. The model date for the deepest sample (20–22 cm, 1916) is considered unreliable because of the large uncertainty value. The ^{210}Pb age model suggests that the unconsolidated sediments in the upper 10 cm represent deposition in the last 10 to 15 years.

In core TZG02, ^{137}Cs activity is at or below the detection limit in the upper 8 cm, then increases with increasing depth to the highest activity in the deepest interval (22–24 cm; fig. 15). The increasing ^{137}Cs with depth without an apparent maximum is consistent with a younger than 1963 deposition date for the depth range of sediments sampled.

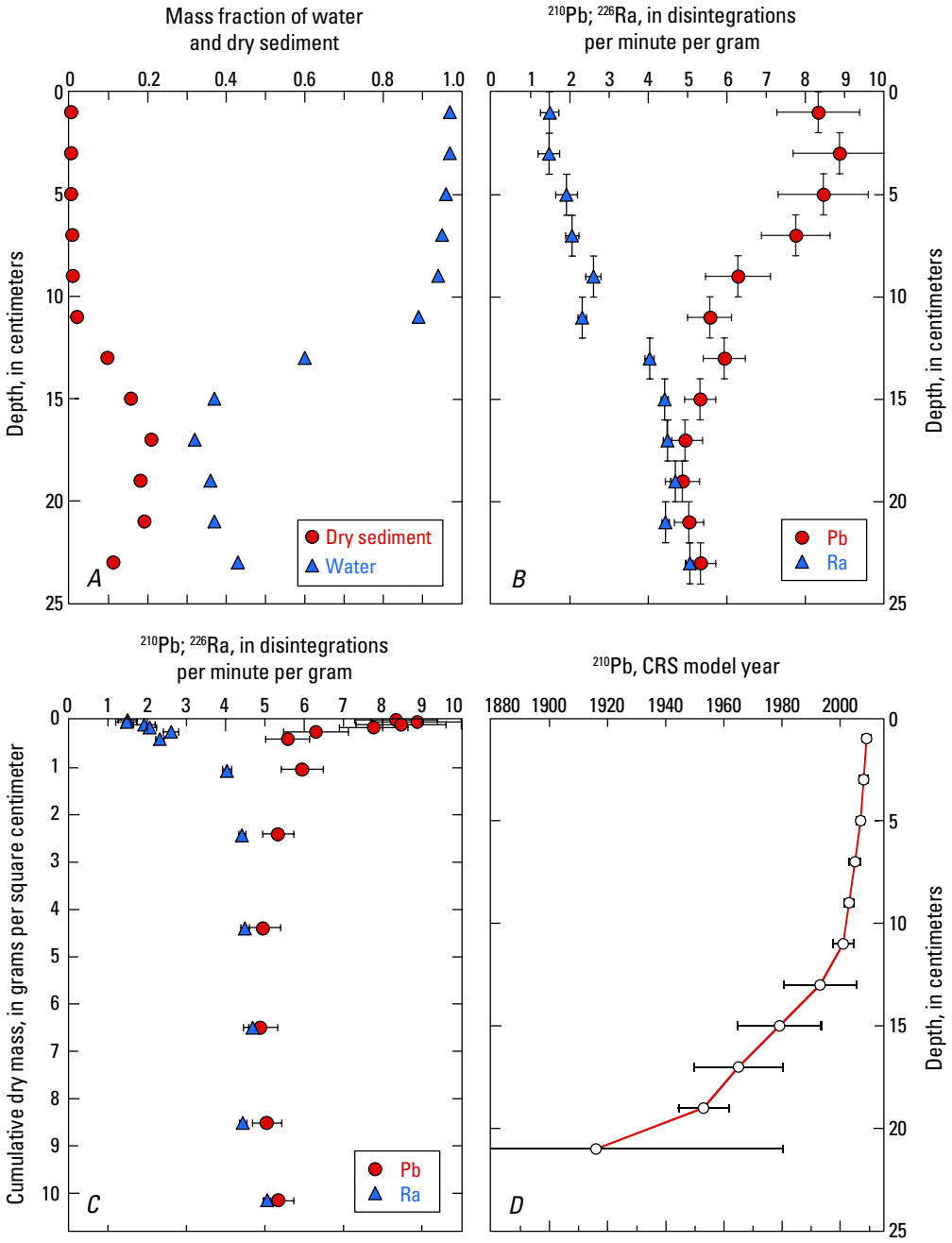

Figure 14. Plots showing water content and radioactivity in sediment core TZG02 from Tavasci Marsh. *A*, Fractional water content of sediment versus depth; ^{210}Pb and ^{226}Ra activity in sediment versus depth (*B*) and versus cumulative dry mass (*C*); *D*, ^{210}Pb CRS Model Date for core TZG02. Horizontal error bars depict 1-sigma uncertainty in the measured activity based on counting statistics. Vertical error bars depict depth range of sample interval.

The ^{137}Cs profile is inconsistent with ^{210}Pb-derived age of greater than 100 years at the core bottom, although there is large error associated with the lowest core section.

At site TZG03, the unconsolidated, higher water content sediments extend deeper (to about 15 cm; fig. 16), and the transition to compacted, low-water-content sediments occurs more gradually than observed in core TZG02. The general features of the ^{210}Pb, ^{226}Ra, and ^{137}Cs activity profiles in this core (figs. 16 and 17) are similar to those for TZG02. The ^{210}Pb chronology for TZG03 using the CRS method also yields deposition dates of younger than 15 years for the unconsolidated zone (fig. 16*D*). The ^{210}Pb model ages for underlying sediments increase rapidly with depth, and have a large associated uncertainty because of the small difference between total ^{210}Pb and the supported activity defined by ^{226}Ra.

Little or no detectable ^{137}Cs was measured in the upper 16 cm, but there was detectable and increasing activity with depth below 16 cm (fig. 17). The ^{137}Cs activity in the 26–28 cm interval of TZG03 (0.61 pCi/g) is about half that of the deepest interval in TZG02 (24–26 cm; 1.21 pCi/g) (figs. 15 and 17), possibly the result of a higher sediment accumulation rate at TZG03. A similar disparity between the apparent ^{210}Pb ages and the increase of ^{137}Cs activity to the bottom of the profile is observed for both TZG03 and TZG02.

The sediment core at TZG04 was collected from a small open water area near the outlet end of the marsh system. In contrast to the previous core sites, consolidated sediments occurred throughout the 58-cm core, with water content decreasing from 59 percent at the core top to 30 percent in the deepest interval (appendix B, table 5). Very low activity and no unsupported ^{210}Pb was measured in multiple intervals throughout the sediment core (fig. 18). The supported activity (^{226}Ra) was fairly constant throughout the core (fig. 18), but about half of the ^{226}Ra activity in the consolidated sediments at TZG02 (fig. 14) and TZG03 (fig. 16), perhaps reflecting a difference in sediment source or composition. The CRS age model was not applied to this profile because the small difference between total ^{210}Pb and the supported activity would result in very large uncertainty in model ages.

Near-constant ^{137}Cs activity was measured throughout the upper 40 cm of TZG04, with a small activity maximum between 47 and 50 cm (fig. 19), which likely reflects the maximum fallout delivery in 1963–64. The activity decreases below but is still measurable in the deepest interval. An overall sedimentation rate of 1.1 cm/year is estimated by assigning a date of 1963 to the mid-depth of the 47–50 cm interval (48.5 cm) and assuming a constant accumulation rate. The ^{137}Cs activities in the TZG04 sediment core are much lower than the highest activities observed at the other two sites (figs. 15 and 17), which may be the result of greater dilution by sediments during deposition at this site.

At site TZG08, unsupported ^{210}Pb generally decreases with depth, with two low values at intermediate depths (8–12 cm), corresponding to a section of mostly plant material (fig. 20). A large root mass was removed from the 4–14 cm depth range (6 to 12 cm cells are shaded in appendix B, table 5 with note about root material) during sectioning and not included in the analysis, and accounting for this mass loss in the accumulation rate would be required in order to calculate a sediment accumulation rate. A sediment mass accumulation could be derived from the ^{210}Pb profile if these intervals are excluded, but because of the issues related to the root and sediment mass, age dates could not be calculated from the ^{210}Pb activities. ^{137}Cs activity is near constant over the upper 16 cm, and then drops off below (fig. 21). Because of this constant activity and the absence of activity maximum corresponding to peak fallout delivery of 1963–64, ^{137}Cs cannot be used to date sediments at this site. The presence of ^{137}Cs throughout the profile to the bottom of the core at 24 cm implies that it was all deposited within the past 60 years.

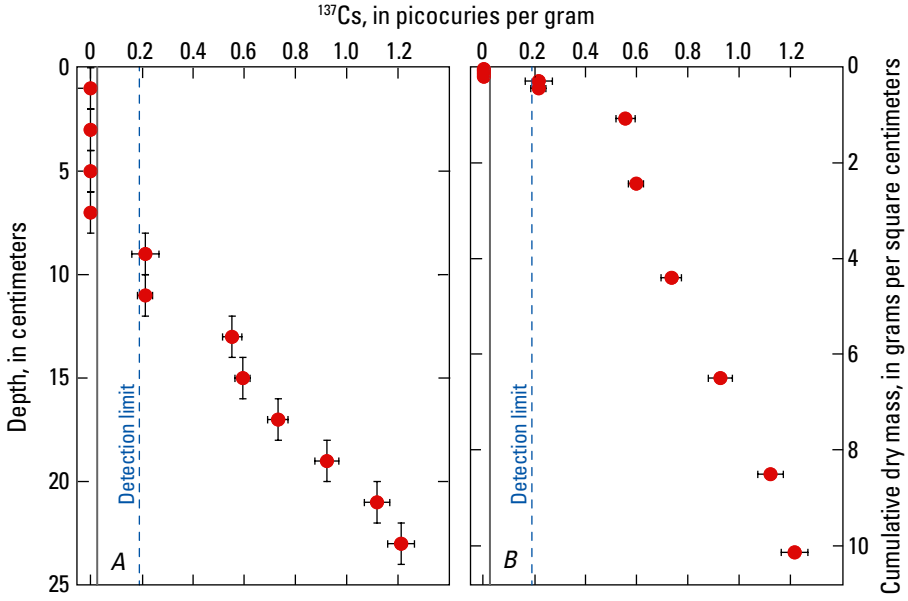

Figure 15. Plots of ^{137}Cs activity in sediment core TZG02 versus depth (*A*) and and versus cumulative dry mass (*B*).

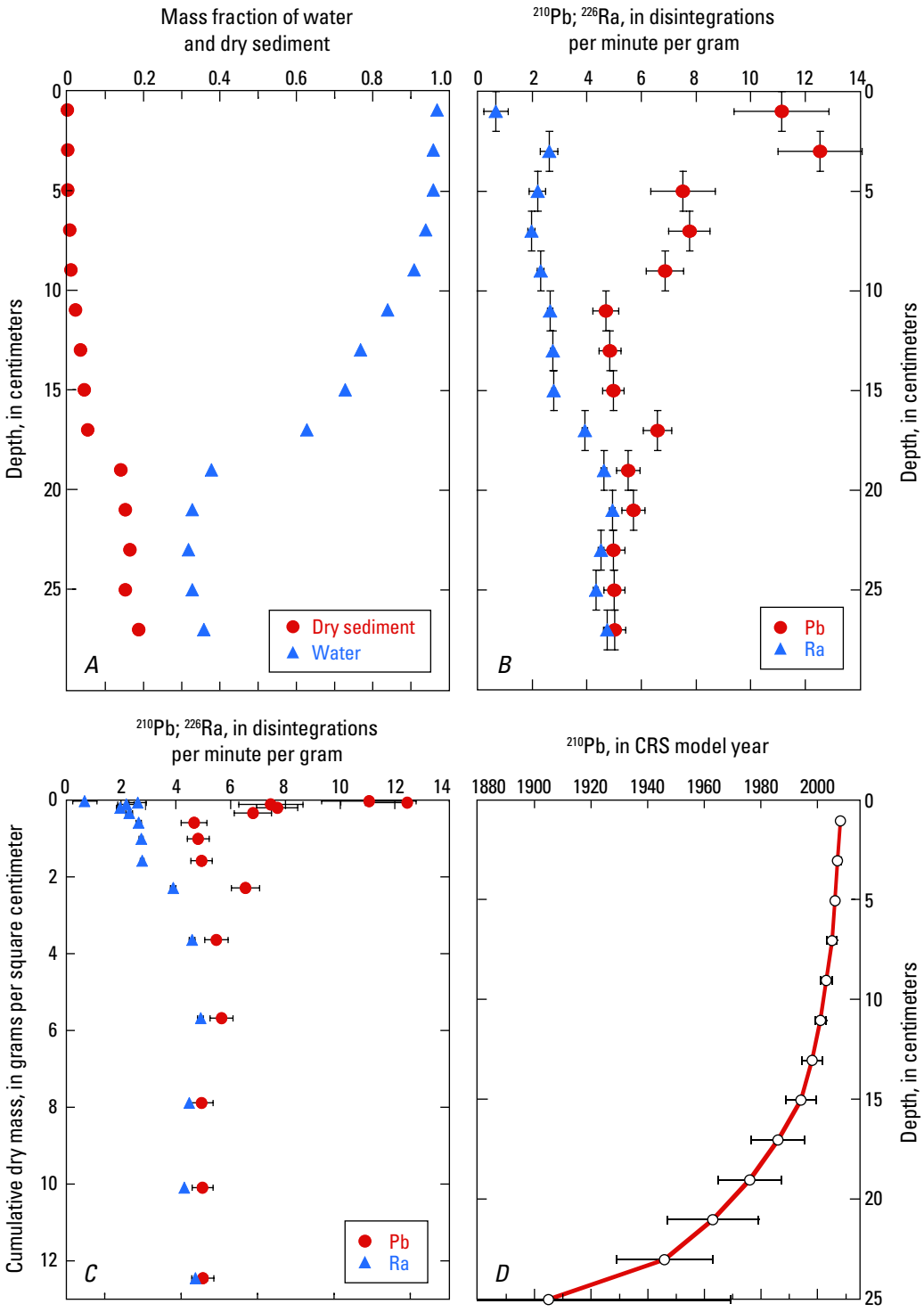

Figure 16. Plots showing water content and radioactivity in sediment core TZG03. *A*, Fractional water content of sediment as a function of depth in core. *B*, ^{210}Pb and ^{226}Ra activity in sediment versus depth; *C*, ^{210}Pb and ^{226}Ra activity versus cumulative dry mass; and *D*, ^{210}Pb CRS age model. Horizontal error bars depict 1-sigma uncertainty in the measured activity based on counting statistics. Vertical error bars depict depth range of sample interval.

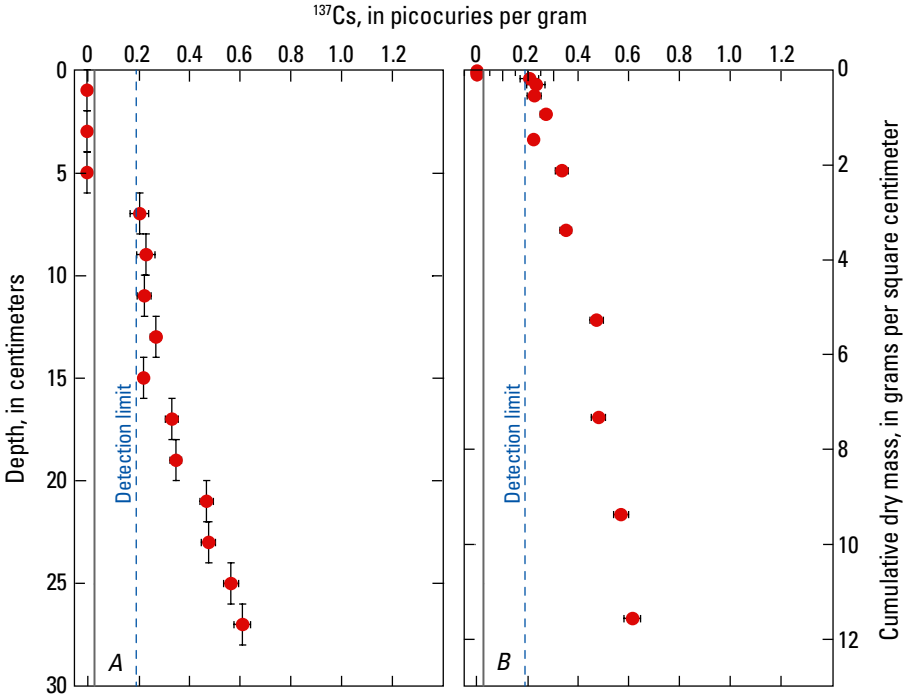

Figure 17. Plots of ^{137}Cs activity in sediment core at TZG03 versus depth (*A*), and cumulative dry mass (*B*).

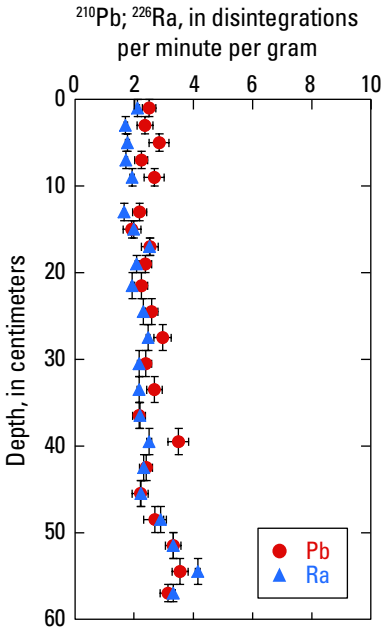

Figure 18. Plot showing activity of ^{210}Pb and ^{226}Ra versus depth in sediment core TZG04.

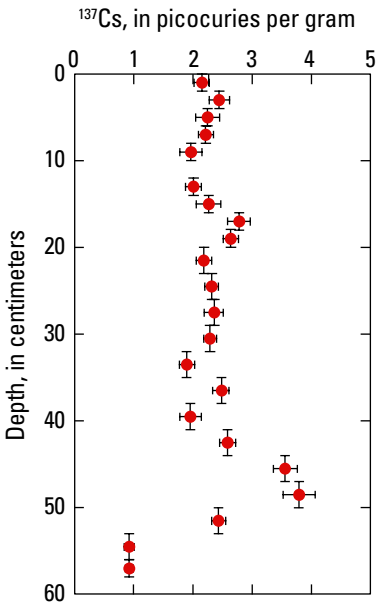

Figure 19. Plot of ^{137}Cs activity versus depth in sediment core TZG04.

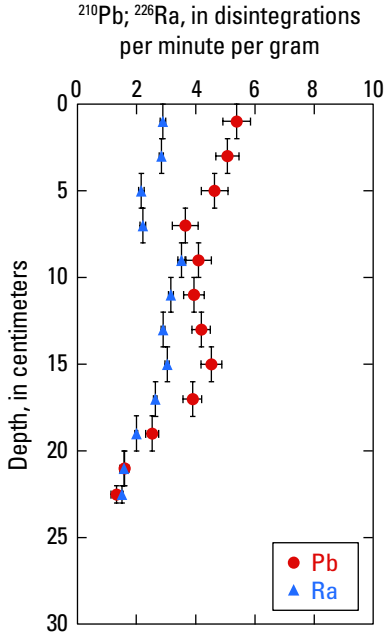

Figure 20. Plot of ^{210}Pb and ^{226}Ra activity versus depth in sediment core TZG08.

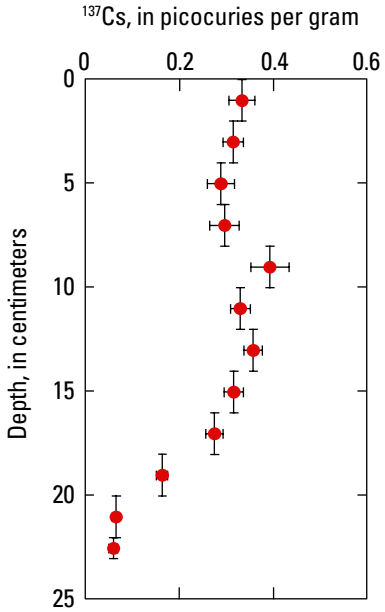

Figure 21. Plot of ^{137}Cs activity versus depth in sediment core TZG08.

At site TZG09, unsupported ^{210}Pb decreases exponentially with depth, excluding the relatively low value at 12–14 cm (fig. 22). ^{137}Cs activity has a very broad subsurface maximum between 10 and 24 cm that is not well defined, with measurable ^{137}Cs present to the bottom of the core (fig. 23). Dating based on ^{137}Cs is limited to concluding that sediment in the upper 34 cm was deposited over the past 60 years.

The western side of Tavasci Marsh includes a man-made irrigation ditch that was designed to convey water from Pecks Lake through Tavasci Marsh in a channelized manner. Historically this ditch was reported to have had about a foot of sediment removed annually beginning a couple of years after the land was leased from UVCC in 1928 (Stoutamire, 2011). Sediment cores TZG08 and -09 were collected near the irrigation ditch (fig. 4) and show a distinct radioisotope pattern with depth compared with the other sediment cores collected from Tavasci Marsh. Sediment cores at TZG08 and -09 are characterized by two divergences of ^{210}Pb and ^{226}Ra (figs. 20 and 22), and the pattern of ^{137}Cs with depth (figs. 21 and 23) mimics ^{210}Pb. These patterns would not be expected from a site with continuous sediment deposition where the unsupported ^{210}Pb is highest in surface sediments then decreases with increasing depth to the supported activity (from ^{226}Ra activity), as observed in TZG02 and -03 (figs. 14 and 16). The deviation from this trend expected for continuous sedimentation observed in sediment cores from TZG08 and -09 may indicate disturbance of sediment above the middle portion of the cores, which could be from sediment removal from the nearby ditch.

The two deepest intervals of TZG08 and -09 have some of the lowest concentrations of ^{226}Ra of all sediment cores and ^{210}Pb is at equilibrium with ^{226}Ra decay, suggesting older sediment likely of a different source. The complexity of the unsupported ^{210}Pb profiles at these sites does not allow application of sediment accumulation rate calculations such as by the CRS method.

Sediment core TZG10 was collected on the northern edge of the marsh at a location with sediment deposits derived from the surrounding hillside, which sits on top of older marsh material. The upper 10 cm of the core had more medium and fine sand than other cores (fig. 13*F*). The high sand content may dilute ^{210}Pb activities, which is consistent with the lower activity between 0 and 10 cm, than in the two intervals below. The increase in unsupported ^{210}Pb down core starting at 10 cm suggests significant disturbance or reworking of the sediment profile (fig. 24) and no age dates could be calculated using the ^{210}Pb and ^{226}Ra activities. ^{137}Cs activity increases slightly over the upper 20 cm with a break in slope following the 12–14 cm core section (fig. 25). No distinct maximum in ^{137}Cs activity is observed and so dates cannot be assigned from ^{137}Cs profile.

The maxima in ^{210}Pb in core TZG10 between 10 and 14 cm are associated with a sudden increase in the amount of plant material in the sediment and suggests that material below 14 cm may be older marsh material that was buried by a small debris flow from the nearby Verde Formation. The plant material was removed from the sample before sediment analysis. Sediment from core sections 10–12 and 12–14 cm are also characterized by a sharp increase in silt and clay, marking the transition to marsh material (fig. 13). Lower ^{210}Pb activity and metal concentrations above 10 cm, along with higher sand content, indicate that the upper core sections are more recent erosional deposits that cover older marsh material below.

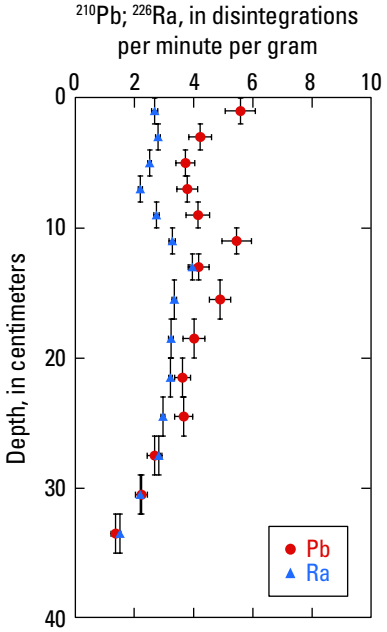

Figure 22. Plot of ^{210}Pb and ^{226}Ra activity versus depth in sediment core TZG09.

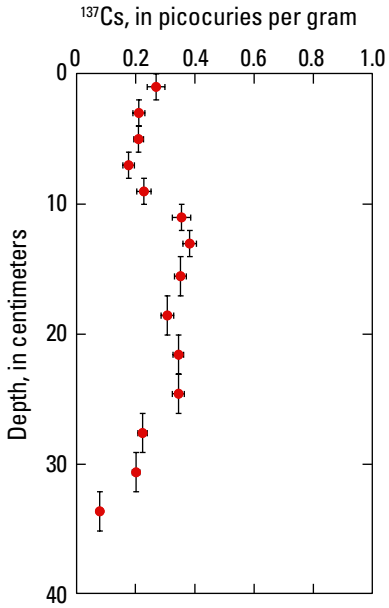

Figure 23. Plot of ^{137}Cs activity versus depth in sediment core TZG09.

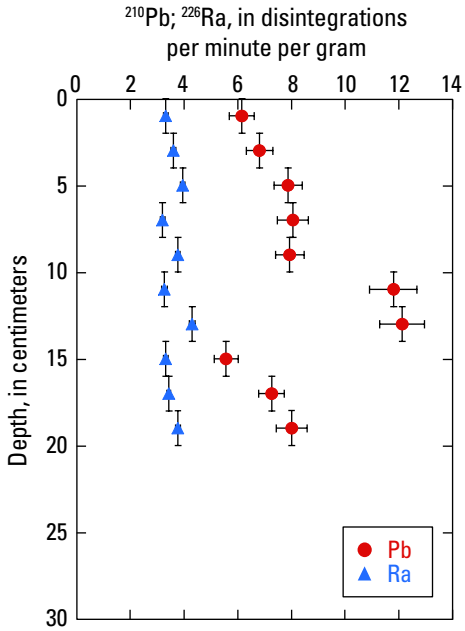

Figure 24. Plot of ^{210}Pb and ^{226}Ra activity versus depth in sediment core TZG10.

The apparent disparity between ^{210}Pb and ^{137}Cs deposition dates may be the result of a combination of (1) low unsupported activities, in part due to low atmospheric deposition of ^{210}Pb in the southwestern U.S. (Fuller and Hammond, 1983; Piliposian and Appleby, 2003) that limits the ability to constrain sediment ages from ^{210}Pb because of large propagated uncertainties in model dates, and (2) the possible postdepositional mobility of ^{137}Cs in highly organic sediments. Mobility of ^{137}Cs independent of sediment particles has been documented in sediments with high organic matter contents and high rates of organic matter degradation. Remobilization of ^{137}Cs results from desorption from clays by cation exchange for ammonium ions produced during diagenesis. Subsequent diffusion of dissolved ^{137}Cs results in deeper penetration of the radionuclide and an upward migration of the activity maximum (Anderson and others, 1987). Postdepositional mobility of ^{137}Cs may have modified the activity profiles in cores from Tavasci Marsh. The ^{210}Pb data cannot be improved with the current analytical capability. The high unsupported ^{210}Pb activities in the upper 10 cm of TZG02 and -03 likely reflect recent fallout deposition combined with little dilution by terrigenous sediment, but these factors only account for a small component of the whole-core unsupported ^{210}Pb inventory. The high activities of ^{210}Pb in the surface layer observed in TZG02 and -03 are not observed in core TZG04, which does not have a similar high-water-content, unconsolidated zone at the surface like the other two cores. The high ^{210}Pb and lack of significant ^{137}Cs in the upper 10 to 15 cm of TZG02 and -03 indicates that the substrate likely was deposited within the past 20 years following the end of ^{137}Cs atmospheric deposition. The high water content and low solid density, likely from high organic content, suggest that little terrigenous sediment is currently transported to and deposited at these sites. However, the observed profiles at TZG02 and -03 showing increasing ^{137}Cs activity with depth would not be expected from this process. The lack of agreement between the ^{137}Cs profile with the apparent chronology derived from ^{210}Pb is difficult to resolve with the present data set. Cores that capture the full ^{137}Cs profile and measurement of other constituents may help resolve this disparity.

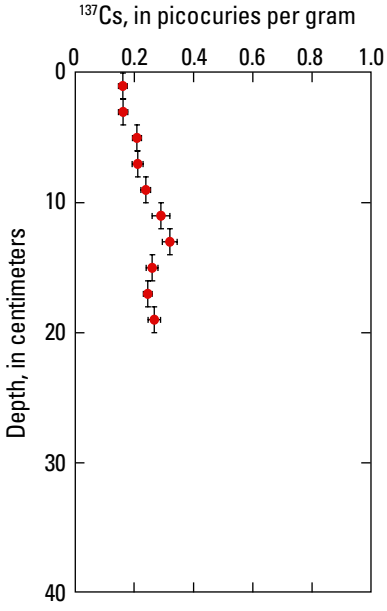

Figure 25. Plot of ^{137}Cs activity versus depth in sediment core TZG10.

Elemental Profiles

Elemental profiles for the nine elements of interest (As, Cd, Cr, Cu, Hg, Ni, Pb, Se, and Zn) are plotted versus depth in figure 26. Arsenic and Se were greatest in the upper sections of cores TZG02 and -03 (fig. 26). Five elements of interest (Cd, Cu, Hg, Pb, and Zn) and five other elements (Bi, In, Sb, Sn, and Te) follow a pattern of increasing concentration with depth at three core sites in the southern half of the marsh (TZG02, -03, and -04) (fig. 26). At TZG08, however, all of these ten elements follow a pattern of decreasing with depth (fig. 26), opposite the trend observed at TZG02, -03, and -04. These ten elements may provide a unique signature indicative of the source of elevated concentrations.

The ten aforementioned elements show a statistically significant (p-value <0.05) strong directional trend (*tau* > 0.5) with depth using Kendall's tau in cores at TZG02, -03, -04, -08, and -10 (fig. 27). All significant strong correlations at TZG10 were positive, which indicates that the upper sections composed of erosional material from the surrounding hillside have lower elemental concentrations than the older, deeper marsh sediments. The erosional deposits at the surface of core TZG10 had some of the lowest As concentrations of all sediment core sections (fig. 26*A*). Most other element concentrations from the surface of core TZG10 were intermediate compared to the range of other shallow-sediment core sections (fig. 26).

For several elements, the concentration of the two deepest core sections is often several times greater than the shallowest two core sections at TZG02, -03, and -04 and less than the top sections at TZG08 and -09 (table 15). Nine of the ten elements (Hg was not measured in all core sections), which increased significantly with depth at TZG02, -03, and -04 (figs. 26 and 27), were at least a factor of 1.7 greater and up to 7.8 times greater in the bottom two sections of the core compared with the top two sections (table 15). In contrast, top and bottom sections from cores TZG08 and -09 were either the same or as low as a factor of 0.2 less in the bottom sections compared with the top sections (table 15). At TZG10, most elements were about 1.5 times greater at the bottom of the core (table 15).

A large proportion of the total mass of metal and trace elements in sediment is usually associated with fine-grained sediments, including clay and silt particles and particulate organic carbon (Shelton and Capel, 1994). Sediment core sections were not sieved before analysis in order to understand metal and trace element concentrations in the raw sediment, but they were analyzed for total and carbonate carbon (from which organic carbon was calculated).

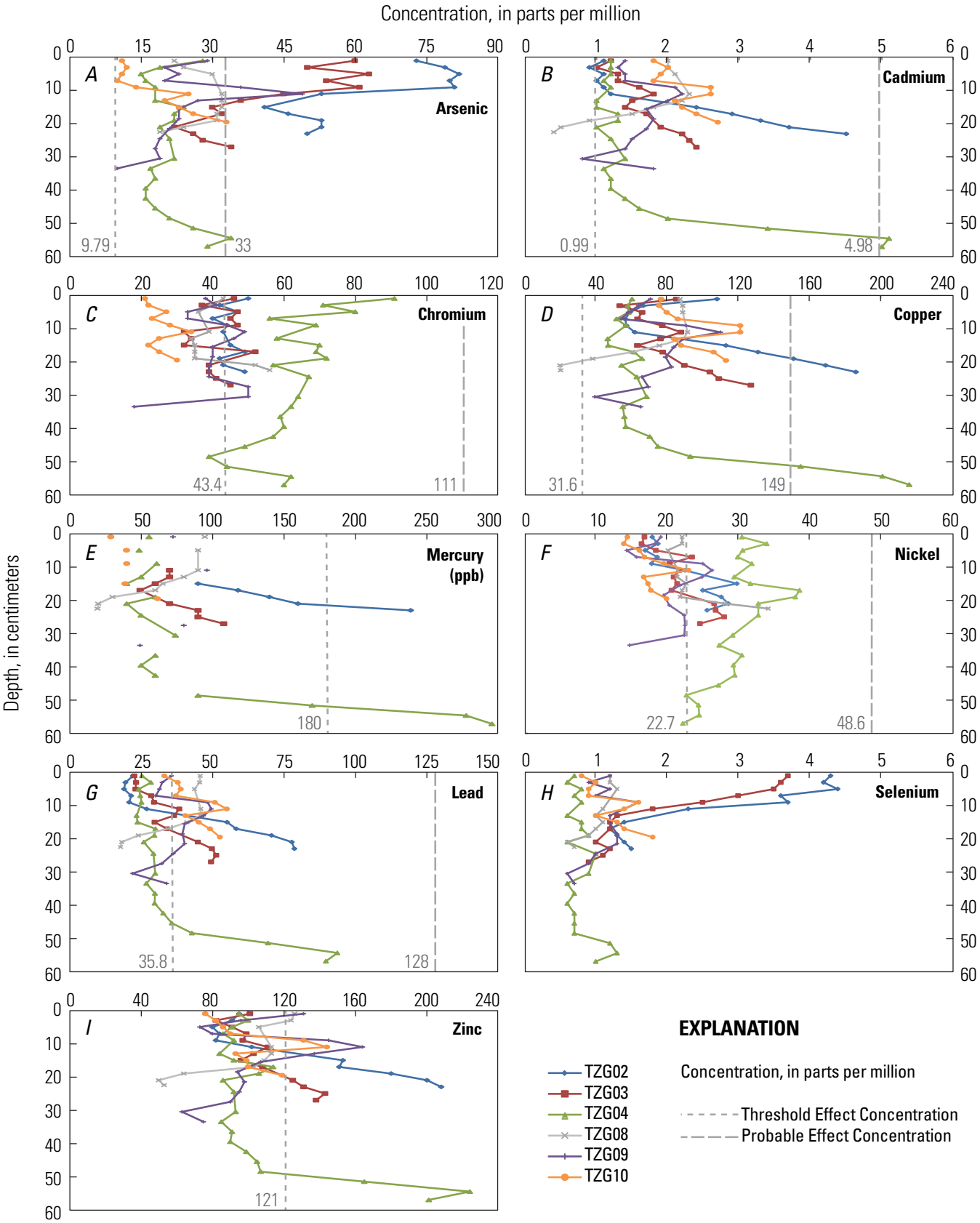

Figure 26. Plots of elemental concentrations in sediment cores at Tavasci Marsh (for sample locations see figure 5). Sediment quality standards are included for reference; *A*, arsenic; *B*, cadmium; *C*, chromium; *D*, copper; *E*, mercury; *F*, nickel; *G*, lead; *H*, selenium; and *I*, zinc. Note that mercury concentrations are given in parts per billion (ppb).

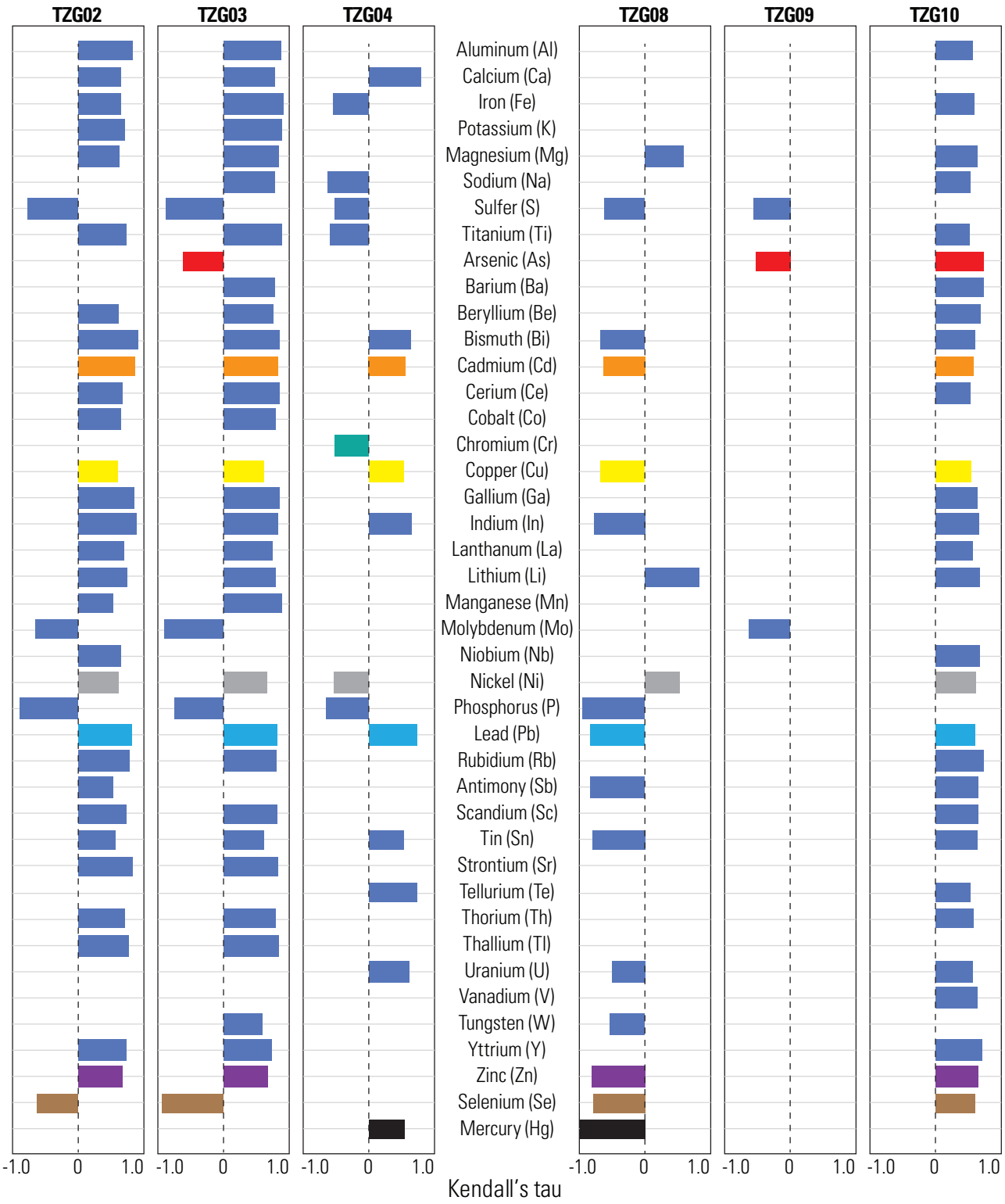

Figure 27. Horizontal bar charts showing major and trace elements having statistically significant trends with depth (p-value < 0.05) and Kendall's tau values greater than 0.5 or less than -0.5 in sediment cores collected at Tavasci Marsh.

The elemental increase with depth in these cores is not associated with a similar proportional change in sediment size or organic carbon (figs. 13, 26, and 28). The highest organic carbon values in the marsh are at the tops of cores TZG02 and -03 then decrease significantly with depth. Arsenic and Se are high in the upper sediments where there is more organic carbon, but the 10 other elements (Cd, Cu, Hg, Pb, Zn, Bi, In, Sb, Sn, and Te) are most concentrated in the lower sediments where there is less organic carbon (figs. 26 and 28*A*,*B*).

At TZG04, organic carbon and particle size distribution are fairly consistent with depth, but this core does exhibit the drastic increase in concentration below about 50 cm for the 10 elements noted above (figs. 13*C*, 26, and 28*C*). At TZG08, the ten elements decrease in concentration with depth, which corresponds with a decrease in organic carbon and the proportion of fine-grained sediments (figs. 13*D*, 26, and 28*D*). Among all of the cores, four elements had significant correlations: As and Se increased with increasing organic carbon, and Ni and Cr decreased with increasing organic carbon (table 16). The other elements of interest (Cd, Cu, Hg, Pb, and Zn) were not strongly correlated with organic carbon and concentration with depth profiles were distinct for these elements, indicating that there is another factor controlling sediment concentration (table 16 and figs. 26 and 28).

In the following discussion of sample results, SQG exceedances refer to sample concentrations that exceeded the SQG with 90 percent confidence (SQG plus uncertainty; table 4). For sample concentrations whose uncertainty may exceed the SQG, exceedance of the SQG is not certain at the 90-percent confidence level. All sediment cores had sections with element concentrations that exceeded or were within uncertainty of at least one SQG.

Table 15. Ratio of average of bottom two core sections compared with the average of the top two core sections at each coring site.

[A value of 0.5 indicates that the average value of the bottom two sections of the core was half the average value of the top two sections of the core, 1 indicates that the top and bottom two sections of the core had the same average value, 2 indicates that the average value of the bottom two sections of the core was twice the average value of the top two sections of the core; values were rounded to the nearest tenth]

Element	TZG02	TZG03	TZG04	TZG08	TZG09	TZG10
Bi	4.5	2.3	4.8	0.3	0.8	1.5
Cd	4.1	2.1	4.2	0.2	1.0	1.3
Cu	2.0	1.7	3.5	0.2	0.8	1.4
In	5.0	2.5	4.5	0.4	0.8	1.8
Pb	3.7	2.2	3.4	0.4	0.8	1.4
Sb	2.5	1.4	2.0	0.6	0.7	1.5
Sn	1.8	1.9	3.7	0.5	0.5	1.5
Te	1.8	1.4	7.8	0.3	1.0	1.4
Zn	2.2	1.5	2.2	0.4	0.6	1.4

Table 16. Correlation and significance of organic carbon and trace elements of interest.

[Grey shaded cells indicate the correlation was significant at the 0.05 level; negative values of Kendall's tau indicate that elemental concentration decreased as organic carbon increased]

Element	Kendall's tau	p value
Arsenic	0.3628	<0.0001
Cadmium	0.0238	0.7644
Chromium	-0.189	0.016
Copper	0.0976	0.21
Lead	-0.0236	0.7615
Mercury	0.0885	0.3875
Nickel	-0.3147	<0.0001
Selenium	0.5757	<0.0001
Zinc	0.0592	0.4491

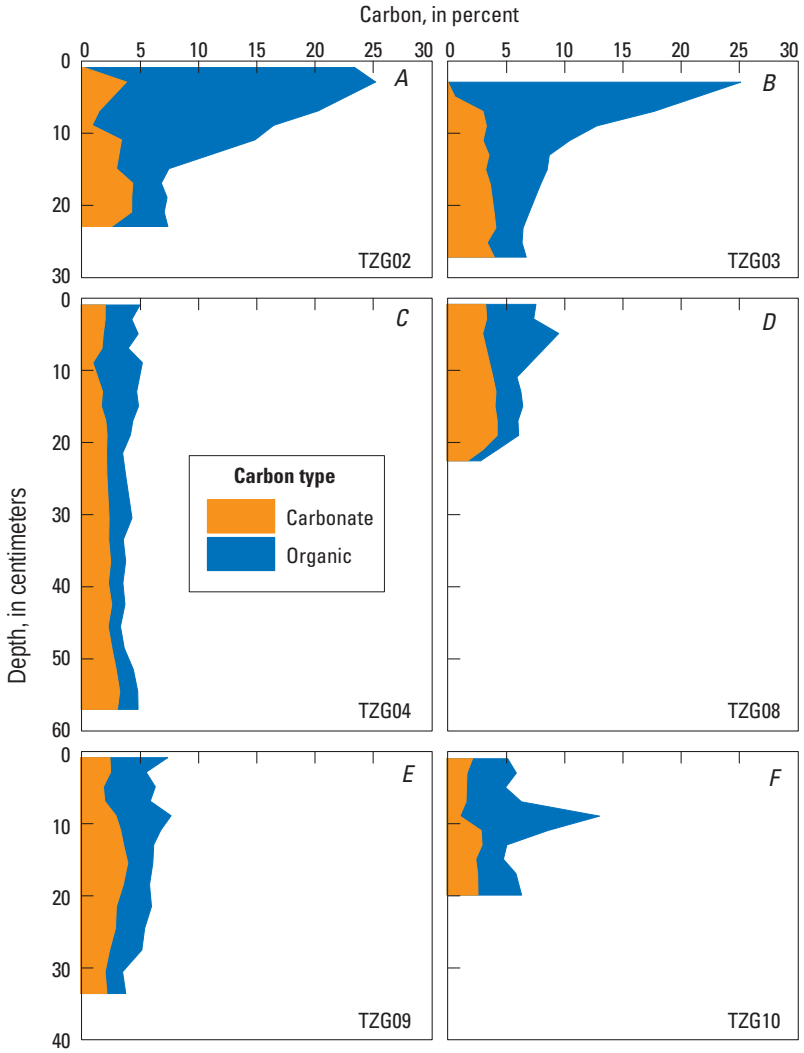

Figure 28. Plots of carbonate and organic carbon from sediment cores at Tavasci Marsh. For sample locations, see figure 4.

Table 17. Exceedance of sediment-quality guidelines (SQG) in cores collected from Tavasci Marsh.

[Exceed refers to concentrations greater than the sediment quality guideline (SQG) plus uncertainty at the 90-percent confidence level; within uncertainty refers to concentrations within the range of uncertainty at the 90-percent confidence level around the SQG; LEL, lowest effect level; SEL, severe effect level; TEL, threshold effects level; PEL, probable effects level; TEC, threshold effect concentration; PEC, probable effect concentration; --, no exceedance. Location of sites shown in figure 4. Elements in bold red exceed or were within uncertainty of the respective column for SEL, PEL, or PEC and exceedance of the respective LEL, TEL, or TEC is implied]

Site (core)	LEL and SEL		TEL and PEL		TEC and PEC	
	Exceed	Within uncertainty	Exceed	Within uncertainty	Exceed	Within uncertainty
TZG02	Cd, Cr, Hg, Ni, Pb, Zn, **As, Cu**	--	Hg, Ni, Pb, Zn, **As, Cd, Cu**	Cr	Cd, Hg, Ni, Pb, Zn, **As, Cu**	Cr
TZG03	Cd, Cr, Ni, Pb, Zn, **As**	**Cu**	Cd, Ni, Pb, Zn, **As**	Cr, **Cu**	Cd, Ni, Pb, Zn, **As**	Cr, **Cu**
TZG04	Cd, Cr, Hg, Ni, Pb, Zn, **Cu**	**As**	As, Cr, Hg, Ni, Pb, Zn, **Cd, Cu**	--	Cd, Cr, Hg, Ni, Pb, Zn, **Cu**	**As, Cd**
TZG08	Cd, Cr, Ni, Pb	Zn, **As, Cu**	As, Cd, Ni, Pb	Cr, Zn, **Cu**	Cd, Cr, Cu, Ni, Pb	Zn, **As**
TZG09	Cd, Cr, Ni, Pb, Zn, **As**	**Cu**	Ni, Pb, Zn, **As**	Cr, **Cu**	Cu, Ni, Pb, Zn, **As**	Cr
TZG10	Cd, Ni, Pb, Zn	Cr, **As, Cu**	As, Cd, Ni, Pb, Zn	**Cu**	Cd, Cu, Pb, Zn	Cr, Ni, **As**

Cumulative Toxic Units in Sediment

Sediment samples collected from Tavasci Marsh during this study exceeded published single-element SQGs (table 7), the highest of which were As, Cd, and Cu (fig. 26). Several other elements such as Hg, Pb, and Zn were elevated in deeper sections of three sediment cores (TZG02, -03, and -04). The presence of multiple trace elements and metals at elevated concentrations warrants further investigation of the potential increased toxicity for aquatic biota exposed to the sediment. Trace element interactions can be additive, where the toxicity increases in proportion to the number of trace elements present, or synergistic, where the toxicity is enhanced by a factor greater than the number of trace elements present (Paul and others, 2012). However, multiple trace element interactions may also be antagonistic, where a trace element can decrease the toxicity of another (Andrewes and others, 2000; Larsen and Bjeeregaard, 1995).

As with the water samples, assessment of CTUs provide an indication of the increased toxicity risk by assuming the effect of multiple trace elements is additive. Given this assumption, CTUs presented in this report should only be considered as an indicator of potential risk. CTUs are calculated by dividing each trace element concentration by its respective SQG and then adding the ratio from each trace element together where values greater than 1 indicate potential toxicity (Besser and others, 2009; Clements and others, 2000; Maret and others, 2003). The PEC from the study by MacDonald and others (2000) was the SQG used for the calculation of the CTU in this report for As, Cd, Cr, Cu, Pb, Hg, Ni, and Zn, and gives values comparable to those presented in Paul and others (2012) for the western United States.

All sediment core sections had CTU values greater than 1, which indicates potential toxicity. Several elements varied greatly between and within core sites in their contribution to the overall CTU value, with As being the most widely variable (fig. 29). Chromium and Ni were the most consistent in their contribution to the overall CTU value (fig. 29). The most drastic change in CTU occurs below 50 cm in core TZG04, where Cd, Cu, Hg, Pb, and Zn concentrations increase and account for a larger proportion of the CTU (fig. 29*C*). These same elements proportionally decrease below about 18 cm at TZG08, which results in smaller CTU values (fig. 29*D*).

Periphyton-Diatoms

Periphyton data are commonly used to assess water quality, and periphyton community information has become recognized as an excellent measure of nutrient enrichment in both lotic and lentic environments (Griffith and others, 2002; Hill and others, 2000; Stevenson and Bahls, 1999). Periphyton respond rapidly and consistently to water quality conditions. Their short colonization, ubiquitous distribution, and ease of sampling make them ideal indicators for regional comparisons. In lentic environments, the sediment that accumulates over time will preserve diatom assemblages, and the investigation of diatoms in sediment cores can be useful for understanding water quality conditions through time. In this investigation, periphyton were analyzed for richness (number of different species present) and abundance (number of organisms present) in eight sections of core TZG04 and changes in communities were assessed with depth relative to trace element concentrations.

Substrate is an important factor for biofilm development, meaning that larger substrates such as cobble and gravel will provide greater surface area for colonization than fine sediments and sand. The particle-size depth-profile for the TZG04 sediment core was fairly homogenous, with silt/clay comprising 50 percent of the total sample near the top of the core and 40 percent near the bottom with various sand

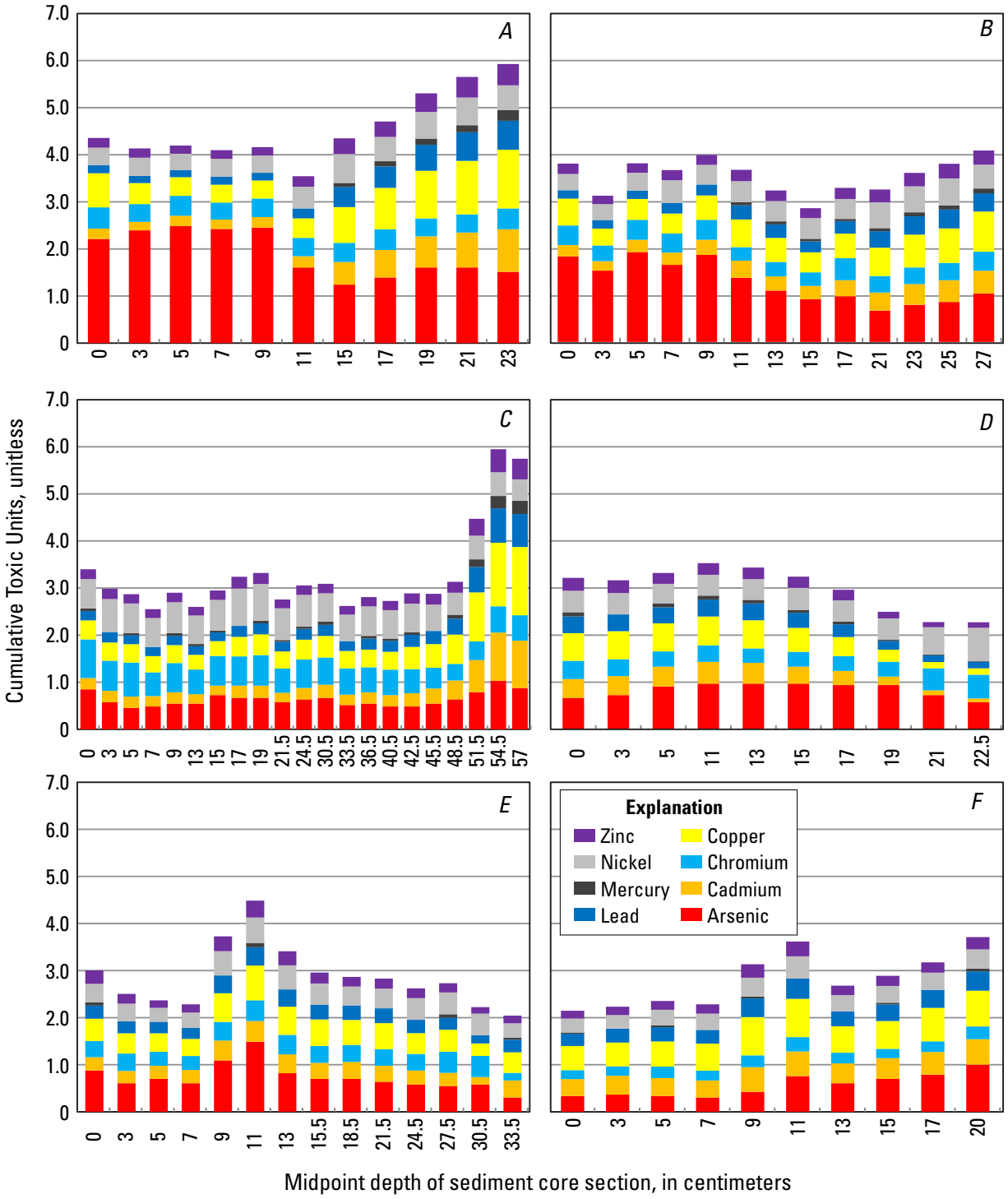

Figure 29. Histograms showing cumulative toxic unit contribution by element for sediment samples collected at Tavasci Marsh.

classes making up the remaining distribution (fig. 13*C*). The homogenous particle-size profile with depth suggests that trends observed in diatom assemblages were less related to changing substrates and most likely related to other factors such as water and sediment chemistry. Several of the trace elements of interest increased between the depth of 41 cm and 58 cm and corresponded to decreases in diatom richness and abundance in these sections compared to the sections between the surface and 32 cm (fig. 26). Periphyton abundance decreased 1 to 2 orders of magnitude in the sections analyzed between 41 and 58 cm. Diatom richness showed a similar decrease with depth and decreased from 51 genera (308 individuals) in section 0–2 cm to 2 genera (4 individuals) in the section 56–58 cm. Several trace elements increased with depth, but only Cu concentrations were negatively correlated to richness and abundance (both *tau*=-0.64, *p*=0.026) and Cd concentrations were negatively correlated with richness (*tau*=-0.62, *p*=0.040).

There were 97 different diatom species identified and they accounted for a total of 1,586 individuals counted in the core sections. The most abundant species throughout the core (cells>100) were *Fragilaria construens* var. *venter* (106 individuals), *Aulacoseira granulata* (178), *Nitzschia girdle* sp. (219), and *Synedra ulna* (256). Several species within the genera *Nitzschia* sp., *Synedra* sp., *Aulacoseira* sp., and *Fragilaria* sp. were not observed below 32 cm. The diatom assemblage (richness and abundance) changed significantly with depth (*tau*=0.33, p=0.018). The assemblages collected between 0 and 32 cm were more similar to each other compared to the assemblages collected in sections between 41 and 58 cm.

Synedra ulna and *Fragilaria* sp. have been documented as being sensitive to metal pollution (Hill and others, 2000; Barranguet and others, 2000). The species *Achnanthes minutissima*, *Nitzschia palea* and *Gomphonema parvulum* have been identified as being tolerant to trace metals (Deniseger and others, 1986; Sabater 2000; Hill and others, 2000). Many of these species were not observed in the last two sections from the core. Species occurring in either of the last two sections, which had elevated trace element concentrations, include *Achnanthes girdle* sp., *Amorpha girdle* sp., *Aulacoseira girdle* sp., *Bacillaria paradoxa*, *Caloneis girdle* sp., *Cocconeis pediculus*, *Cymbella girdle* sp., *Fragilaria brevistriata* var. *inflata*, *Fragilaria girdle* sp., *Fragilaria leptostauron*, *Fragilaria virescens*, *Gomphonema girdle* sp., *Hantzschia amphioxys*, *Melosira varians*, *Nitzschia inconspicua*, Unknown *Pennate girdle* sp., and *Rhoicosphenia abbreviata*. The last section in the core was contained only *Rhoicosphenia abbreviata* and *Fragilaria brevistriata* var. *inflata*. There are some *Fragilaria* present in the bottom core sections, which other studies found to be sensitive to metal pollution, and as such this conflicting observation indicates there may be other factors contributing to the diatom assemblages or that this site is different compared with the other studies.

While there was a clear shift in the assemblage of the diatoms with depth and it corresponds to an increase in the CTUs (fig. 30), other unknown factors should be considered, such as the changing habitat (cattail proliferation) and variable discharge/wetness of the marsh. Variable physical settings in the marsh could have had significant changes in the diatom community. Periphyton as indicators of water quality are more commonly used in stream and lake applications that focus on changes in longitudinal or regional gradients. Diatom assemblages were used in a unique application to provide additional information about water quality in the marsh over time. The strong correlation of diatom richness and abundance compared with trace element concentrations indicates the successful application of this technique to this study.

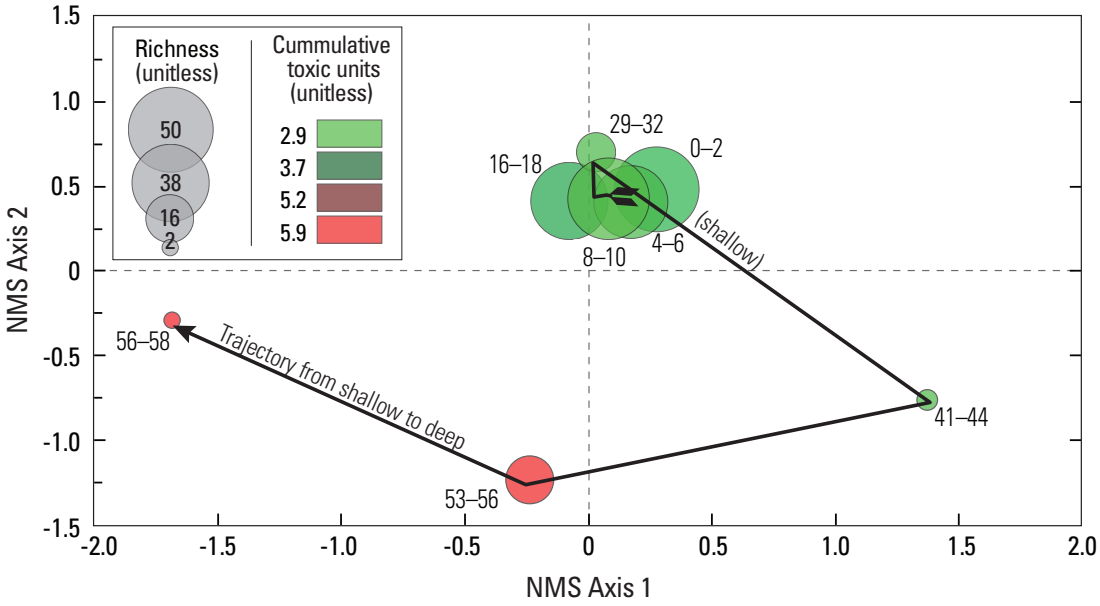

Figure 30. Nonmetric multidimensional scaling plot using a square root transformation and bray-curtis distance showing how diatom richness changes with increasing cumulative toxic units and depth in the sediment core collected at site TZG04, Tavasci Marsh. Seriation Rho of 0.33 and p value of 0.018. Numbers next to colored circles indicate sediment core section depth in centimeters.

Organic Material

In addition to analyzing elemental carbonate and organic carbon, sediment core sections were analyzed for organic material properties to understand source and decomposition. FI values in cores TZG02, -03, and -04 (0.99–1.16), which were obtained using the less aggressive $Na_4P_2O_7$ extraction method, were less than FI values in cores TZG08, -09, and -10 (1.16–1.52), which were obtained using the more aggressive NaOH extraction method (fig. 31). This finding is consistent with that of Klapper and others (2002) and Wolfe and others (2002). Wolfe and others (2002) suggest that the $Na_4P_2O_7$ extraction method underestimates the yield of tightly bound terrestrial humic substances, and therefore the NaOH extraction method may be necessary to fully characterize the source of the organic material. While the application of different extraction methodologies limits the ability to compare absolute FI values among sediment cores extracted with the two different methods, relative patterns in FI with depth can be interpreted to provide useful information.

FI values were highest at the surface and decreased with depth for the cores collected at TZG02, -03, -04, and -10 (fig. 31). This trend indicates that organic material extracted from the surface of the cores was from more of a microbial source than the organic material deeper in the cores. The lower FI values from the deeper sections of these cores could indicate a greater relative contribution of terrestrially or higher-plant-derived organic carbon at depth, but may also be reflective of biogeochemical processing of more labile organic material with higher FI values. The relative importance of changes in source material versus biogeochemical processing in determining the observed patterns in FI warrants further investigation. FI patterns with depth in the cores collected from TZG08 and -09 were variable. Of note is that there was a sustained increase in FI in the core collected at TZG08 from 12 to 23 cm, indicating the presence of microbially derived organic material at depth. FI was invariant from 17–35 cm in the core collected at TZG09. The trend of the trace element profiles with depth at TZG02, -03, -04, -08 and -10 are, in general, opposite the FI profiles (increasing trace element concentrations correspond to decreasing FI values) and may indicate that trace element concentration is related to the source of organic material.

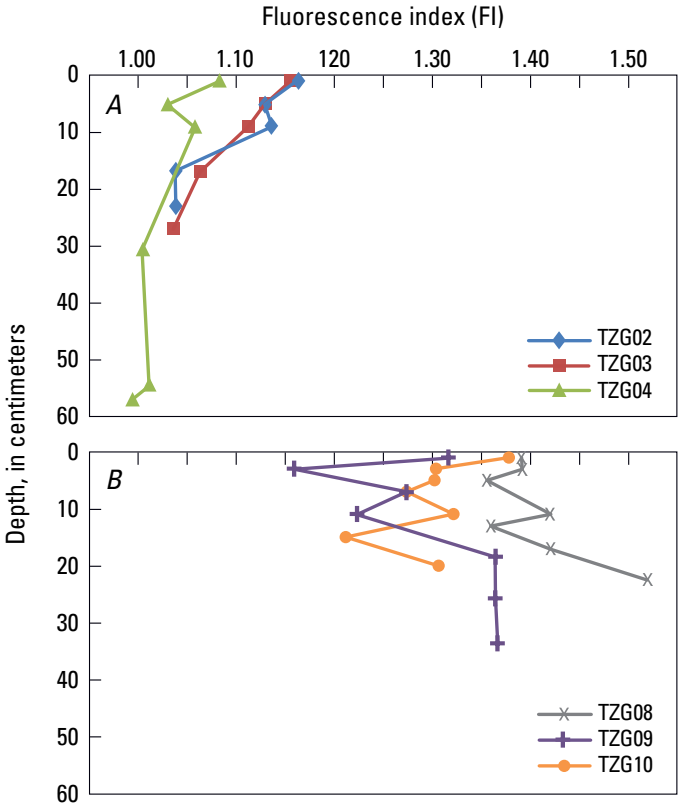

Figure 31. Plots showing depth profiles for fluorescence index (FI) of organic material extracted from sediment cores. *A*, FIs for sediment cores collected at TZG02, -03, and -04, from which organic material was extracted using the $Na_4P_2O_7$ method. *B*, FIs for sediment cores TZG08, -09, and -10, from which organic material was extracted using the NaOH method.

Regional Sediment Comparison

An anomaly threshold value was determined as part of a regional study investigating mining impacts in Prescott National Forest, Yavapai County, Arizona to be distinctly higher than normal, generally the 75th to 90th percentile interval (Nash and others, 1996) (table 8). Additionally, concentrations in the range of 100 to 600 ppm for Cu, Pb, or Zn are considered very high geochemically (Nash and others, 1996), and several sediment samples from Tavasci Marsh exceeded 100 ppm for Cu and Zn. Elevated elemental concentrations measured in the bottoms of sediment cores TZG02, -03, and -04 exceed the anomaly threshold values for all elements reported by Nash and others (1996), including As, Cd, Cu, Pb, and Zn (tables 8 and 18).

Surface soil samples from the Nash and others (1996) study had greater elemental concentrations compared with deep soil samples, which is in contrast with the concentrations that increase with depth in the sediment cores at Tavasci Marsh. The difference may be due to depositional environment, where Tavasci Marsh has standing water through which sediment particles deposit over time and older sediments become buried more quickly compared to terrestrial soil, which forms slowly and retains surface elemental concentrations, especially in arid environments. The surface soil samples located near old mines and mine processing sites appear to have retained the elevated elemental concentrations likely deposited during mining related activities, almost a century prior to sample collection (Nash and others, 1996).

A sediment sample was collected from the eastern bank of the Verde River to the northwest of Tavasi Marsh (Verde reference) in a side channel with ponded water containing cattails and aquatic macrophytes as a reference location.

Table 18. Trace-element concentrations in sediment from Tavasci Marsh and the Verde reference site.

[All values are in parts per million (ppm), except for mercury in ppb; nc, not computed; other local, regional, and national sediment data are presented in table 8]

Element	Arsenic (As)	Cadmium (Cd)	Chromium (Cr)	Copper (Cu)	Mercury (Hg) (ppb)	Lead (Pb)	Nickel (Ni)	Selenium (Se)	Zinc (Zn)
Tavasci Marsh surface sediment (average)	22.4	2.02	51.6	118	nc	40.4	26.4	1.57	147
Tavasci Marsh sediment core (average)	31.3	1.79	45.2	82.7	82.8	38.3	23.6	1.39	109
Tavasci Marsh sediment core TZG02, -03, and -04 bottom 2 intervals (average)	38	3.83	50	168	195	73.4	25.6	1.2	186
Tavasci Marsh sediment core TZG08 and -09 bottom 2 intervals (average)	18	0.88	44	36	29.6	23.1	24.8	0.65	60.2
Verde reference fines (<63 micron)	18	1.8	56	68.1	nc	34.6	34.8	0.50	97
Verde reference coarse (>63 micron)	7	0.6	55	19.3	nc	12.1	25.7	<0.2	37

The sediment sample was separated into two subsamples by wet sieving through a 63-µm mesh. The coarser material contained trace element concentrations similar to or less than the national and western baseline stream sediment values (tables 8 and 18). Some of the lowest trace element concentrations from all sediment core sections in Tavasci Marsh were observed in the bottom two intervals at TZG08 and -09, which may reflect a background metal concentration for the marsh, and are also more similar to western U.S. baseline bed-sediment samples (tables 8 and 18).

Trace element concentrations in the finer part of the Verde River reference sample (less than 63 µm) were greater than the larger particle size sample, and As, Cd, Pb, and Zn concentrations exceeded the Prescott National Forest anomaly thresholds determined by Nash and others (1996). These concentrations in the fine fraction of the reference sample were similar to shallow core sections from Tavasci Marsh, the shallow core section elemental concentrations were about two times less than the deeper core sections at sites TZG02, -03, and -04 (table 18). Because only one sediment sample was collected at the Verde River reference site, variation in sample concentration cannot be determined, but the sample gives an indication of regional trace element concentrations in a setting similar to Tavasci Marsh.

The Verde River sample location is considered to be a reference site rather than a background sample as it is located within 2 miles of the historical Clarkdale smelter. Nash and others (1996) found elevated metal concentrations within 3 miles of smelters in Prescott National Forest (fig. 32). Surface soil samples collected by Nash and others (1996) in the vicinity of Tavasci Marsh were all derived from the Verde Formation except for one sample in a quaternary deposit. Copper concentrations range from <50 to 350 ppm in soil from the same geologic unit (Verde Formation–undivided sedimentary rocks) (fig. 32). The tailings pile next to Tavasci Marsh had Cu concentrations of 953 ppm (table 8, Ecology and Environment Inc., 1994), which is several times greater than the elevated soil concentrations (figs. 26 and 32).

Concentrations of Cd, Cu, Pb, and Zn in sediment and rock samples from all available studies in and around Tavasci Marsh were compared using a cluster analysis to understand how sediment samples collected during this study compare to previous studies and nearby locations (fig. 33). Sediment samples collected in Tavasci Marsh (both surface and sediment cores) were most similar to surface soil samples from Nash and others (1996) and Tavasci Marsh and Pecks Lake sediments collected in the study by Ecology and Environment, Inc. (1994). Verde River reference sediment was most similar to Tavasci Marsh sediment and wash surface soil from URSGWC (1999) and deep soil samples from Nash and others (1996). The sediments were all more similar to each other than to the rock samples surrounding the marsh collected from the URSGWC (1999) study (fig. 33).

Analysis of CTUs from stream sediment samples in the western U.S. from Paul and others (2012) indicates that potential toxicity at mining-affected sites was significantly greater than at undeveloped sites (fig. 34). Values greater than 4 CTU exceeded the 75th percentile of all 201 sediment samples analyzed from throughout the western U.S. and are considered moderately high enrichment sites (Paul and others, 2012). Values greater than 7.5 CTU occurred only at mining-affected sites and were considered high enrichment sites (Paul and others, 2012). Surface sediment samples collected from Tavasci Marsh during this study ranged from 2.5 to 7 CTU with an average and standard deviation of 3.5±1.3 CTU. Sediment core samples collected from Tavasci Marsh during this study ranged from 2 to 5.9 CTU with an average and standard deviation of 3.3±0.9 CTU (fig. 34). Sediment cores at TZG02, -03, and -04, which showed an increasing trend with depth for Bi, Cd, Cu, Hg, In, Pb, Sb, Sn, Te, and Zn, had an average and standard deviation of 5.0±1.1 CTU in the bottom two core sections indicating moderately high enrichment.

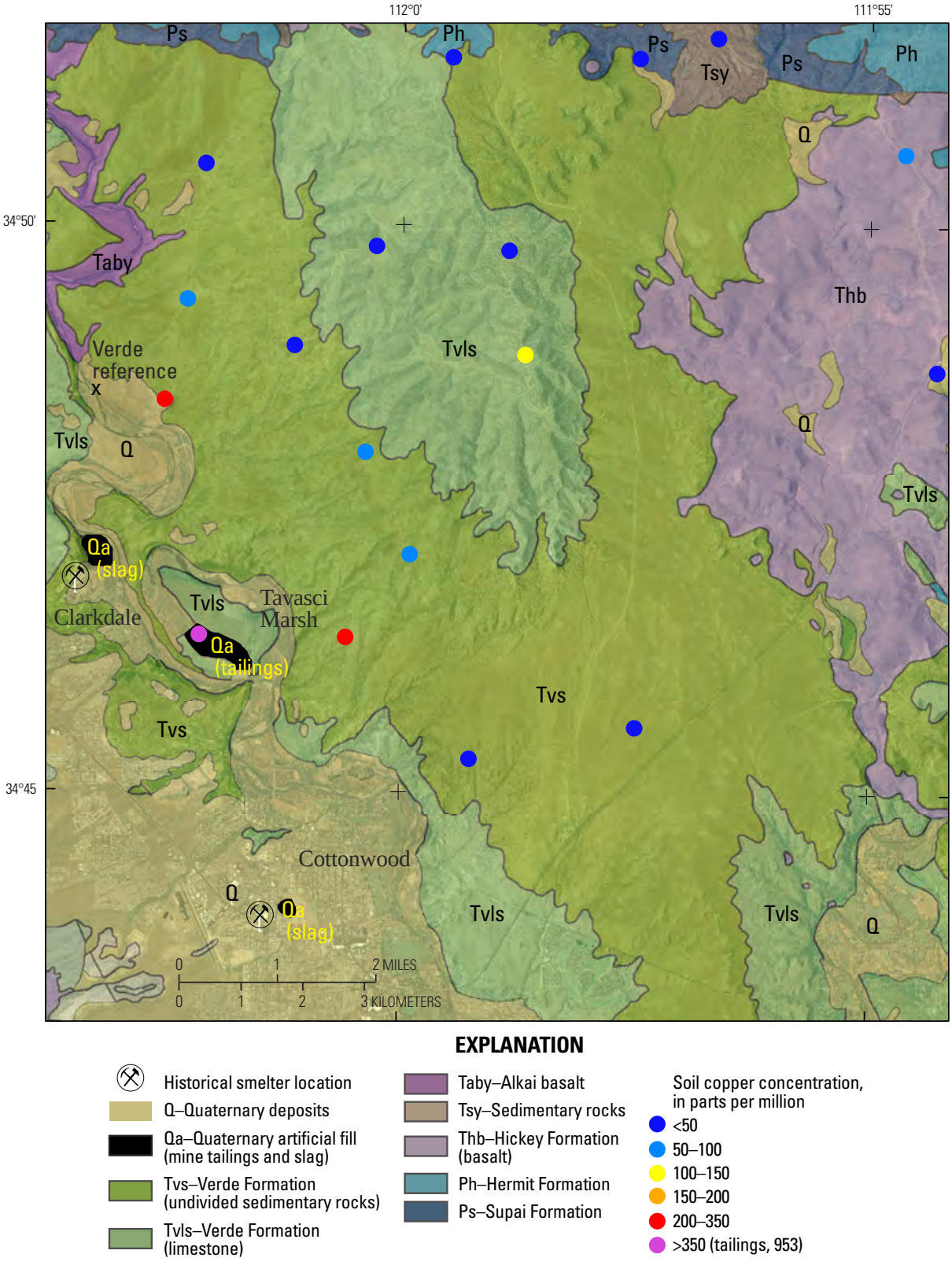

Figure 32. Geologic map showing copper concentration in surface soils in relation to historical smelter and tailings locations. Modified from Nash and others (1996); tailings concentration from Ecology and Environment, Inc. (1994). Geology from DeWitt and others (2008).

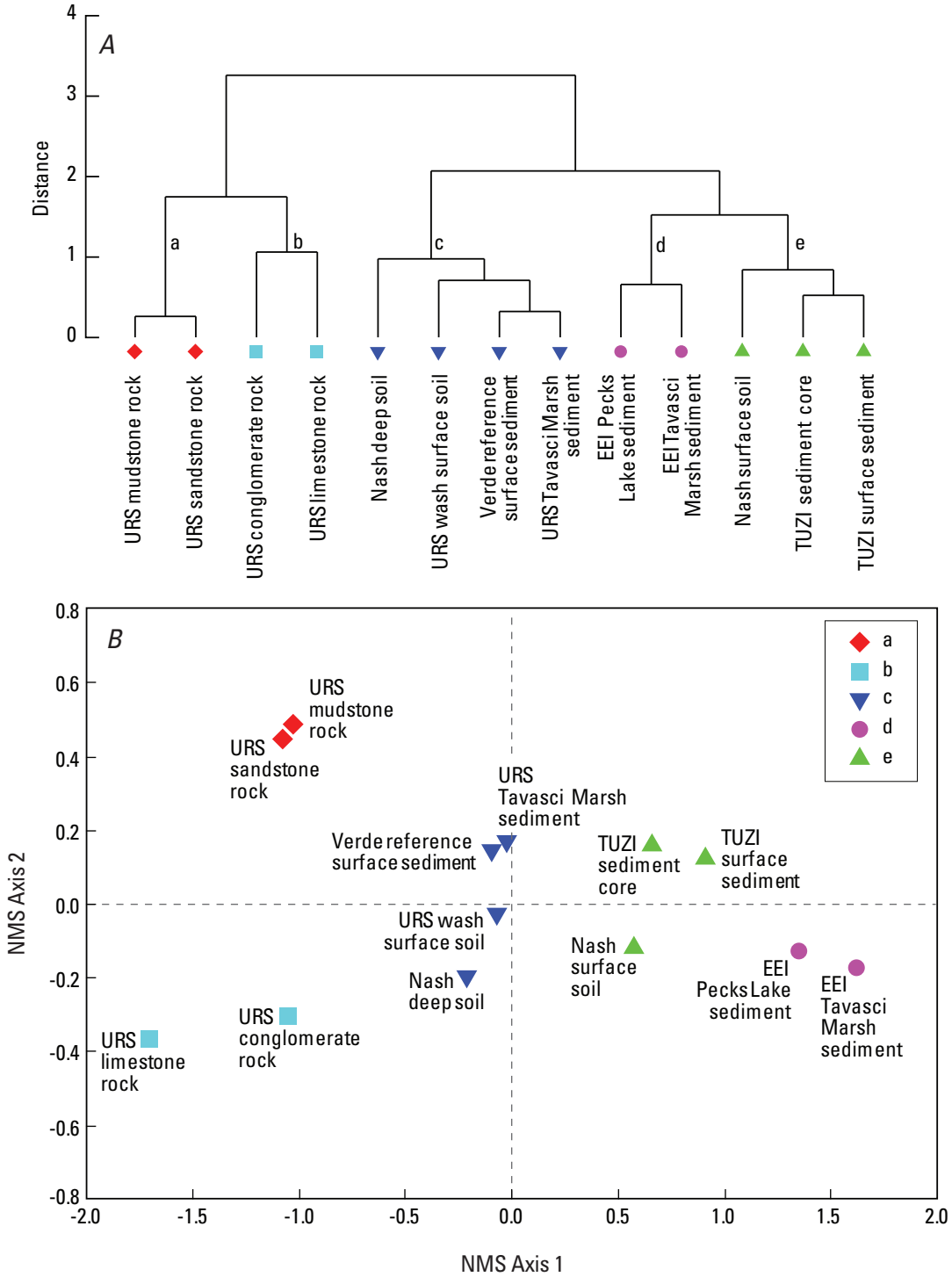

Figure 33. Plots of multivariate group average cluster analysis on log10 transformation of normalized data using Euclidean distance to determine distinct groups of samples (*A*) and nonmetric multidimensional scaling plot using the groups determined in the cluster analysis as different symbols (*B*) as a comparison of Cd, Cu, Pb, and Zn concentrations in sediment and rock samples from the Tavasci Marsh area.

Determination of source of elevated metal and trace element concentrations found in Tavasci Marsh during this study cannot be uniquely determined based on concentration alone. However, given that several elements exceed SQGs, sediment anomalies associated with mining, and regional values of mining impacted sediments, it is highly probable that Cd, Cu, Hg, Pb, and Zn, concentrations in sediment from Tavasci Marsh are elevated because of past mining activities.

Plants

Certain trace elements are required for plant growth and some plants have evolved specific mechanisms to adapt to growth media (for example, water or sediment) with elevated trace element concentrations. The interactions between plants and trace elements are very complex and the accumulation of trace elements is not only related to the plant species but also to the physical, chemical, and biological conditions of the plant's environment. A single species can have tolerance to a range of metal concentrations. Seventeen trace elements (Al, B, Br, Cl, Co, Cu, F, Fe, I, Mn, Mo, Ni, Rb, Si, Ti, V, and Zn) are known to be essential for all plants, while others such as As, Cd, Hg, and Pb have no known function in plants and animals (Kabata-Pendias, 2010; Mertz, 1981). Trace elements are taken up at varying efficiencies and transferred to different morphological components of the plant, which is why it is important to analyze different components of the plants as well as the growth media where trace elements originate and transfer to the plant.

Typha spp. (cattails) are the most abundant emergent aquatic macrophyte in the marsh and *Typha domingenis* and *Typha latifolia* are the two dominant species reported in the marsh (Schmidt and others, 2005). Cattails are able to tolerate and thrive in elevated levels of metals without sustaining damaging effects and they are commonly used in wetlands for the phytoremediation of contaminated waters (Deng and others, 2004; Grisey and others, 2012; Karpiscak and others, 2001; Ye and others, 1997; Sasmaz and others, 2008; Taylor and Crowder, 1983).

Of the 44 elements analyzed, 6 (As, Cd, Co, Ni, Mo and W) had higher concentrations in the cattail root samples compared to the associated surface sediment at one or more sites (appendix B, table 2; appendix C, table 1). Except for the six elements mentioned previously, most of the surface sediment trace element concentrations were greater than any of the cattail plant parts. Arsenic concentrations were greater in root samples for all sites but TZG01. Manganese concentrations were greater in the cattail leaves compared to the roots at all but TZG03, and concentrations of Li, Hg, Te, Tl, and W were greater in the leaves than in the roots at one or more sites (appendix C, table 1). Metal concentrations generally increase in the order of green leaves < non-green

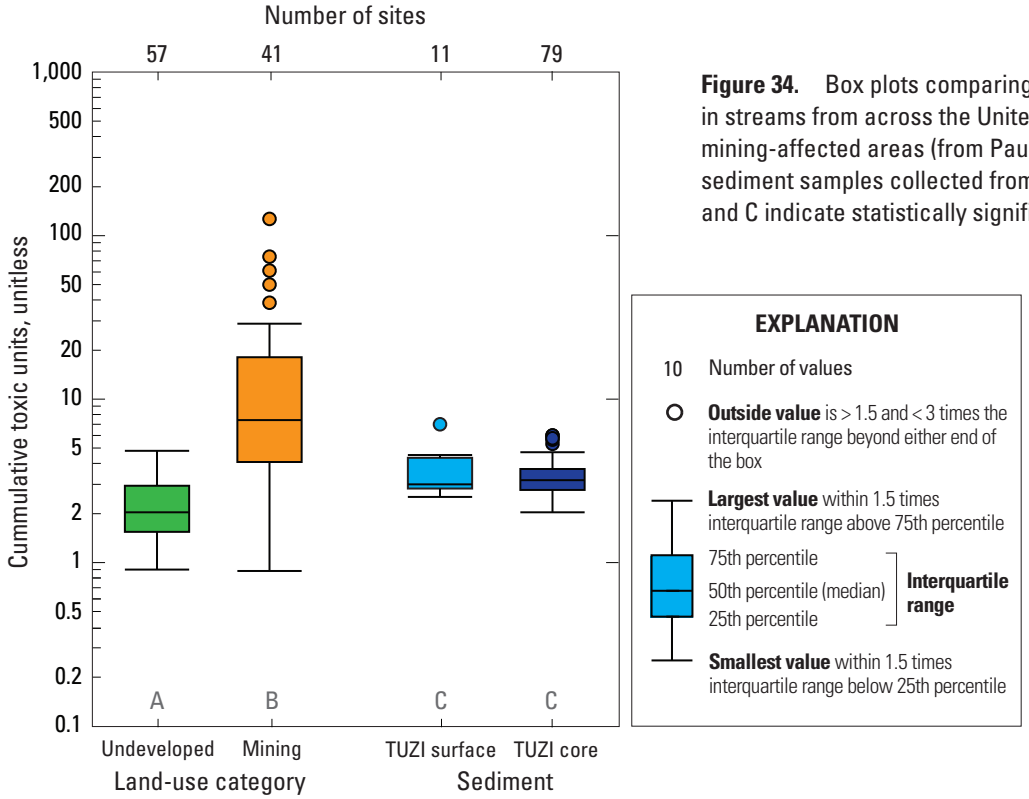

Figure 34. Box plots comparing bed-sediment concentrations in streams from across the United States in undeveloped and mining-affected areas (from Paul and others, 2012) compared to sediment samples collected from Tavasci Marsh. Letters A, B, and C indicate statistically significant groups ($p<0.005$).

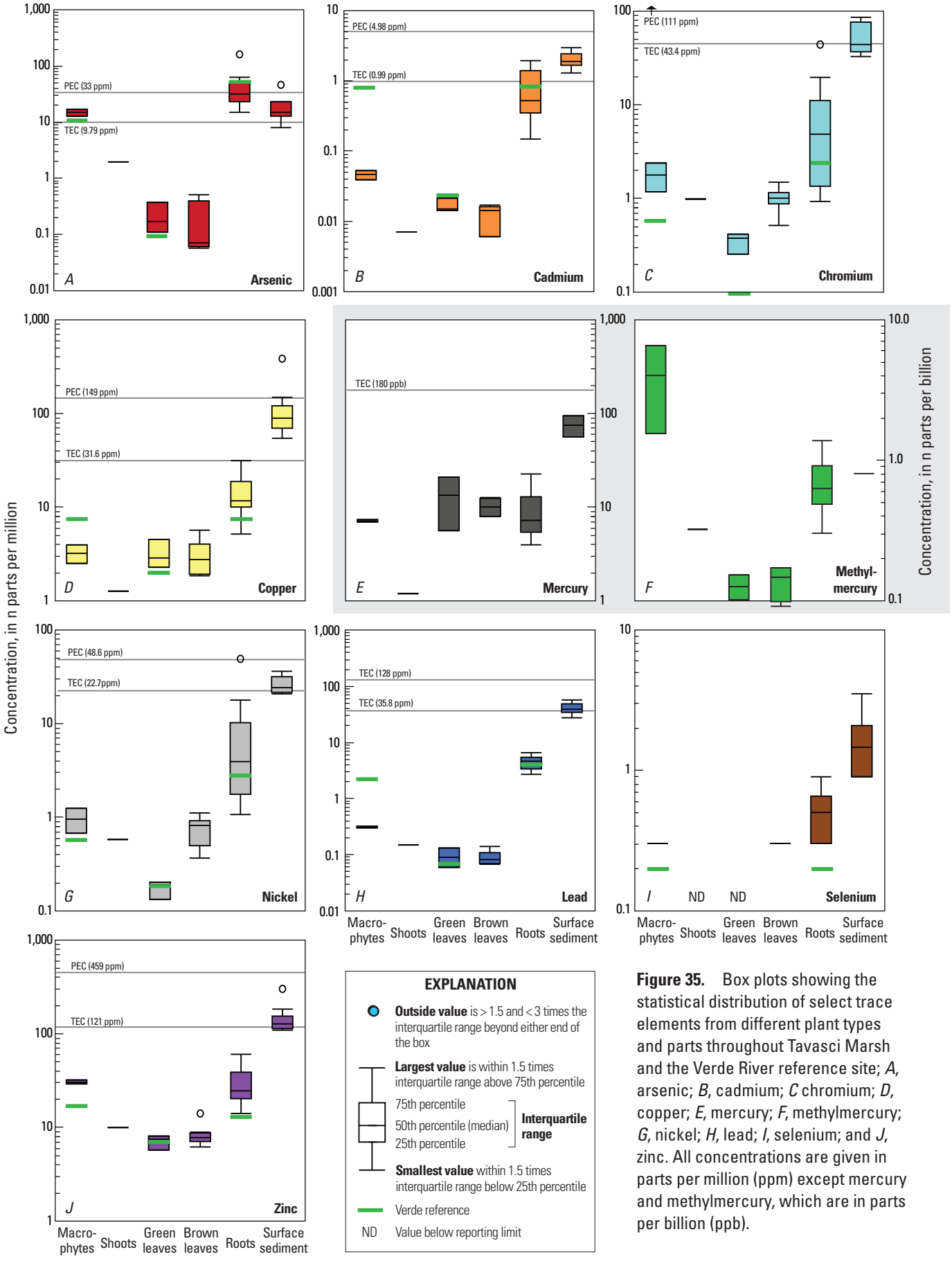

Figure 35. Box plots showing the statistical distribution of select trace elements from different plant types and parts throughout Tavasci Marsh and the Verde River reference site; *A*, arsenic; *B*, cadmium; *C* chromium; *D*, copper; *E*, mercury; *F*, methylmercury; *G*, nickel; *H*, lead; *I*, selenium; and *J*, zinc. All concentrations are given in parts per million (ppm) except mercury and methylmercury, which are in parts per billion (ppb).

leaves < rhizomes < roots for many studies analyzing trace elements in cattails (Letachowicz and others, 2006; Grisey and others, 2012; Taylor and Crowder, 1983), unless transfer factors are high, and hyperaccumulation occurs where leaves have levels on the order of greater than 100 ppm for Cd, 1,000 ppm for Co, Cu, Ni, Pb, and 10,000 for Mn and Zn (Kabata-Pendias, 2010). The increase of metal concentrations with plant parts with greatest concentration in roots and least in leaves found in other studies was observed for a majority of the trace elements analyzed in cattails from Tavasci Marsh.

For the elements of interest, each plant sample was compared to the TEC and PEC SQGs to better understand the magnitude of the concentration (fig. 35). Several of the root samples had concentrations of As that exceeded the PEC, one sample exceeded the PEC for Ni, and some root concentrations of Cd exceeded the TEC.

Concentrations of metals in cattail root samples were highly variable among sample sites in Tavasci Marsh (fig. 35). Cattail roots at site TZG04 had the greatest concentrations of As, Hg, and methylmercury. The cattail root samples from TZG06 and -07 were higher in concentrations of Cd, Cr, Cu, Ni, and Zn compared to the other sites in the marsh (fig. 35). Concentrations in cattail root samples at sites TZG06 and -07 were more than 5 and 15 times greater for Cr and Ni, respectively, than those in roots from the Verde River reference site (fig. 35). The ecological implications of these levels are unclear; the Verde River reference site may also have unknown atmospheric impacts from historical mining practices.

At TZG03 samples of watermilfoil, cattail emergent shoots, green leaves, roots, and surface sediments were collected to investigate metal and trace element concentrations in different plant tissue. The watermilfoil, a submergent aquatic macrophyte,

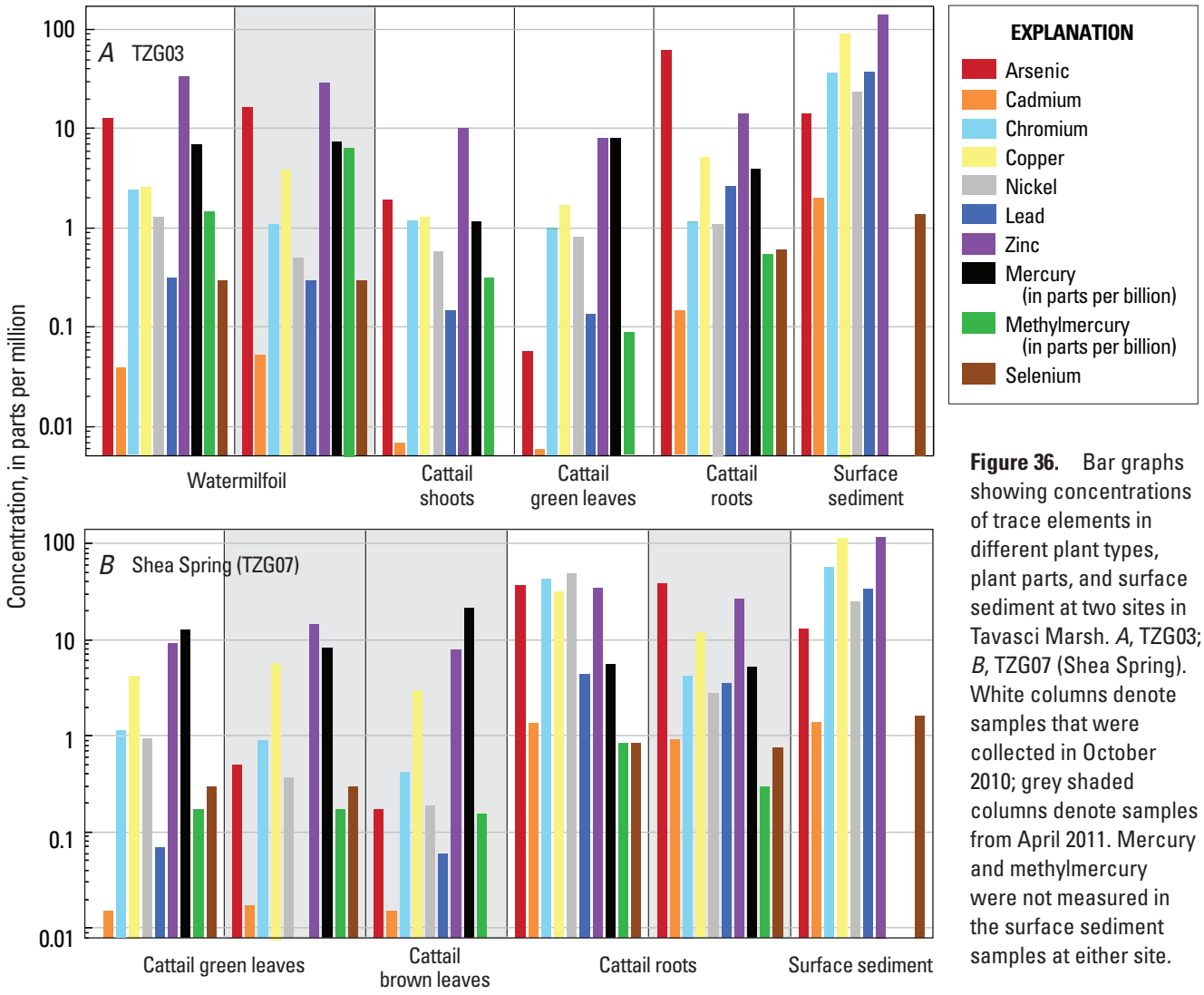

Figure 36. Bar graphs showing concentrations of trace elements in different plant types, plant parts, and surface sediment at two sites in Tavasci Marsh. *A*, TZG03; *B*, TZG07 (Shea Spring). White columns denote samples that were collected in October 2010; grey shaded columns denote samples from April 2011. Mercury and methylmercury were not measured in the surface sediment samples at either site.

collected at TZG03 had metal and trace element concentrations as great as or greater than the shoots and green leaves of cattails for As, Cd, Cr, Cu, methylmercury, Pb, Se, and Zn (fig. 36*A*). The watermilfoil had greater methylmercury and Zn concentrations than all other cattail parts and greater Hg concentrations than the cattail shoots and roots.

Sediments collected near the cattails at TZG03 had higher trace element concentrations than plant tissue with exception of As, which was greater in the cattail roots (fig. 36*A*). Cattail roots had greater concentrations of most elements compared with the green leaves and shoots, except for Hg, which was greatest in cattail green leaves.

At Shea Spring (TZG07), most trace elements followed similar patterns as at TZG03, where surface sediment had the highest concentrations, except for As and Ni, which were both greater in at least one root sample (fig. 36*B*). Again, Hg was the only element that was lower in the roots than the leaf samples. In April 2011, both green and brown cattail leaves were present at Shea Spring (TZG07). Cadmium and methylmercury were the same concentration in both leaves; As, Cr, Cu, Ni, Se, and Zn were greater in the green leaves, and Hg and Pb were greater in the brown leaves. The aforementioned comparisons are based on single samples, so more samples would be needed to demonstrate these differences with statistical confidence.

To date there are few studies that have sampled cattails at mining affected wetlands and analyzed different morphological components (roots, shoots, leaves, flowers) as a means to understand the bioaccumulation and uptake processes of metals. Four studies that analyzed the accumulation of metals in *T. latifolia* (Taylor and Crowder, 1983; Ye and others, 1997; Sasmaz and others, 2008; and Grisey and others, 2012) are discussed herein to provide context for metal concentrations found in cattails from Tavasci Marsh (table 9). The concentrations presented from the literature should be viewed as supporting information and not interpreted as directly comparable, because metal uptake is related to a multiple chemical and physical properties that vary with region, climate, and types of anthropogenic impacts.

Concentrations of Cu, Ni, and Zn in cattail roots from Tavasci Marsh were lower than those in cattail roots collected from wetlands near smelter sites in Ontario, Canada (Taylor and Crowder, 1983). Compared to cattail roots in a settling pond from a Pb/Zn mine in China, cattail root samples from TZG06 had greater Cd concentrations, but all other samples from Tavasci Marsh cattails were less than Cd, Pb and Zn concentrations from that site (Ye and others, 1997). The concentrations of Cr, Cu, Ni, Pb, and Zn in cattail roots from Tavasci Marsh were lower than those collected from wetlands supplied with treated effluent in Turkey, but several Cd concentrations in cattail roots in Tavasci Marsh were greater (Sasmaz and others, 2008). Several Cr, Cu and Ni concentrations from cattail roots in Tavasci Marsh were greater than cattail roots collected from the inflow of a landfill leachate pond in France (Grisey and others, 2012). All cattail leaf samples from Tavasci Marsh had concentrations of Cd, Cr, Cu, Ni, Pb, and Zn that were lower than the aforementioned studies.

Seasonal Analysis

At four of the sampling locations in Tavasci Marsh (TZG01, -03, -06, and Shea Spring [TZG07]), plant samples were collected in the fall (October 2010) and the spring (April 2011) to capture seasonal variability in the uptake of metals.

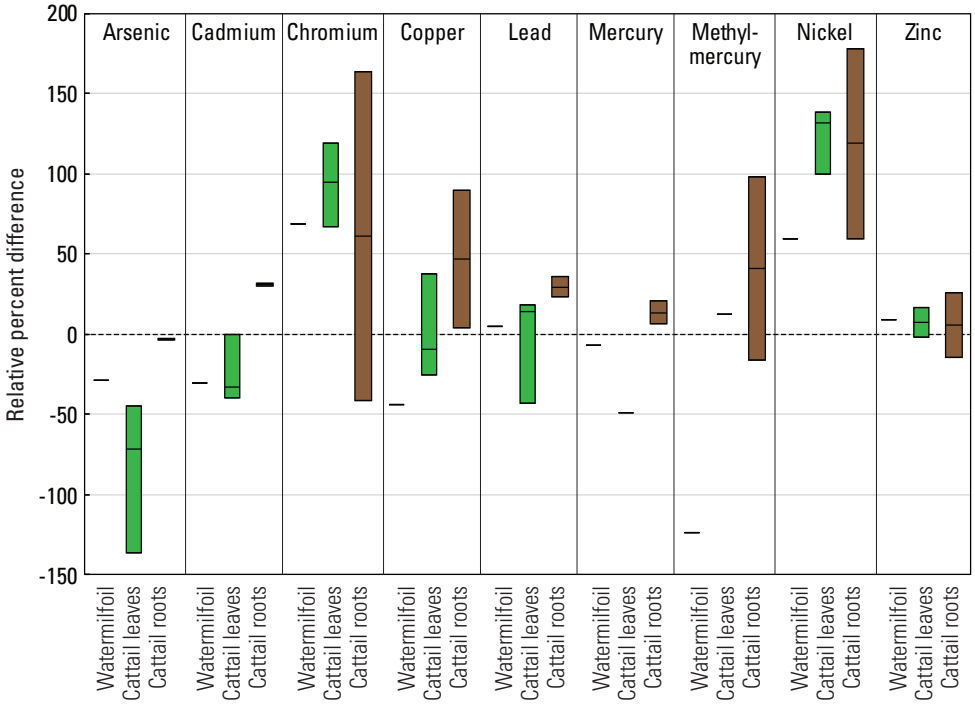

Figure 37. Bar plot of relative percent difference between fall and spring samples as observed in watermilfoil and cattail samples from Tavasci Marsh. Zero, which represents the case in which samples from fall and spring site visits had identical concentrations, is denoted by the black line in the middle of the plot. Positive values indicate that fall samples had greater concentrations than spring samples and vice versa for negative values.

The relative percent difference (RPD) was calculated between seasons for the nine elements of interest to understand seasonal differences in the concentrations of metals in each of the plant types (watermilfoil, cattail leaves, and roots). Positive RPD values indicate that the fall concentration was greater than the spring concentration and negative indicate that spring concentration was greater than fall concentration.

The fall and spring watermilfoil samples collected at TZG03 were similar (±50 percent RPD) with the exception of Cr, Ni, and methylmercury (fig. 37). Methylmercury was more than four times greater in the spring than in the fall.

The trace elements Cr and Ni showed the greatest positive RPDs for cattail leaves and roots, indicating greater concentrations occurred in the fall (fig. 37). Concentrations of Cd, Pb, Hg, and Zn showed RPDs within 50 percent for all plant types and parts, suggesting less seasonal variability than Cr and Ni. The RPDs for Cu and methylmercury were greater for roots in the fall, and As concentration was greater in leaves in the spring. While seasonal comparisons were limited to 2 or 3 samples, there was some indication that season influences the sequestration of metals in watermilfoil and cattails in addition to the different parts of the cattails. Grisey and others (2012) also observed significant variability between seasons in roots and shoots for most metals analyzed (notably Cu, Ni, Pb, and Zn) (table 9). These differences are likely related to physical and biological conditions associated with seasonality (for example, temperature, dissolved oxygen, pH, microbial interactions, and metabolic timing of plants).

Organic Material

Average FIs of organic matter extracted from different parts of cattails ranged from 1.30±0.03 for the brown leaves collected in April 2011 to 1.58±0.16 for burned green leaves collected in October 2010. The average FIs for green leaves (1.57±0.06) and shoots (1.58) collected in October 2010 were nearly identical to the average FI of the burned green leaves. The average FI of the roots collected in October 2010 (1.40±0.10) was intermediary between the brown leaves and other plant parts. The FI for watermilfoil was 1.58.

The fact that the FIs for the burned green leaves were similar to those of the unburned green leaves suggests that, if green leaves were burned historically in the marsh (and indeed, we know that the marsh was burned annually), any potential signal would not be expected to show up as a shift in FI in the sediment core data. However, it is possible the burning of green leaves could result in a detectable change in other organic (or inorganic) material in the sediment core parameters not measured here. Of interest is that the root material, and even more so the brown leaves collected in the spring, had consistently lower FIs than the other plant parts. These results support the idea that the measured gain in terrestrially-derived DOC during transport from the assumed source areas (Shea Spring [TZG07] and shallow groundwater at the north end of the marsh) to the TZG03 and outflow sites could be largely from degradation of the abundant cattails. More specifically, these results suggest that brown leaves and (or) root material may be the parts of the cattails that contribute most to changes in marsh water quality. While it seems likely that brown leaves, which are generally the part of the plant that degrades in the marsh as new cattails replace older ones, are likely contributors to water quality in the marsh, this contention warrants further investigation, especially given that these results are based on a small number of samples and because we did not investigate the potential for green leaf material to contribute to patterns in marsh water quality over a timescale of seasons to years.

Dragonfly Larvae

Dragonfly larvae samples were collected at four sites throughout Tavasci Marsh to understand spatial variability of trace element concentration. Results are reported for each element of interest and results for As, Cd, Cu, Hg, Pb, and Zn are compared to four other studies, summarized in table 10. All concentrations are reported as dry weight.

Arsenic concentrations were roughly ten times greater at TZG04 (22.3 ppm) relative to the concentrations observed at TZG01, -03, and -08 (2.3 to 3.2 ppm; fig. 38*A*). The As concentration of 22.3 ppm observed at TZG04 was elevated relative to the comparative studies for both polluted and nonpolluted sites, which ranged from 2.21 to 5.62 ppm (table 10). The concentrations of other elements in samples from Tavasci Marsh are within the ranges of the other studies.

The patterns observed in the distribution of As concentrations were similar to those observed in the dragonfly larvae Cd concentrations. TZG04 had a concentration of 0.4 ppm, which was twice the concentration observed at TZG03, and an order of magnitude greater than TZG01 and -08 (0.02 and 0.05 ppm; fig. 38*B*). Concentrations of metals in caddisfly and other macroinvertebrate samples collected at mining affected sites (2.16 to 6.68 ppm, table 10) were generally an order of magnitude greater than what was observed in Tavasci Marsh.

Cadmium in sediment from the Idaho studies (Farag and others, 1998 and Maret and others, 2003) was at least 5 times greater than the maximum surface sediment sample from Tavasci Marsh, while the Cd concentration in sediment from mining sites in the California study (Cain and others, 2000) was similar to Tavasci Marsh, but the caddisfly Cd concentrations were greater (table 10). Reference concentrations from unmined and unpolluted sites (0.06 to 0.58 ppm, table 10) are similar to Tavasci Marsh concentrations.

Chromium concentration was high at TZG03 (11.3 ppm) compared with the other sites in Tavasci Marsh, which ranged from 0.94 to 3.5 ppm (fig. 38*C*). With the exception of the one high Cr concentration at TZG03, Tavasci Marsh concentrations were similar to both a polluted and nonpolluted site in Spain (0.567 and 1.10 ppm, respectively;Lavilla and others, 2010).

Copper concentrations were similar among Tavasci Marsh sites, with all four samples' concentrations between 22.5 and 27.6 ppm (fig. 38*D*). These concentrations are slightly less than mining affected sites in Idaho and California (32 and 37.5 ppm respectively, table 10) and similar to the

sites in Spain for both polluted and nonpolluted sites (20.9 and 25.6 ppm respectively, table 10).

Mercury concentrations decreased between sites TZG03, -04, -08, and -05 from 109 to 23.8 ppb. Mercury concentration was greatest in the fall sample collected from TZG03 (109 ppb), which was 45.1 ppb greater than the spring sample (fig. 38*E*). Seasonal difference between fall and spring samples at TZG04 was only 14.3 ppb. The concentration for the TZG05 fall sample was the lowest of all the sites for Hg (23.8 ppb). The range of concentrations from Tavasci Marsh overlaps the range of reference and mining sites from Idaho and California (40–110 ppb, table 10).

Similar to Cr, there was one anomalous Ni concentration of 26.7 ppm at TZG03, which was an order of magnitude greater than the other sites (which ranged from 0.47 to

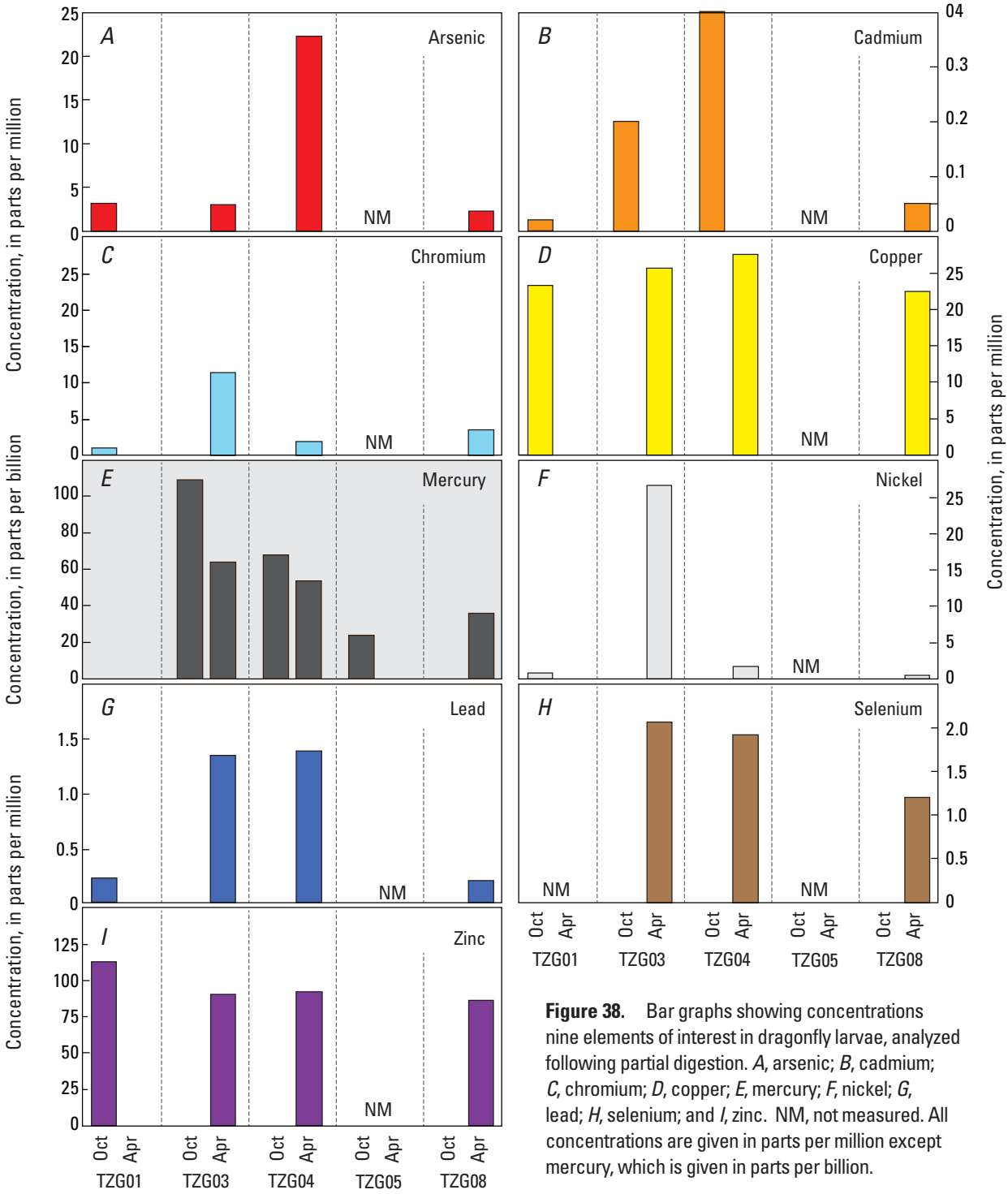

Figure 38. Bar graphs showing concentrations nine elements of interest in dragonfly larvae, analyzed following partial digestion. *A*, arsenic; *B*, cadmium; *C*, chromium; *D*, copper; *E*, mercury; *F*, nickel; *G*, lead; *H*, selenium; and *I*, zinc. NM, not measured. All concentrations are given in parts per million except mercury, which is given in parts per billion.

1.7 ppm; fig. 38*F*). With the exception of the one high Ni concentration at TZG03, the concentrations observed in the dragonfly larvae at Tavasci Marsh were similar to both a polluted and nonpolluted site in Spain (0.413 and 1.03 ppm, respectively; Lavilla and others, 2010).

Lead concentrations in dragonfly larvae followed a similar pattern as Cd, where sites TZG03 and -04 (1.34 and 1.38 ppm) were about an order of magnitude greater than TZG01 and -08 (0.2 and 0.22 ppm; fig. 38*G*). Lead concentrations from dragonfly larvae in Tavasci Marsh were similar to most other compared studies in table 10 (0.59 to 2.94 ppm), except for mining sites in Idaho, which were much greater (74 to 142 ppm, table 10). Previously mentioned mining sites in Idaho had much larger sediment Pb concentrations (1,851 to 2,390 ppm, table 10) compared with Tavasci Marsh surface sediment (27 to 56 ppm).

Selenium was only analyzed in samples collected at TZG03, -04, and -08. concentrations of Se in dragonfly larvae from Tavasci Marsh were similar across the three sites and ranged from 1.21 to 2.08 ppm (fig. 38*H*).

Zinc concentrations in dragonfly larvae were fairly similar among all sampling sites and ranged from 86.5 to 113 ppm (fig. 38*I*). Zinc concentrations in dragonfly larvae from Tavasci Marsh were similar to most other comparative studies (which ranged from 59.7 to 181 ppm, table 10), except for mining sites in Idaho, which were much greater (707 to 973 ppm, table 10). Previously mentioned mining sites in Idaho had much larger sediment Zn concentrations (2,022 to 2,543 ppm, table 10) compared with Tavasci Marsh surface sediment (112 to 308 ppm).

Site TZG03 had the greatest concentrations of Cr, Hg, Ni, and Se, while TZG04 had the greatest concentrations of As, Cd, Cu, and Pb and TZG01 had the greatest concentration of Zn. Lavilla and others (2010) found that the majority of As is adsorbed onto the outside of the dragonfly larvae and most can be removed by rinsing, which may suggest that the anomalously large concentration at TZG04 was the result of inadequate rinsing of the sample before analysis. Conversely, most Cd, Cu and Zn are localized inside of the dragonfly larvae (Cain and others, 2000; Lavilla and others, 2010), which may explain why the concentrations are consistent among sampling sites. Overall, trace element concentrations in dragonfly larvae were generally similar or less than mining affected sites in other comparative studies.

Fish

Several fish species were collected throughout the marsh to investigate variability in metal bioaccumulation in different trophic guilds. For comparison with other studies (FWS and OTHER USGS—see the Data Used for Comparison section for details), fish were grouped into three general categories, and species collected from Tavasci Marsh are given in parentheses: sunfish (including samples of bluegill, green sunfish, and largemouth bass), catfish (yellow bullhead), and small minnows/livebearers (western mosquitofish). As in the dragonfly larvae section, results are reported for each element of interest, values are compared to other studies, and summarized in table 11 and appendix D, table 9. All concentrations are reported as dry weight.

Arsenic concentrations in fish from Tavasci Marsh were consistent within the same fish group but varied strongly between groups—concentrations of As ranged from 0.3 to 2.4 ppm. The western mosquitofish samples had the greatest As concentrations, 2.3 and 2.4 ppm (fig. 39*A*). Arsenic concentrations in the sunfish group were within the IQR of the FWS and OTHER USGS distributions. Yellow bullhead exceeded the 75th percentile of both the FWS and OTHER USGS distributions. Western mosquitofish greatly exceeded the 75th percentile for the FWS the 50th percentile of the OTHER USGS distributions (fig. 39*A*). Overall, As concentrations in the western mosquitofish and yellow bullhead samples collected from Tavasci Marsh were elevated relative to other regional studies, especially in comparison to many of the FWS studies that focused on mining-affected sites.

Cadmium in fish from Tavasci Marsh was consistent within the same fish groups. Concentrations of Cd in the fish from Tavasci Marsh were generally low (<0.006 to 0.03 ppm) but western mosquitofish and yellow bullhead concentrations were an order of magnitude greater than the sunfish group (fig. 39*B*). Cadmium was below the 25th percentile for all three fish groups compared to both FWS and OTHER USGS studies (fig. 39*B*).

Unlike Cd, Cr in fish from Tavasci Marsh varied within the fish groups. Concentrations of Cr ranged from 0.25 to 8.1 ppm, where the lowest concentration was in the largemouth bass fillet and the greatest was in a yellow bullhead (fig. 4039*C*). Within the sunfish group, a largemouth bass (2 ppm) and green sunfish (1.6 ppm) sample were an order of magnitude greater than the other samples (0.25 to 0.38 ppm). The two greatest Cr concentrations in sunfish samples were within the IQR while the rest of the sunfish samples were less than the 25th percentile of both the FWS and other USGS studies (fig. 39*C*). For yellow bullhead, the highest sample exceeds the 75th percentile and the lowest is below the 25th percentile of both FWS and OTHER USGS studies. For western mosquitofish, both samples are below the 25th percentile of the FWS study, and are outside the IQR of the OTHER USGS study. Overall, there was high variability in sample concentrations of Cr, which was also observed in replicate RPD, which ranged from 20 to 53 percent (appendix D, table 7). Standard reference sample percent recovery was good for Cr, which indicates that there may be inherent environmental variability of Cr concentrations in fish from Tavasci Marsh that need to be investigated further.

Copper concentrations in fish from Tavasci Marsh were fairly consistent within the fish groups. Concentrations of Cu ranged from 1.47 to 11.1 ppm and the western mosquitofish samples had the greatest Cu concentrations, 7.47 and 11.1 ppm (fig. 39*D*). Copper was within the IQR of sunfish and catfish groups and western mosquitofish were greater than the 50th percentile for small minnow/ livebearer groups compared to both FWS and OTHER USGS studies (fig. 39*D*).

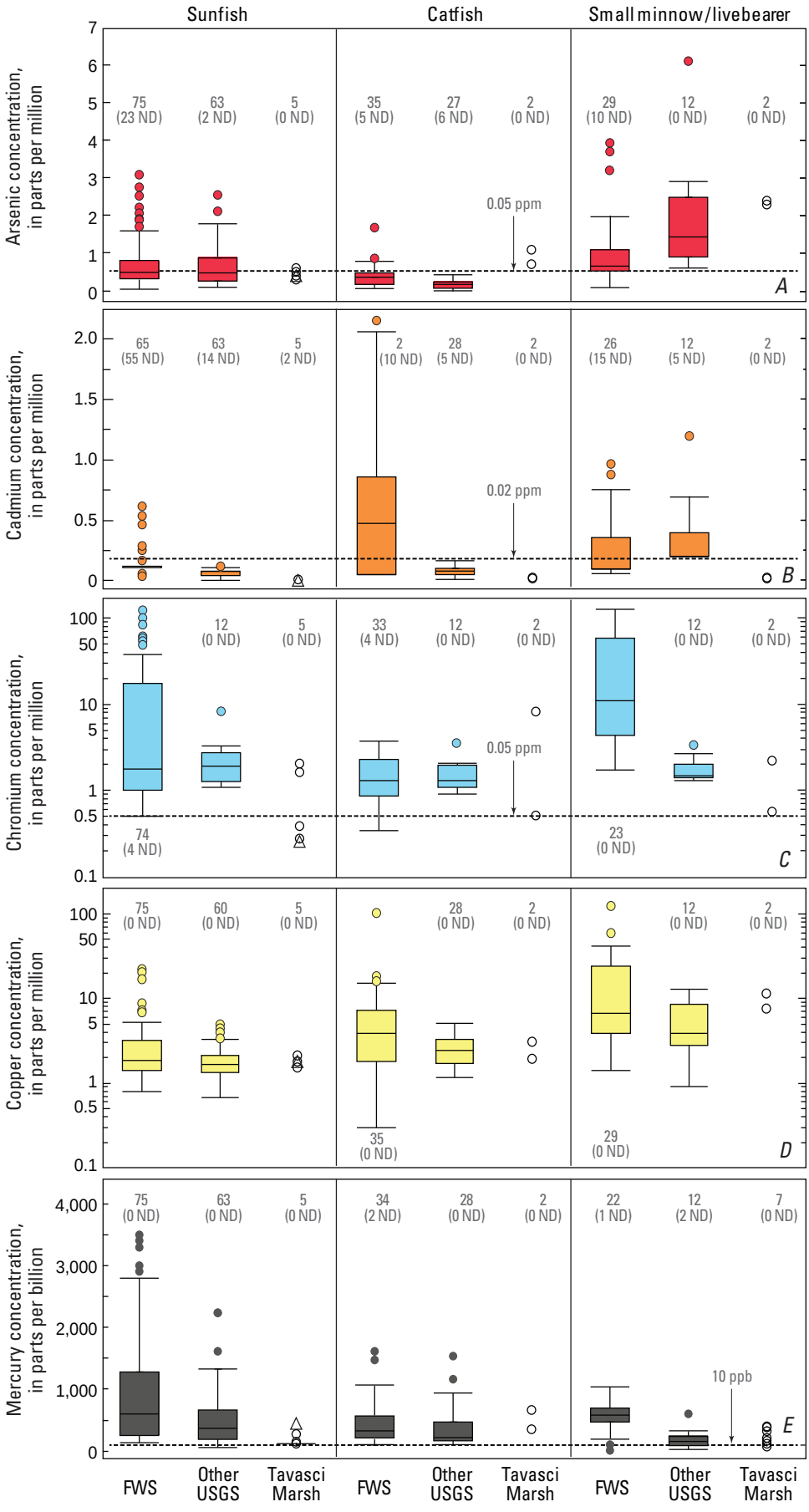

Figure 39. Box plots of trace element concentrations in fish samples from Tavasci Marsh (this study), FWS and OTHER USGS studies. *A*, arsenic; *B*, cadmium; *C*, chromium; *D*, copper; *E*, mercury; *F*, nickel; *G*, lead; *H*, selenium; and *I*, zinc. ND, value less than laboratory reporting limit.

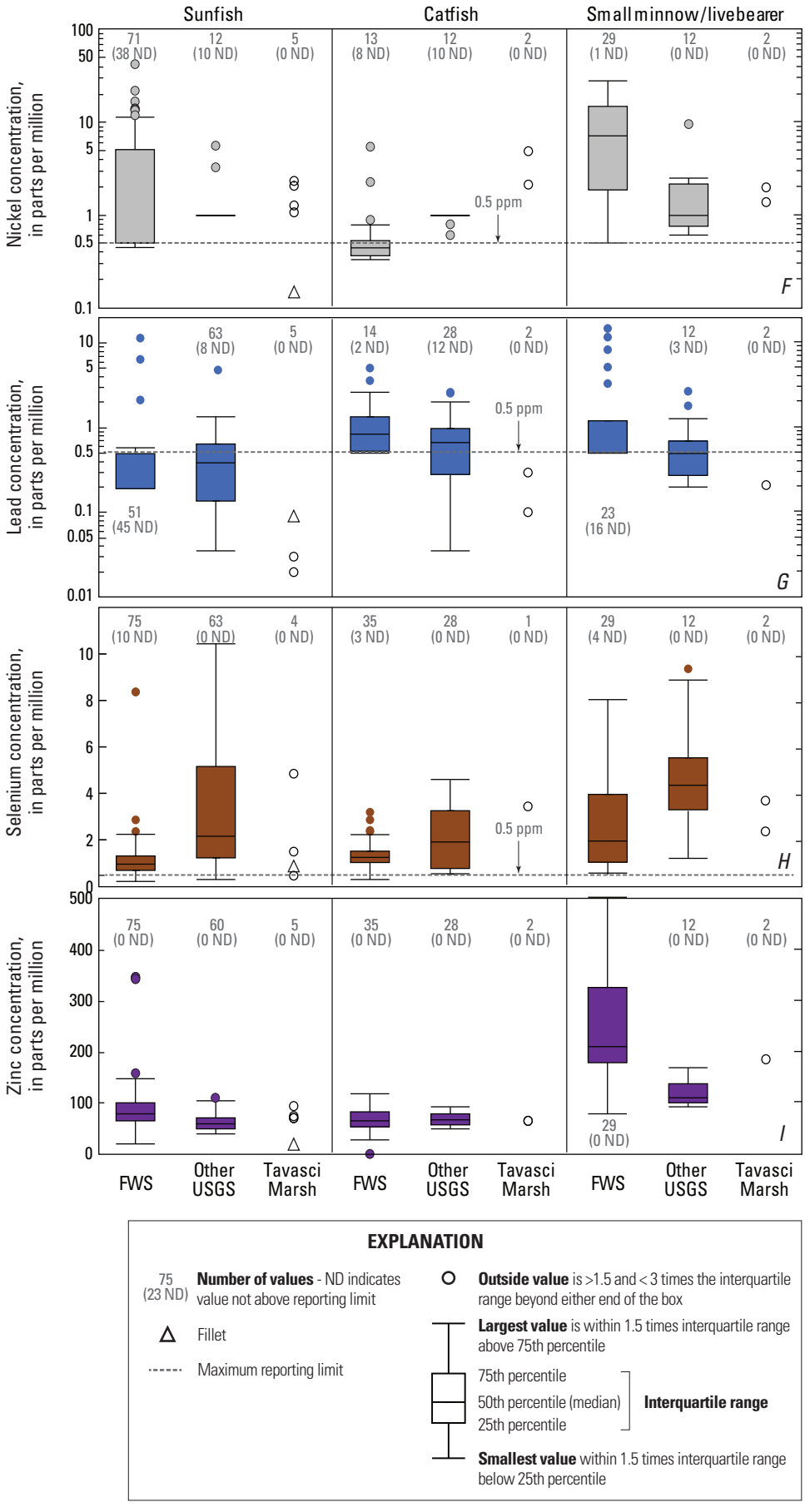

Figure 39.—Continued

Mercury in fish from Tavasci Marsh varied within the fish groups. Concentrations of Hg in the fish from Tavasci Marsh ranged from 67.6 to 662 ppb, and yellow bullhead had the highest concentrations, 357 and 662 ppb (fig. 39*E*). Within the sunfish group, the largemouth bass fillet was the only sample to exceed the 50th percentile of the OTHER USGS study. The lower concentration yellow bullhead sample exceeded the 50th percentile and the higher concentration exceeded the 75th percentile of both the FWS and OTHER USGS studies (fig. 39*E*). The western mosquitofish from Tavasci Marsh all had Hg concentrations lower than the 25th percentile of the FWS study, while the range of concentrations from Tavasci Marsh bracketed the IQR: one sample was less than the 25th percentile and 3 samples greater than the 75th percentile of the OTHER USGS study (fig. 39*E*).

Nickel concentrations in fish from Tavasci Marsh varied within some of the fish groups but was fairly similar between groups, ranging from 0.15 to 4.9 ppm (fig. 39*F*). The Ni concentration in the largemouth bass fillet (0.15 ppm) was an order of magnitude less than the sunfish group (which ranged from 1.1 to 2.4 ppm). Sunfish group samples (excluding the fillet) were within the IQR of the FWS study and were less than the outliers for the OTHER USGS study (fig. 39*F*). Yellow bullhead Ni concentrations were greater than the 75th percentile of both the FWS and OTHER USGS studies. Western mosquitofish Ni concentrations were at or less than the 25th percentile of the FWS study and bracketed the 75th percentile of the OTHER USGS study (fig. 39*F*).

Lead in fish from Tavasci Marsh varied within some of the fish groups. Concentrations of Pb in the fish from Tavasci Marsh were generally low (0.03 to 0.3 ppm) and western mosquitofish and yellow bullhead concentrations were an order of magnitude greater than the sunfish group (fig. 39*G*). Lead was less than the 25th percentile for all three fish groups compared with both FWS and OTHER USGS studies, except for one yellow bullhead sample which was just above the 25th percentile for the OTHER USGS studies (fig. 39*G*).

Selenium concentrations in fish from Tavasci Marsh varied within some of the fish groups but was fairly similar between groups. Concentrations of Se in the fish from Tavasci Marsh ranged from 0.47 to 3.7 ppm (fig. 39*H*). Sunfish group concentrations bracket the IQR of the FWS study with one sample less than the 25th percentile and two above the 75th percentile. Two sunfish group fish are within the IQR of the OTHER USGS study and two are below the 25th percentile. The Se concentration in the yellow bullhead is greater than the 75th percentile of both the FWS and OTHER USGS studies (fig. 39*H*). Western mosquitofish Se concentrations were within the IQR of the FWS study and bracketed the 25th percentile of the OTHER USGS study (fig. 39*H*).

Zinc concentrations in fish from Tavasci Marsh were similar among the whole-fish samples, ranging from 17.5 to 186 ppm. The lowest concentration was found in the largemouth bass fillet, an order of magnitude less than the two western mosquitofish (fig. 39*I*). The largemouth bass fillet was less than the 25th percentile of both FWS and OTHER USGS studies. The whole-fish samples from the sunfish group were within the IQR of the FWS study and bracketed the 75th percentile of the OTHER USGS study (fig. 39*I*). Yellow bullhead Zn concentrations were within the IQR of both the FWS and OTHER USGS studies. Western mosquitofish Zn concentrations were less than the 50th percentile of the FWS study and greater than the 75th percentile of the OTHER USGS study (fig. 39*I*).

The largemouth bass fillet, compared to the whole-fish samples in the sunfish group, had lower concentrations of three elements of interest (Cr, Ni, and Zn) and higher concentrations of two (Hg and Pb), suggesting that certain trace elements may partition to different parts of largemouth bass. More than one sample would be needed to confirm this observation with certainty, but it may warrant further investigation. Yellow bullhead samples had the greatest concentration among all fish collected in Tavasci Marsh during this study for four elements (Cr, Hg, Ni, and Pb). Cadmium concentration was greatest in yellow bullhead and western mosquitofish.The greatest concentration of As, Cu, and Zn was from western mosquito fish. Selenium concentration was greatest in a largemouth bass sample.

Comparison Between Sediment, Plant, Dragonfly Larvae, and Fish

Trace element concentrations in water samples were generally low with the exception of As. Water concentrations are reported in mass per volume units, and while water concentrations do influence concentrations in other sample media, they are not directly comparable to the solid samples, which are reported in mass per mass units. The following discussion focuses on comparison among the solid samples.

Statistical distributions of surface sediment, core sediment, plants, dragonfly larvae, and fish were calculated for the elements of interest (As, Cd, Cr, Cu, Hg, Ni, Pb, Se, and Zn) to understand how each element partitioned in the Tavasci Marsh ecosystem. Arsenic concentrations were greatest in sediment and cattail roots and were generally much lower in the dragonfly larvae and fish (fig. 40*A*). Most of the other elements of interest (Cd, Cr, Cu, Ni, and Pb) were greatest in the sediment and much lower in the plants, dragonfly larvae, and fish (figs. 40*B–D* and *G–H*). Mercury concentrations were greatest in fish samples, and methylmercury concentrations were several orders of magnitude greater in the fish and dragonfly larvae compared with the sediment core and cattail samples, and watermilfoil samples had intermediate concentrations (figs. 40*E–F*). Selenium and Zn concentrations were similar across the different sample types, except for plants, which were the least concentrated. Dragonfly larvae and fish sample concentrations were similar or greater than the sediment (figs. 40*I–J*).

Bioaccumulation of a few elements of interest appears to be occurring in some aquatic biota from Tavasci Marsh. Arsenic concentrations in the cattail roots are often greater than the surrounding surface sediment. Mercury concentrations in the dragonfly larvae are similar to the sediment samples, and

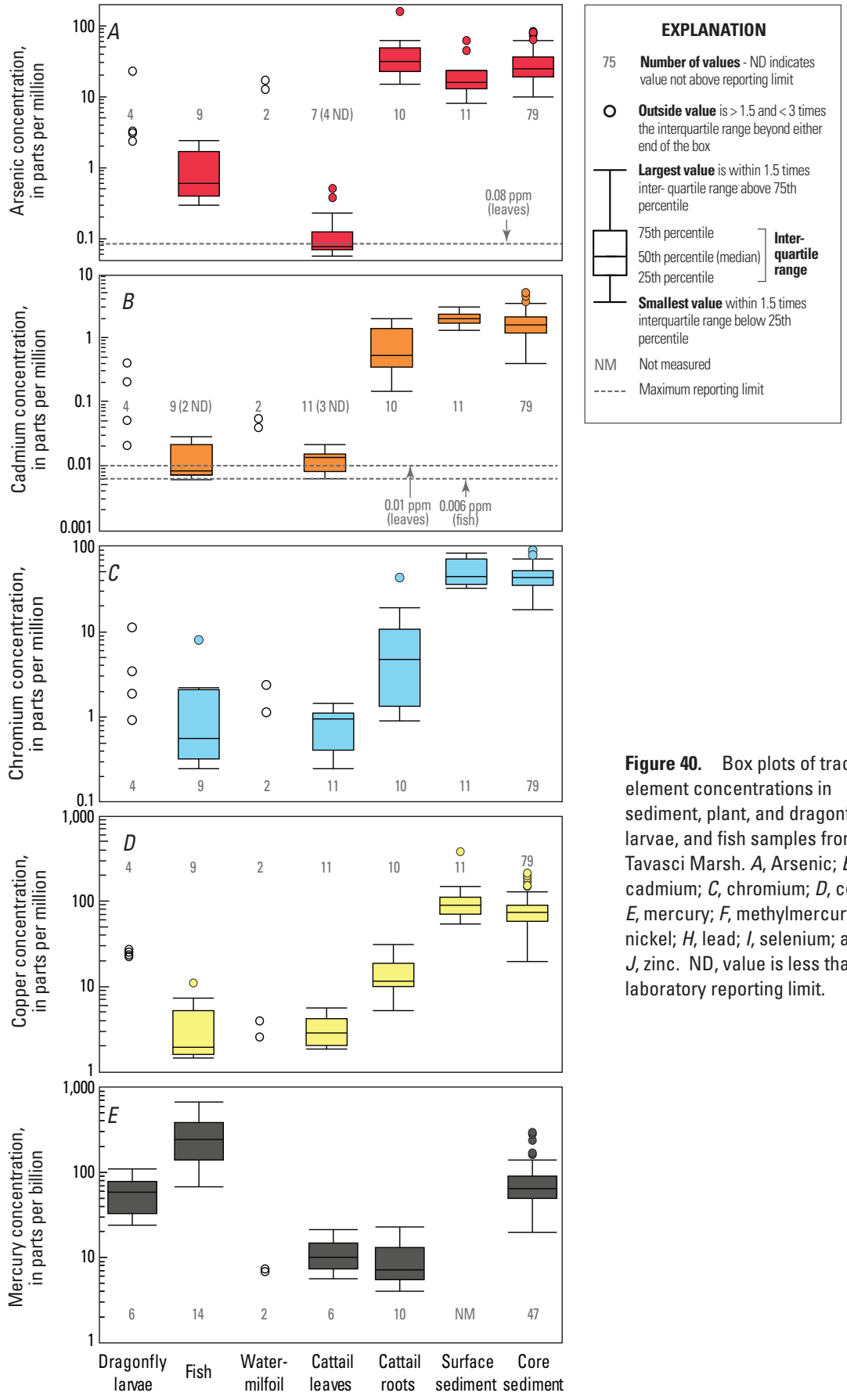

Figure 40. Box plots of trace element concentrations in sediment, plant, and dragonfly larvae, and fish samples from Tavasci Marsh. *A*, Arsenic; *B*, cadmium; *C*, chromium; *D*, copper; *E*, mercury; *F*, methylmercury; *G*, nickel; *H*, lead; *I*, selenium; and *J*, zinc. ND, value is less than laboratory reporting limit.

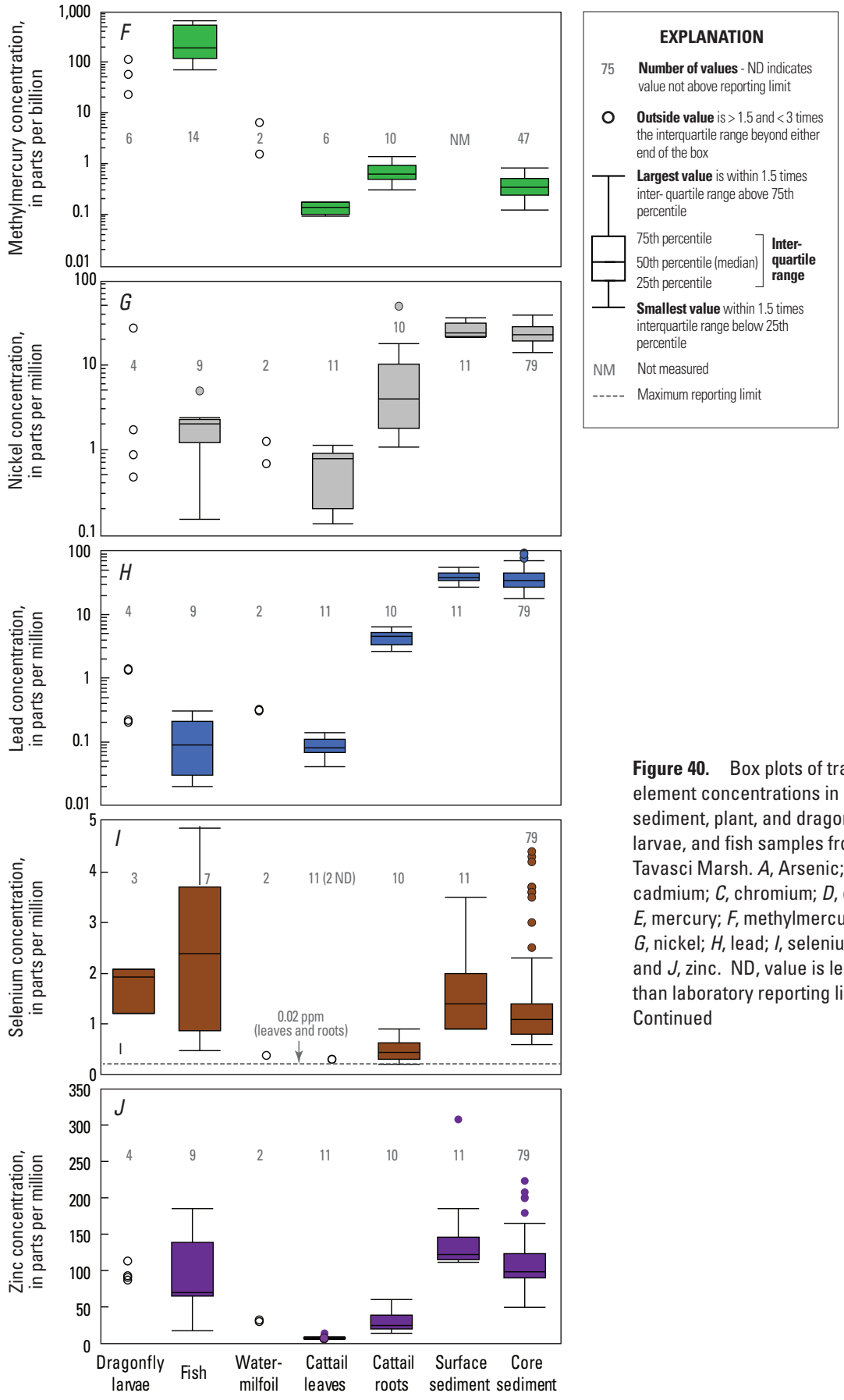

Figure 40. Box plots of trace element concentrations in sediment, plant, and dragonfly larvae, and fish samples from Tavasci Marsh. *A*, Arsenic; *B*, cadmium; *C*, chromium; *D*, copper; *E*, mercury; *F*, methylmercury; *G*, nickel; *H*, lead; *I*, selenium; and *J*, zinc. ND, value is less than laboratory reporting limit.—Continued

concentrations in fish are significantly greater than the sediment samples, and, as noted above, methylmercury concentrations in the dragonfly larvae and fish are several orders of magnitude greater than the sediment samples (fig. 40).

Principal-component analysis on the majority of the elements of interest (As, Cd, Cr, Cu, Ni, Pb, and Zn) indicates that surface sediment has the greatest concentration of trace elements, followed by cattail roots (fig. 41). Plant samples were characterized by greater concentrations of As, Cd, Ni, and Zn compared to the surface sediment, dragonfly larvae, and fish. Cattail leaves had the least concentration of trace elements, and watermilfoil samples were intermediate between cattail leaves and roots. Dragonfly larvae and fish were characterized having greater concentrations of Cu, Cr, and Zn, as did the surface sediment samples (fig. 41).

It is important to consider that the plants, dragonfly larvae, and fish were only exposed to the surface sediment, which was lower in concentration than the elevated trace element concentrations at depth in three of the sediment cores from the marsh (outliers for core sediment are shown in figure 40 for Cd, Cu, Hg, Pb, Zn) except for one surface sediment site (an outlier in surface sediment in figure 40 for Cu and Zn [Hg was not measured in surface sediments]). If deeper sediments are disturbed and brought into contact with surface waters and habitat for the biota of Tavasci Marsh, further samples should be collected to understand the bioaccumulation from the new substrate.

Summary

Tavasci Marsh is a large freshwater marsh within the Tuzigoot National Monument unit of the National Park system in central Arizona and is the largest freshwater marsh in Arizona unconnected to the Colorado River. The marsh has been altered significantly by mining activities nearby during the first half of the 20th century and subsequent management, and the National Park Service is evaluating the possibility of restoring the marsh. In light of this history, we conducted evaluations of water, sediment, plant, dragonfly larvae, and fish in the marsh. The evaluations were focused on nine metals and trace elements of interest (As, Cd, Cr, Cu, Hg, Ni, Pb, Se, and Zn) that are commonly associated with mining activities, together with isotopic and geochemical analysis of water and sediment in order to understand the sources and timing of sediment inputs to the marsh and concentrations of metals and trace elements in plants, dragonfly larvae, and fish.

Two distinct sources of water contributed to Tavasci Marsh during the study, one from older high-elevation (>6,000 ft) recharge entering the marsh at Shea Spring (as well as a number of unnamed seeps and springs on the north eastern edge of the marsh) and the other source present as shallow groundwater at the northern end of the marsh, originating from younger low-elevation recharge or water from Pecks Lake that has been altered due to evaporation.

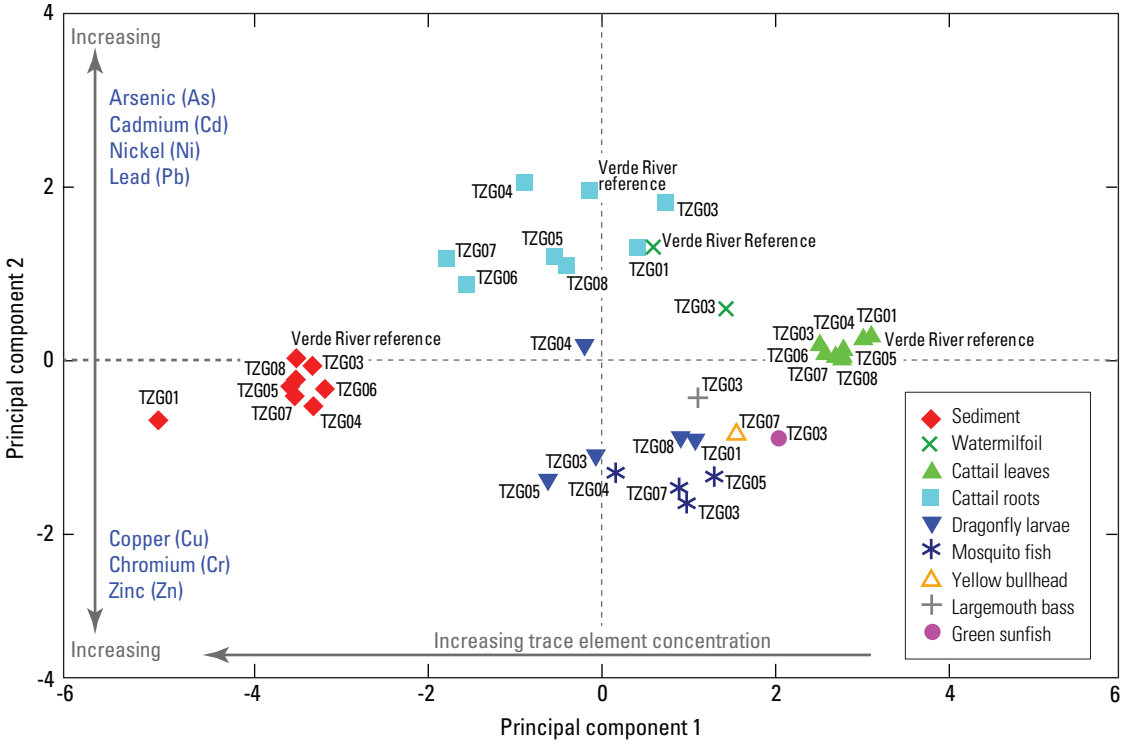

Figure 41. Principal component analysis graph of solid samples from Tavasci Marsh for As, Cd, Cr, Cu, Ni, Pb, and Zn. Symbols are grouped by type of sample and location of symbols on the graph are related to changes in overall trace element concentration (principal component 1) and changes in specific trace element concentration (principal component 2).

Water concentrations of As exceeded the U.S. Environmental Protection Agency primary drinking water standard of 10 µg/L at all sampling sites, ranging from 14.8 to 161 µg/L. Arsenic is known to be naturally elevated in water of the Verde River watershed, typically associated with certain geologic formations such as the sandstone member of the Verde Formation.

Surface waters at Tavasci Marsh may contain conditions favorable for methylmercury production. We found that methylmercury was an average of 29 percent of the total mercury measured.

All surficial and core sediment samples exceeded or were within sample concentration variability of at least one sediment-quality guideline for As, Cd, Cr, Cu, Hg, Ni, Pb, and Zn. Several sediment sites were also above or were within sample variability of severe or probable-effect sediment quality guidelines for As, Cd, and Cu. Three sediment cores collected in the marsh (at sites TZG02, -03, and -04) had elevated metal and trace element concentrations at the bottom of the core (for Bi, Cd, Cu, Hg, In, Pb, Sb, Sn, Te, and Zn). The elevated metal and trace element concentrations are associated with sediment deposited before 1963 (based on ^{137}Cs radioisotope dating), but detailed chronology at the bottom of the sediment cores was not possible due to large uncertainties in the age-dating method using ^{226}Ra and unsupported ^{210}Pb.

Arsenic concentration was greater in the cattail roots than the surrounding sediment for all but one sample site in Tavasci Marsh. Concentrations of As and Cd in cattail roots exceeded severe or probable-effect sediment quality guidelines and Ni exceeded sediment quality guidelines at some sites. Chromium and Ni showed the greatest seasonal variability in plant samples with greater concentrations in the fall samples.

Concentrations of Cd were greatest in western mosquitofish and yellow bullhead from Tavasci Marsh. Arsenic, Cu, and Zn concentrations were greater in western mosquitofish than all other fish. Yellow bullhead had greater concentrations of Cr, Hg, Ni, and Pb. Concentrations of As, Ni, and Se in yellow bullhead were greater than the 75th percentile similar studies from Arizona and the western U.S.

Mercury concentrations in dragonfly larvae and fish from Tavasci Marsh were similar to or greater than sediment, including those elevated concentrations from the bottom of three sediment cores.

A principal component analysis on the majority of the elements of interest, As, Cd, Cr, Cu, Ni, Pb, and Zn indicates that surface sediment has the greatest trace element concentration among all solid samples followed by cattail roots. Dragonfly larvae and fish and surface sediment samples had the greatest concentrations of Cu, Cr, and Zn.

Future Research

In order to understand the spatial extent of the elevated metals concentrations observed at depth in three of the sediment cores, more deep sediment cores should be collected at other open water sections of the marsh with the goal of obtaining sediment present in the marsh before mining activities to better understand background concentrations. The radioisotope age dating of sediment core samples from this study was limited by not being able to collect cores with a complete ^{137}Cs profile as well as only being able to apply the CRS method using ^{226}Ra and unsupported ^{210}Pb to two cores, which had large errors at depth. Better chronology of additional sediment cores is needed to understand the trace element profile with depth in Tavasci Marsh. Additionally, a geophysical survey to map the thickness of marsh sediment would guide the selection of core sampling sites and help quantify the volume of sediments in Tavasci Marsh. Dissolved oxygen measurements of surface water should be made at a larger number of sites in the marsh, and biochemical oxygen demand should be measured throughout the marsh to better understand the processes contributing to the depletion of oxygen in the marsh. Further investigation of factors influencing Hg bioaccumulation in the marsh would help park managers understand this issue. An ecological risk assessment by the U.S. Geological Survey has begun based on the results presented in this report.

Continued monitoring of water quality throughout the marsh would provide valuable information related to changes in water transported to the marsh from Pecks Lake under various lake management regimes. Stable isotopes and major ions, analyzed during this study, were shown to be distinct indicators of water sources to the marsh.

References Cited

Alenius, E.M.J., 1968, A brief history of the United Verde Open Pit, Jerome, Arizona, The Arizona Bureau of Mines Bulletin 178.

Allert, A.L., DiStefano, R.J., Fairchild, J.F., Schmitt, C.J., McKee, M.J., Girondo, J.A, Brumbaugh, W.G., and May, T.W., 2013, Effects of historical lead-zinc mining on riffle-dwelling benthic fish and crayfish in the Big River of southeastern Missouri, USA: Ecotoxicology, v. 22, p. 506–521, doi:10.1007/s10646-013-1043-3.

Anderson, C.A., and Creasey, S.C., 1958, Geology and ore deposits of the Jerome area Yavapai County, Arizona: U.S. Geological Survey Professional Paper 308, 194 p., http://pubs.er.usgs.gov/publication/pp308.

Anderson, R.A., Schiff, S.L., and Hesslein, R.H., 1987, Determining sediment accumulation and mixing rates using ^{210}Pb, ^{137}Cs and other tracers—Problems due to postdepositional mobility or coring artifacts: Canadian Journal of Fisheries and Aquatic Sciences, v. 44, p. 231–250.

Andrewes, P., Cullen, W.R., and Polishchuk, E., 2000, Arsenic and antimony biomethylation by *Scopulariopsis brevicaulis*—Interaction of arsenic and antimony compounds: Environmental Science and Technology, v. 34, p. 2249–2253.

Andrews, B.J., and King, K.A., 1997, Environmental contaminants in sediment and fish of Mineral Creek and the Middle Gila River, Arizona: U.S. Fish and Wildlife Service Environmental Contaminants Report, Phoenix Ecological Services Field Office, Arizona, 17 p., http://www.fws.gov/southwest/es/arizona/Documents/ECReports/MineralCreekMidGilaRiverAZ.pdf

Andrews, B.J., King, K.A., and Baker, D.L., 1995, Radionuclides and trace elements in fish and wildlife of the Puerco and Little Colorado Rivers, Arizona: U.S. Fish and Wildlife Service Environmental Contaminants Report, Phoenix Ecological Services Field Office, Arizona, 20 p., http://www.fws.gov/southwest/es/documents/r2es/radionuclidesaz.pdf

Appleby, P.G., and Oldfield, F., 1992, Application of ^{210}Pb to sedimentation studies, chap. 21 in Ivanovich, M., and Harmon. R.S., eds., Uranium-series Disequilibrium—Application to Earth, Marine, and Environmental Sciences, 2d ed.: Oxford, Clarendon Press, p. 731–778.

Arizona Department of Environmental Quality, Peck's Lake Total Maximum Daily Load Assessment, September, 2001: Arizona Department of Environmental Quality, 41 p.,.

Baker, D.L., and King. K.A., 1994, Environmental contaminant investigation of water quality, sediment and biota of the upper Gila River basin, Arizona: U.S. Fish and Wildlife Environmental Contaminants Report, Phoenix Ecological Services Field Office, Arizona, 25 p., http://www.fws.gov/southwest/es/Documents/R2ES/UpperGilaRiver1994.pdf

Barker, L.M., 1930, Concentrating plant of United Verde Copper Company: Mining Congress Journal, v. 16, p. 363–367, https://uair.arizona.edu/system/files/usain/download/azu_m9791_m666u_w.pdf/.

Barranguet, C. Charantoni, L., Plans, M., and Admiraal, W., 2000, Short-term response of monospecific and natural algal biofilms to copper exposure: European Journal of Phycology, v. 35, p. 397–406, http://dx.doi.org/10.1080/09670260010001736001/.

Besser, J.M., Brumbaugh, W.G., Allert, A.L., Poulton, B.C., Schmitt, C.J., and Ingersoll, C.G., 2009, Ecological impacts of lead mining on Ozark streams—Toxicity of sediment and pore water: Ecotoxicology and Environmental Safety, v. 72, no. 2, p. 516–526, http://dx.doi.org/10.1016/j.ecoenv.2008.05.013/.

Blasch, K.W., Hoffmann, J.P., Graser, L.F., Bryson, J.R., and Flint, A.L., 2006, Hydrogeology of the upper and middle Verde River watersheds, central Arizona: U.S. Geological Survey Scientific Investigations Report 2005–5198, 102 p., 3 plates, http://pubs.usgs.gov/sir/2005/5198/.

Brenton, R.W., and Arnett, T.L., 1993, Methods of analysis by the U.S. Geological Survey National Water Quality Laboratory—Determination of dissolved organic carbon by uv-promoted persulfate oxidation and infrared spectrometry: U.S. Geological Survey Open-File Report 92-480, 12 p., http://pubs.er.usgs.gov/publication/ofr92480/.

Briggs, P.H., and Meier, A.L., 2002, The determination of forty-two elements in geological samples by inductively coupled plasma-atomic emission spectrometry, chap. G *in* Taggart, J.E., Jr., ed., Analytical methods for chemical analysis of geologic and other materials: U.S. Geological Survey Open-File Report 02-223-G, p. G1–G18, http://pubs.usgs.gov/of/2002/ofr-02-0223/.

Cain, D.J., Carter, J.L., Fend, S.V., Luoma, S.N., Alpers, C.N., and Taylor, H.E., 2000, Metal exposure in a benthic macroinvertebrate, *Hydropsyche californica*, related to mine drainage in the Sacramento River: Canadian Journal of Fisheries and Aquatic Sciences, v. 57, p. 380–390.

Callender, E., and Robbins, J.A., 1993, Transport and accumulation of radionuclides and stable elements in a Missouri River reservoir: Water Resources Research, v. 29, no. 6, p. 1787–1804, doi:10.1029/93WR00387.

Cassell, D.T., 1980, Sedimentary petrography and depositional models for the non-marine carbonate rocks of the Verde Formation, northern Verde Valley, Arizona: Flagstaff, Ariz., Northern Arizona University, M.S. thesis.

Chapman P.M., Adams, W.J., Brooks, M.L., Delos, C.G., Luoma, S.N., Maher, W.A., Ohlendorf, H.M., Presser, T.S., and Shaw, D.P., 2009, Ecological assessment of selenium in the aquatic environment: Summary of a SETAC Pellston Workshop. Pensacola FL (USA): Society of Environmental Toxicology and Chemistry (SETAC).

Church, S.E., von Guerard, P., and Finger, S.E., eds., 2007, Integrated investigations of environmental effects of historical mining in the Animas River watershed, San Juan County, Colorado: U.S. Geological Survey Professional Paper 1651, 1,096 p. plus CD-ROM [In two volumes.], http://pubs.usgs.gov/pp/1651/.

Cidu, R., and Frau, F., 2007, Influence of fine particles on the concentration of trace elements in river waters, Bullen and Wand ed., Water-Rock Interaction, Proceedings of the 12th international symposium on water-rock interaction, Kunming, China, 31 July – 5 August 2007; Taylor and Francis, 2007.

Clark, I.D., and Fritz, P., 1997, Environmental isotopes in hydrogeology: New York, Lewis Publishers, 328 p.

Clarke, K.R., 1993, Non-parametric multivariate analyses of changes in community structure: Australian Journal of Ecology, v. 18, no. 1, p. 117–143, doi: 10.1111/j.1442-9993.1993.tb00438.x.

Clarke, K.R., and Gorley, R.N., 2006, Primer v6—User manual/tutorial: Plymouth, United Kingdom, PRIMER-E, Ltd., 190 p.

Clarke, K.R., and Warwick, R.M., 2001, Change in marine communities—an approach to statistical analysis and interpretation, chapter 4 *in* Clarke, K.R. and Gorley, R.N. eds. PRIMER-E, 2d ed.: Plymouth, United Kingdom, PRIMER-E, Ltd., 8 p.

Clements, W.H., Carlisle, D.M., Lazorchak, J.M., and Johnson, P.C., 2000, Heavy metals structure benthic communities in Colorado mountain streams: Ecological Applications, v. 10, no. 2, p. 626–638.

Cory, R.M., Miller, M.P., McKnight, D.M., Guerard, J.J., and Miller, P.L., 2010, Effect of instrument-specific response on the analysis of fulvic acid fluorescence spectra: Limnology and Oceanography Methods, v. 8, p. 67–78, doi:10.4319/lom.2010.8.67.

Cutshall, N.H., Larsen, I.L., and Olsen, C.R., 1983, Direct analysis of ^{210}Pb in sediment samples—self-absorption corrections: Nuclear Institute and Methods, v. 206, p. 309–312, http://dx.doi.org/10.1016/0167-5087(83)91273-5.

Deng, H., Ye, Z.H., and Wong, M.H., 2004, Accumulation of lead, zinc, copper and cadmium by 12 wetland plant species thriving in metal-contaminated sites in China: Environmental Pollution, v. 132, p. 29–40, http://dx.doi.org/10.1016/j.envpol.2004.03.030.

Deniseger, J., Austin, A., and Lucey, W.P., 1986, Periphyton communities in a pristine mountain stream above and below heavy metal mining operations: Freshwater Biology, v. 16, p. 209–218, doi:10.1111/j.1365-2427.1986.tb00965.x.

Denny, F.W., 1930, Cottrell plant of the United Verde Copper Company: Mining Congress Journal, v. 16, p. 370–375, https://uair.arizona.edu/system/files/usain/download/azu_m9791_m666u_w.pdf/.

DeWild, J.F., Olson, M.L., and Olund, S.D., 2001, Determination of methyl mercury by aqueous phase ethylation followed by gas chromatographic separation with cold vapor atomic fluorescence detection: U.S. Geological Survey Open-File Report 01-445, http://pubs.usgs.gov/of/2001/ofr-01-445/.

DeWild, J.F., Olund, S.D., Olson, M.L., and Tate, M.T., 2005, Methods for the preparation and analysis of solids and suspended solids for methylmercury: U.S. Geological Survey Techniques and Methods, book 5, chapter 7, section A, 13 p., http://pubs.usgs.gov/tm/2005/tm5A7/.

DeWitt, E., Langenheim, V., Force, E., Vance, R.K., Lindberg, P.A., and Driscoll R.L., 2008, Geologic map of the Prescott National Forest and the headwaters of the Verde River, Yavapai and Coconino Counties, Arizona: U.S. Geological Survey Scientific Investigations Map 2996, scale 1:100,000, http://pubs.usgs.gov/sim/2996/.

Ecology and Environment, Inc., 1994, Expanded site inspection summary report (analysis of ESI results) Phelps Dodge Verde Mine, submitted to U.S. Environmental Protection Agency, EPA ID# AZD983475773.

Farag, A.M., Woodward, D.F., Goldstein, J.N., Brumbahgh, W., and Meyer, J.S., 1998, Concentrations of metals associated with mining waste in sediments, biofilm, benthic macroinvertebrates, and fish from the Coeur d'Alene River Basin, Idaho: Archives of Environmental Contamination and Toxicology, v. 34, p. 119–127.

Fishman, M.J., ed., 1993, Methods of analysis by the U.S. Geological Survey National Water Quality Laboratory--Determination of inorganic and organic constituents in water and fluvial sediments: U.S. Geological Survey Open-File Report 93–125, 217 p., http://pubs.er.usgs.gov/publication/ofr93125/.

Fishman, M.J., and Friedman, L.C., 1989, Methods for determination of inorganic substances in water and fluvial sediments: U.S. Geological Survey Techniques of Water-Resources Investigations, book 5, chapter A1, 545 p., http://pubs.usgs.gov/twri/twri5-a1/.

Foust, R.D., Mohapatra, P., Compton-O'Brien, A.M., and Reifel, J., 2004, Groundwater arsenic in the Verde Valley in central Arizona, USA: Applied Geochemistry, v. 19, p. 251–255, http://dx.doi.org/10.1016/j.apgeochem.2003.09.011/.

Fuller, C.C., and Hammond, D.E., 1983, The fallout rate of Pb-210 on the western coast of the United States: Geophysical Research Letters, v. 10, p. 1164–1167, doi:10.1029/GL010i012p01164.

Fuller, C.C., vanGeen, A., Baskaran, M., and Anima, R., 1999, Sediment chronology in San Francisco Bay defined by ^{210}Pb, ^{234}Th, ^{137}Cs, and ^{239,240}Pu: Marine Chemistry, v. 64, p. 7–27, http://dx.doi.org/10.1016/S0304-4203(98)00081-4/.

Garbarino, J.R., Kanagy, L.K., and Cree, M.E., 2006, Determination of elements in natural-water, biota, sediment, and soil samples using collision/reaction cell inductively coupled plasma–mass spectrometry: U.S. Geological Survey Techniques and Methods, book 5, chapter 1, section B, 88 p., http://pubs.usgs.gov/tm/2006/tm5b1/.

Goodyear, K.L. and McNeill, S., 1999, Bioaccumulation of heavy metals by aquatic macro-invertebrates of different feeding guilds—A review: Science of the Total Environment, v. 229, p. 1–19, http://dx.doi.org/10.1016/S0048-9697(99)00051-0/.

Grisey, E., Laffray, X., Contoz, O., Cavalli, E., Mudry, J. and Aleya, L. 2012, The bioaccumaulation performance of reeds and cattails in a constructed treatment wetland for removal of heavy metals in landfill leachate treatment (Etueffont, France): Water, Air, and Soil Pollution, v. 223, p. 1723–1741, doi:10.1007/s11270-011-0978-3.

Griffith, M.B., Hill, B.H., Herligy, A.T., and Kaufman, P.R., 2002, Multivariate analysis of periphyton assemblages in relation to environmental gradients in Colorado Rocky Mountain streams: Journal of Phycology, v. 38, p. 83–95, doi:10.1046/j.1529-8817.2002.01117.x/.

Hargis, T. G., and Twilley, R.R., 1994, Improved coring device for measuring soil bulk density in a Louisiana deltaic marsh: Journal of Sedimentary Research Section A—Sedimentary Petrology and Processes, v. 64, p. 681–683.

Hart, R., Nelson, S.T., and Eggett, D., 2010, Uncertainty in ^{14}C model ages of saturated zone waters—The influence of soil gas in terranes dominated by C3 plants: Journal of Hydrology, v. 392, p. 83–95, doi:10.1016/j.jhydrol.2010.08.001.

Helsel, D.R., 2005, Nondetects and data analysis—statistics for censored environmental data: Hoboken, N.J., John Wiley and Sons, Inc., 250 p.

Helsel, D.R., and Hirsch, R.M., 2002, Statistical methods in water resources: U.S. Geological Survey Techniques of Water Resources Investigations, Book 4, chapter A3, 522 p., http://pubs.usgs.gov/twri/twri4a3/.

Hill, B. H., Herlihy, A.T., Kaufmann, P.R., Stevenson, R.J., McCormick, F.H., and Johnson, C. Burch, 2000, Use of periphyton assemblage data in an index of biotic integrity: Journal of the North American Benthological Society, v. 19, no. 1, p. 50-67.

Hill, B.H., Willingham, W.T., Parrish, L.P., and McFarland, B.H., 2000, Periphyton community responses to elevated metal concentrations in a Rocky Mountain Stream: Hydrobiologia, v. 428, p. 161–169, doi:10.1023/A:1004028318542.

Hinck, J.E., Blazer, V.S., Denslow, N.D., Gross, T.S., Echols, K.R., Davis, A.P., May, T.W., Orazio, C.E., Coyle, J.J., and Tillitt, D.E., 2006, Biomonitoring of Environmental Status and Trends (BEST) Program—Environmental contaminants, health indicators, and reproductive biomarker in fish from the Colorado River Basin: U.S. Geological Survey Scientific Investigations Report 2006–5163, 132 p., http://pubs.usgs.gov/sir/2006/5163/.

Horowitz, A.J., and Stephens, V.C., 2008, The effects of land use on fluvial sediment chemistry for the conterminous U.S.—Results from the first cycle of the NAWQA Program—Trace and major elements, phosphorus, carbon, and sulfur: Science of the Total Environment, v. 400, p. 290–314, http://dx.doi.org/10.1016/j.scitotenv.2008.04.027.

Ingersoll, C.G., Haverland, P.S., Brunson, E.L., Canfield, T.J., Dwyer, F.J., Henke, C.E., Kemble, N.E., Mount, D.R., and Fox, R.G., 1996, Calculation and evaluation of sediment effect concentrations for the amphipod *Hyalella azteca* and the midge *Chironomus riparius*: Journal of Great Lakes Research, v. 22, no. 3, p. 602–623, http://dx.doi.org/10.1016/S0380-1330(96)70984-X.

Ingerson, R., and Pearson, F.J., 1964, Estimation of age and rate of motion of groundwater by the ^{14}C method *in* Miyake, Y., and Koyama, T., eds., Recent research in the field of hydrosphere, atmosphere and nuclear chemistry: Tokyo, Maruzen Company, Sugawara Festival Volume, p. 263-283.

Johnson, R.H., DeWitt, E., Wirt, L., Arnold, L.R., and Horton, J.D., 2011, Water and rock geochemistry, geologic cross sections, geochemical modeling, and groundwater flow modeling for identifying the source of groundwater to Montezuma Well, a natural spring in central Arizona: U.S. Geological Survey Open-File Report 2011–1063, 62 p., http://pubs.usgs.gov/of/2011/1063/.

Kabata-Pendias, A., 2010, Trace elements in soils and plants, 4th ed: Boca Raton, Fla., CRC Press, 520 p.

Karpiscak, M.M., Whiteaker, L.R., Artiola, J.F., and Foster, K.E. 2001, Nutrient and heavy metal uptake and storage in constructed wetland systems in Arizona, Water Science and Technology, vol. 44, p. 455-462.

Keith, S.B., Gest, D.B., DeWitt, Ed, Toll, N.B., and Person, B.E., 1983, Metallic mineral districts and production in Arizona: Tucson, Arizona Bureau of Geology and Mineral Technology, 58 p; map scale 1:1,000,000.

King, K.A. and Andrews, 1996, Contaminants in fish and wildlife collected from the Lower Colorado River and irrigation drains in the Yuma Valley, Arizona: U.S. Fish and Wildlife Service Environmental Contaminants Report, Phoenix Ecological Services Field Office, Arizona, 22 p.

King, K.A., Baker, D.L., and Kepner, W.G., 1992, Organochlorine and trace element concentrations in the San Pedro River Basin, Arizona: U.S. Fish and Wildlife Service Environmental Contaminants Report, Phoenix Ecological Services Field Office, Arizona, 17 p., http://www.fws.gov/southwest/es/arizona/Documents/ECReports/FinalReportSanPedro.pdf/.

King, K.A., Andrews, B.J., Martinez, C.T., and Kepner, W.G., 1997, Environmental contaminants in fish and wildlife of the Lower Gila River, Arizona: U.S. Fish and Wildlife Service Environmental Contaminants Report, Phoenix Ecological Services Field Office, Arizona, 64 p., http://library.fws.gov/Pubs2/ci/LowerGila97.pdf/.

Klapper, L., McKnight, D.M., Fulton, J.R., Blunt-Harris, E.L., Nevin, K.P., Lovley, D.R., and Hatcher, P.G., 2002, Fulvic acid oxidation state detection using fluorescence spectroscopy: Environmental Science and Technology, v. 36, p. 3170–3175.

Lanning, J.E., 1930, Historical growth of the United Verde smelting plant at Clarkdale, Arizona: Mining Congress Journal, v. 16, p. 354–360.

Larsen, L.F., and Bjeeregaard, P., 1995, The effect of selenium on the handling of mercury in the shore crab *Carcinus maenas*: Marine Pollution Bulletin, v. 31, no. 1–3, p. 78–83.

Lavilla, I., Rodriguez-Linares, G., Garrido, J., and Bendicho, C., 2010, A biogeochemical approach to understanding the accumulation patterns of trace elements in three species of dragonfly larvae—evaluation as biomonitors: Journal of Environmental Monitoring, v. 12, p. 724–730.

Letachowicz, B., Krawczyk, A., and Klink, A., 2006, Accumulation of heavy metals in organs of *Typha latifolia* L.: Polish Journal of Environmental Studies, v. 15, p. 407–409.

Lindgren, Waldemar, 1926, Ore deposits of the Jerome and Bradshaw Mountains quadrangles, Arizona: U.S. Geological Survey Bulletin 782, 192 p., 2 pls., http://pubs.er.usgs.gov/publication/b782/.

Lindsay, B.A., 2000, Soil survey of Tuzigoot National Monument, Arizona: U.S. Geological Survey Technical Report No. 67., 54 p.

MacDonald, D.D., Ingersoll, C.G., and Berger, T.A., 2000, Development and evaluation of consensus-based sediment quality guidelines for freshwater ecosystems: Archives of Environmental Contamination and Toxicology, v. 39, p. 20–31.

Manning, A.H., 2009, Ground-water temperature, noble gas, and carbon isotope data from the Española Basin, New Mexico: U.S. Geological Survey Scientific Investigations Report 2008–5200, 69 p.

Maret, T.R., Cain, D.J., MacCoy, D.E., and Short, T.M., 2003, Response of benthic invertebrate assemblages to metal exposure and bioaccumulation associated with hard-rock mining in northwestern streams, USA: Journal of the North American Benthological Society, v. 22, no. 4, p. 598–620.

Marr, C., 2008, Contaminants in fish and wildlife of Lynx Lake, Arizona, U.S. Fish and Wildlife Service Environmental Contaminants Report, Phoenix Ecological Services Field Office, Arizona, 55 p., http://www.fws.gov/southwest/es/arizona/Documents/ECReports/lynx%20lake%2008%20final%20report.pdf

Marr, C., and Schotborgh, H.M., 2003, Contaminants in fish and birds of Watson Lake, Arizona 2000-2001: U.S. Fish and Wildlife Service Environmental Contaminants Report, Phoenix Ecological Services Field Office, Arizona, p. 47. http://www.fws.gov/southwest/es/arizona/Documents/ECReports/WATSON_LAKE_EC_REPTfinal.pdf

Mason, R. P., Laporte, J.-M., and Andres, S., 2000, Factors controlling the bioaccumulation of mercury, methylmercury, arsenic, selenium, and cadmium by freshwater invertebrates and fish: Archives of Environmental Contamination and Toxicology, v. 38, p. 283–297.

McKnight, D.M., Boyer, E.W., Westerhoff, P.K., Doran, P.T., Kulbe, T., and Anderson, D.T., 2001, Spectrofluorometric characterization of dissolved organic matter for indication of precursor organic material and aromaticity: Limnology and Oceanography, v. 46, p. 38–48.

Mertz, W., 1981, The essential trace elements: Science, v. 213, no. 4514, p. 1332–1338.

Miller, M.P., Simone, B.E., McKnight, D.M., Cory, R.M., Williams, M.W., and Boyer, E.W., 2010, New light on a dark subject—comment: Aquatic Sciences, v. 72, p. 269–275.

Mladenov, N., Zheng, Y., Miller, M.P., Nemergut, D.R., Legg, T., Simone, B., Hageman, C., Rahman, M.M., Ahmed, K.M., and McKnight, D.M., 2010, Dissolved organic matter sources and consequences for iron and arsenic mobilization in Bangladesh aquifers: Environmental Science and Technology, v. 44, p. 123–128.

Munsell Color, 2009, Munsell soil-color charts with genuine Munsell color chips: Grand Rapids, Mich., X-Rite, Inc.

Naftz, D.L., Cederberg, J.R., Krabbenhoft, D.P., Beisner, K.R., Whitehead, J., Gardberg, J., 2011, Diurnal trends in methylmercury concentration in a wetland adjacent to Great Salt Lake, Utah, USA: Chemical Geology, v. 283, no. 1–2, p. 78–86.

Nash, T.J., Miller, W.R., McHugh, J.B., and Meier, A.L., 1996, Geochemical characterization of mining districts and mining-related contamination in the Prescott National Forest area, Yavapai County, Arizona—a preliminary assessment of environmental effects: U.S. Geological Survey Open-File Report 96–687, 80 p.

National Research Council Canada, 1983, TORT-1 Lobster hepatopancreas marine reference material for trace metals and other elements, description sheet.

National Research Council Canada, 2008a, DORM-3 Fish protein certified reference material for trace metals, available online at http://archive.nrc-cnrc.gc.ca/obj/inms-ienm/doc/crm-mrc/eng/DORM-3_e.pdf

National Research Council Canada, 2008b, DOLT-4 Dogfish liver certified reference material for trace metals, available online at http://archive.nrc-cnrc.gc.ca/obj/inms-ienm/doc/crm-mrc/eng/DOLT-4_e.pdf

Ohno, T., 2002, Fluorescence inner-filtering correction for determining the humification index of dissolved organic matter: Environmental Science and Technology, v. 36, p. 742–746.

Olund, S.D., DeWild, J.F., Olson, M.L., and Tate, M.T., 2005, Methods for the preparation and analysis of solids and suspended solids for total mercury: U.S. Geological Survey Techniques and Methods, book 5, chap. 8, section A, 15 p., http://pubs.usgs.gov/tm/2005/tm5A8/.

Owen-Joyce, S.J., and Bell, C.K., 1983, Appraisal of water resources in the upper Verde River area, Yavapai and Coconino Counties, Arizona: Arizona Department of Water Resources Bulletin 2, 219 p.

Patton, C.J., and Kryskalla, J.R., 2011, Colorimetric determination of nitrate plus nitrite in water by enzymatic reduction, automated discrete analyzer methods: U.S. Geological Survey Techniques and Methods, book 5, chap. B8, 34 p., http://pubs.usgs.gov/tm/05b08/.

Paul, A.P., Paretti, N.V., MacCoy, D.E., and Brasher, A.M.D., 2012, The occurrence of trace elements in bed sediment collected from areas of varying land use and potential effects on stream macroinvertebrates in the conterminous western United States, Alaska, and Hawaii, 1992–2000: U.S. Geological Survey Scientific Investigations Report 2012–5272, 55 p., http://pubs.water.usgs.gov/sir/2012/5272.

Persaud, D., Jaagumagi, R., and Hayton, A., 1993, Guidelines for the protection and management of aquatic sediment quality in Ontario: Toronto, Ontario Ministry of the Environment Water Resources Branch, 27 p.

Piliposian, G.T., and Appleby, P.G., 2003, A simple model of the origin and transport of ^{222}Rn and ^{210}Pb in the atmosphere: Continuum Mechanics and Thermodynamics, v. 15, p. 503–518.

Plumb R.H., 1999, Characterization of mine leachates and the development of a ground-water monitoring strategy for mine sites: U.S. Environmental Protection Agency Report 600-R99-007.

Révész, K., and Coplen, T.B., 2008a, Determination of the $\delta(^2H/^1H)$ of water—RSIL lab code 1574, chap. C1 *of* Révész, K., and Coplen, T.B., eds., Methods of the Reston Stable Isotope Laboratory: U.S. Geological Survey Techniques and Methods book 10, chap. C1, 27 p., http://pubs.usgs.gov/tm/2007/tm10c1/#pdf/.

Révész, Kinga, and Coplen, Tyler, B., 2008b, Determination of the $\delta(^{18}O/^{16}O)$ of water—RSIL lab code 489, chap. C2 *of* Révész, Kinga, and Coplen, Tyler B., eds., Methods of the Reston Stable Isotope Laboratory: U.S. Geological Survey Techniques and Methods, book 10, chap. C2, 28 p., http://pubs.usgs.gov/tm/2007/tm10c2/#pdf/.

Ryan, A., and Parsons, L., 2009, Tavasci Marsh wetland assessment—Wetland vegetation communities, condition, and functions: National Park Service, 45 p.

Sabater, S., 2000, Diatom communities as indicators of environmental stress in the Guadiamar River, S-W. Spain, following a major mine tailings spill: Journal of Applied Phycology, v. 12, p. 113–124.

SAS Institute Inc., 2007, JMP Statistics and Graphics Guide: Cary, N.C., SAS Institute Inc., 1048 p., http://www.jmp.com/support/downloads/pdf/jmp_stat_graph_guide.pdf

Sasmaz, A., Obek, E., and Hasar, H., 2008, The accumulation of heavy metals in *Typha latifolia* L. grown in a stream carrying secondary effluent: Ecological Engineering, v. 33, p. 278–284.

Schmidt, C.A., Powell, B.F., and Halvorson, W.L., 2005, Vascular plant and vertebrate inventory of Tuzigoot National Monument: U.S. Geological Survey Open-File Report 2005–1347.

Schmitt, C.J., 1998, Environmental contaminants *in* Mac, M.J., Opler, P.A., Puckett Haecker, C.E., and Doran, P.D., eds., Status and trends of the Nation's biological resources, Part 1—Factors affecting biological resources: Reston, Va., U.S. Geological Survey, p. 131–144, http://www.nwrc.usgs.gov/sandt/.

Schmitt, C.J., and Brumbaugh, W.G., 1990, National Contaminant Biomonitoring Program—concentrations of Arsenic, Cadmium, Copper, Lead, Mercury, Selenium, and Zinc in U.S. freshwater fish, 1976-1984: Archives of Environmental Contamination and Toxicology, v. 19, p. 731–747.

Schnitzer, M., 1982, Organic matter characterization, *in* Page, A.L, Miller, R.H., and Keeney, D.R., eds., Methods of Soil Analysis, Part 2, 2d edition, Agronomy Monograph 9: , Madison, Wisc., American Society of Agronomy and Soil Science Society of America, p. 581–593.

Shelton, C.J., and Capel, P.D., 1994, Guidelines for collecting and processing samples of streambed sediment for analysis of trace elements and organic contaminants for the National Water-Quality assessment program: U.S. Geological Survey Open-File Report 94–458, 20 p., http://water.usgs.gov/nawqa/pnsp/pubs/ofr94-458/.

Smith, D.B., 1995, United States Geological Survey Certificate of Analysis, Cody Shale, SCo-1, available online at http://crustal.usgs.gov/geochemical_reference_standards/pdfs/codyshale.pdf/.

Stevenson, R.J., and Bahls. L.L., 1999, Periphyton protocols, *in* Barbour, M.T., Gerritsen, J., Synder, B.D., and Stribling, J.B., eds., Rapid bioassessment protocols—For use in streams and wadeable rivers—Periphyton, benthic macroinvertebrates, and fish, 2nd ed.: Washington, D.C., U.S. Environmental Protection Agency Office of Water publication EPA 841-B-99-002, p. 6–1 to 6–22.

Stoutamire, W., 2011, Water in the desert—A history of Arizona's Tavasci Marsh 1865-2005: Santa Fe, N.M., National Park Service Intermountain Cultural Resource Management Professional Paper No. 77.

Stute, M., and Schlosser, P., 2000, Atmospheric noble gases, *in* Cook, P.G., and Herczeg, A.L., eds., Environmental tracers in subsurface hydrology Boston, Mass., Kluwer, p. 349–377.

Tamers, M.A., 1967, Radiocarbon ages of groundwater in an arid zone unconfined aquifer, *in* Isotope Techniques in the Hydrological Cycle, AGU Monograph 11, p. 143–152, doi:10.1029/GM011p0143

Taylor, G.J., and Crowder, A.A., 1983, Uptake and accumulation of heavy metals by *Typha latifolia* in wetlands of the Sudbury, Ontario region: The Canadian Journal of Botany, v. 61, p. 63–73.

Turnipseed, D.P., and Sauer, V.B., 2010, Discharge measurements at gaging stations: U.S. Geological Survey Techniques and Methods book 3, chap. A8, 87 p., http://pubs.usgs.gov/tm/tm3-a8/.

URS Greiner Woodward Clyde (URSGWC), 1999, Tavasci Marsh Supplemental Sampling Report: prepared for Bureau of Land Management, Safford, Ariz., at the request of Phelps Dodge Corporation, Phoenix, Ariz., project no. 6800044364.00.

U.S. Environmental Protection Agency, 1997, The incidence and severity of sediment contamination in surface waters of the United States, volume 1—National sediment quality survey: U.S. Environmental Protection Agency publication EPA 823–R–97–006 [variously paged].

U.S. Environmental Protection Agency, 2007, Aquatic life ambient freshwater quality criteria—copper, 2007 revision, United States Environmental Protection Agency Office of Water, Office of Science and Technology publication EPA 822-R-03-026.

U.S. Environmental Protection Agency, 2013a, Drinking water contaminants: U.S. Environmental Protection Agency database, accessed January 13, 2014, at http://www.epa.gov/safewater/contaminants/index.html.

U.S. Environmental Protection Agency, 2013b, Current national recommended water quality criteria for aquatic life: U.S. Environmental Protection Agency database, accessed January 23, 2014, at http://www.epa.gov/waterscience/criteria/wqcriteria.html.

U.S. Environmental Protection Agency, 2013c, ProUCL Software, Statistical software ProUCL 5.0.00 for environmental applications for data sets with and without nondetect observations, available at http://www.epa.gov/osp/hstl/tsc/software.htm.

U.S. Geological Survey, 2013a, Analytical contract laboratory method summaries, methods 8, 10, and 19 available online at http://minerals.cr.usgs.gov/projects/analytical_chem/references.html.

U.S. Geological Survey, 2013b, National Water Information System, USGS Water-quality data for Arizona, accessed January 13, 2014, at http://waterdata.usgs.gov/az/nwis/qw/.

U.S. Geological Survey, variously dated, National field manual for the collection of water-quality data: U.S. Geological Survey Techniques of Water-Resources Investigations, book 9, chaps. A1–A9, available online at http://pubs.water.usgs.gov/twri9A.

Van Metre, P.C., Wilson, J.T., Fuller, C.C., Callender, Edward, and Mahler, B.J., 2004, Collection, analysis, and age dating of sediment cores from 56 U.S. lakes and reservoirs sampled by the U.S. Geological Survey, 1992–2001: U.S. Geological Survey Scientific Investigations Report 2004–5184, 180 p.

Verde Historical Society, 2013, Clemenceau Heritage Museum accessed at:www.clemenceaumuseum.com/history.html

Weishaar, J.L., Aiken, G.R., Bergamaschi, B.A., Fram, M.S., Fuji, R., and Mopper, K, 2003, Evaluation of specific ultraviolet absorbance as an indicator of the chemical composition and reactivity of dissolved organic carbon: Environmental Science and Technology, v. 37, p. 4702–4708.

Wildhaber, M.L., and Schmitt, C.J., 1996, Estimating aquatic toxicity as determined through laboratory tests of Great Lakes sediments containing complex mixtures of environmental contaminants: Environmental Monitoring and Assessment, v. 41, p. 255–289.

Wilson, S., 2001, United States Geological Survey Certificate of Analysis, Green River Shale, SGR-1, available online at http://crustal.usgs.gov/geochemical_reference_standards/pdfs/shale.pdf

Wolf, R.E., Todd, A.S., Brinkman, S., Lamothe, P.J., Smith, K.S., Ranville, J.F., 2009, Measurement of total Zn and Zn isotope ratios by quadrupole ICP-MS for evaluation of Zn uptake in gills of brown trout (Salmo trutta) and rainbow trout (Oncorhynchus mykiss): Talanta, v. 80, p. 676–684.

Wolfe, A.P., Kaushal, S.S., Fultin, J.R., and McKnight, D.M., 2002, Spectrofluorescence of sediment humic substances and historical changes of lacustrine organic matter provenance in response to atmospheric nutrient enrichment: Environmental Science and Technology, v. 36, p. 3217–3223.

Western Regional Climate Center, 2013, Western Regional Climate Center, Tuzigoot, Arizona station number 028904, accessed January 13, 2014, http://www.wrcc.dri.edu/cgi-bin/cliMAIN.pl?az8904.

Ye, Z.H., Baker, A.J.M., Wong, M.H., and Willis, A.J., 1997, Zinc, lead and cadmium tolerance, uptake and accumulation by Typha latifolia: New Phytologist, v. 136, no. 3, p. 469–480.

Menlo Park Publishing Service Center, California
Manuscript approved for publication April 18, 2014
Edited by Claire M. Landowski
Design and layout by Jeanne S. DiLeo

http://dx.doi.org/10.3133/sir20145069
ISSN 2328-0328 (online)